Published for SISSA by Springer

Received: *August 8, 2013*
Revised: *September 16, 2013*
Accepted: *September 27, 2013*
Published: *October 21, 2013*

# Search for new phenomena in final states with large jet multiplicities and missing transverse momentum at $\sqrt{s} = 8$ TeV proton-proton collisions using the ATLAS experiment

**The ATLAS collaboration**

*E-mail:* atlas.publications@cern.ch

Abstract: A search is presented for new particles decaying to large numbers (7 or more) of jets, with missing transverse momentum and no isolated electrons or muons. This analysis uses 20.3 fb$^{-1}$ of $pp$ collision data at $\sqrt{s} = 8$ TeV collected by the ATLAS experiment at the Large Hadron Collider. The sensitivity of the search is enhanced by considering the number of $b$-tagged jets and the scalar sum of masses of large-radius jets in an event. No evidence is found for physics beyond the Standard Model. The results are interpreted in the context of various simplified supersymmetry-inspired models where gluinos are pair produced, as well as an mSUGRA/CMSSM model.

Keywords: Hadron-Hadron Scattering, Jet physics, Supersymmetry, Exotics

Open Access, Copyright CERN,
for the benefit of the ATLAS collaboration

doi:10.1007/JHEP10(2013)130

JHEP10(2013)130

source: https://doi.org/10.7892/boris.58435 | downloaded: 17.4.2024

## Contents


**1 Introduction** **1**

**2 The ATLAS detector and data samples** **3**

**3 Physics object selection** **4**

**4 Event selection** **5**
- 4.1 The multi-jet + flavour stream 6
- 4.2 The multi-jet + $M_J^{\Sigma}$ stream 6
- 4.3 Summary of signal regions 6

**5 Standard model background determination** **8**
- 5.1 Monte Carlo simulations 8
- 5.2 Multi-jet background 9
- 5.3 Systematic uncertainties in the multi-jet background determination 10
- 5.4 Leptonic backgrounds 12
- 5.5 Systematic uncertainties in the leptonic background determination 16

**6 Results** **17**
- 6.1 Simultaneous fit in the multi-jet + flavour stream 19
- 6.2 Simultaneous fit in the multi-jet + $M_J^{\Sigma}$ stream 22
- 6.3 Fit results 22

**7 Interpretation** **22**

**8 Conclusion** **29**

**The ATLAS collaboration** **34**


JHEP10(2013)130

## 1 Introduction

Many extensions of the Standard Model of particle physics predict the presence of TeV-scale strongly interacting particles that decay to weakly interacting descendants. In the context of R-parity-conserving supersymmetry (SUSY) [1–5], the strongly interacting parent particles are the partners of the quarks (squarks, $\tilde{q}$) and gluons (gluinos, $\tilde{g}$), and are produced in pairs. The lightest supersymmetric particle (LSP) is stable, providing a candidate that can contribute to the relic dark-matter density in the universe [6, 7]. If they are kinematically accessible, the squarks and gluinos could be produced in the proton-proton interactions at the Large Hadron Collider (LHC) [8].

Such particles are expected to decay in cascades, the nature of which depends on the mass hierarchy within the model. The events would be characterised by significant missing transverse momentum from the unobserved weakly interacting descendants, and by a large number of jets from emissions of quarks and/or gluons. Individual cascade decays may include gluino decays to a top squark (stop, $\tilde{t}$) and an anti-top quark,

$$\tilde{g} \;\rightarrow\; \tilde{t} + \bar{t} \tag{1.1a}$$

followed by the top-squark decay to a top quark and a neutralino LSP, $\tilde{\chi}_1^0$,

$$\tilde{t} \rightarrow t + \tilde{\chi}_1^0. \tag{1.1b}$$

Alternatively, if the top squark is heavier than the gluino, the three-body decay,

$$\tilde{g} \;\rightarrow\; t + \bar{t} + \tilde{\chi}_1^0 \tag{1.2}$$

may result. Other possibilities include decays involving intermediate charginos, neutralinos, and/or squarks including bottom squarks. A pair of cascade decays produces a large number of Standard Model particles, together with a pair of LSPs, one from the end of each cascade. The LSPs are assumed to be stable and only weakly interacting, and so escape undetected, resulting in missing transverse momentum.

In this paper we consider final states with large numbers of jets together with significant missing transverse momentum in the absence of isolated electrons or muons, using the $pp$ collision data recorded by the ATLAS experiment [9] during 2012 at a centre-of-mass energy of $\sqrt{s} = 8$ TeV. The corresponding integrated luminosity is $20.3\,\text{fb}^{-1}$. Searches for new phenomena in final states with large jet multiplicities — requiring from at least six to at least nine jets — and missing transverse momentum have previously been reported by the ATLAS Collaboration using LHC $pp$ collision data corresponding to $1.34\,\text{fb}^{-1}$ [10] and to $4.7\,\text{fb}^{-1}$ [11] at $\sqrt{s} = 7$ TeV. Searches with explicit tagging of jets from bottom quarks ($b$-jets) in multi-jet events were also performed by ATLAS [12] and CMS [13–15]. These searches found no significant excess over the Standard Model expectation and provide limits on various supersymmetric models, including decays such as that in eq. (1.2) and an mSUGRA/CMSSM [16–21] model that includes strong production processes. The analysis presented in this paper extends previous analyses by reaching higher jet multiplicities and utilizing new sensitive variables.

Events are first selected with large jet multiplicities, with requirements ranging from at least seven to at least ten jets, reconstructed using the anti-$k_t$ clustering algorithm [22, 23] and jet radius parameter $R = 0.4$. Significant missing transverse momentum is also required in the event. The sensitivity of the search is further enhanced by the subdivision of the selected sample into several categories using additional information. Event clasification based on the number of $b$-jets gives enhanced sensitivity to models which predict either more or fewer $b$-jets than the Standard Model background. In a complementary stream of the analysis, the $R = 0.4$ jets are clustered into large ($R = 1.0$) composite jets to form an event variable, the sum of the masses of the composite jets, which gives additional discrimination in models with a large number of objects in the final state [24]. Events



JHEP10(2013)130

containing isolated, high transverse-momentum ($p_{\mathrm{T}}$) electrons or muons are vetoed in order to reduce backgrounds involving leptonic $W$ boson decays. The previous analyses [10, 11] had signal regions with smaller jet multiplicities; those are now omitted since the absence of significant excesses in earlier analyses places stringent limits on models with large cross sections.

Searches involving final states with many jets and missing transverse momentum have been confirmed to have good sensitivity to decays such as those in eqs. (1.1) and (1.2) [11], but they also provide sensitivity to any model resulting in final states with large jet multiplicity in association with missing transverse momentum. Such models include the pair production of gluinos, each of them decaying via an off-shell squark, as

$$\tilde{g} \to \bar{q} + q' + \tilde{\chi}_1^{\pm} \to \bar{q} + q' + W^{\pm} + \tilde{\chi}_1^0, \tag{1.3a}$$

or alternatively

$$\tilde{g} \to \bar{q} + q' + \tilde{\chi}_1^{\pm} \to \bar{q} + q' + W^{\pm} + \tilde{\chi}_2^0 \to \bar{q} + q' + W^{\pm} + Z^0 + \tilde{\chi}_1^0. \tag{1.3b}$$

Another possibility is the pair production of gluinos which decay as in eq. (1.1a) and the subsequent decay of the $\tilde{t}$-squark via

$$\tilde{t} \to b + \tilde{\chi}_1^{\pm},$$

or via the R-parity-violating decay

$$\tilde{t} \to \bar{b} + \bar{s}. \tag{1.4}$$

Several supersymmetric models are used to interpret the analysis results: simplified models that include decays such as those in eqs. (1.1)–(1.4), and an mSUGRA/CMSSM model with parameters[1] $\tan\beta = 30$, $A_0 = -2m_0$ and $\mu > 0$, which accommodates a lightest Higgs boson mass compatible with the observed Higgs boson mass at the LHC [25, 26].

## 2 The ATLAS detector and data samples

The ATLAS experiment is a multi-purpose particle physics detector with a forward-backward symmetric cylindrical geometry and nearly $4\pi$ coverage in solid angle.[2] The layout of the detector is defined by four superconducting magnet systems, which comprise a thin solenoid surrounding the inner tracking detectors (ID), and a barrel and two end-cap toroids generating the magnetic field for a large muon spectrometer. The ID provides precision reconstruction of tracks in the region $|\eta| < 2.5$. The calorimeters lie

[1] A particular mSUGRA/CMSSM model point is specified by five parameters: the universal scalar mass $m_0$, the universal gaugino mass $m_{1/2}$, the universal trilinear scalar coupling $A_0$, the ratio of the vacuum expectation values of the two Higgs fields $\tan\beta$, and the sign of the higgsino mass parameter $\mu$.

[2] ATLAS uses a right-handed coordinate system with its origin at the nominal interaction point (IP) in the centre of the detector and the $z$-axis along the beam pipe. The $x$-axis points from the IP to the centre of the LHC ring, and the $y$-axis points upward. Cylindrical coordinates $(r, \phi)$ are used in the transverse plane, $\phi$ being the azimuthal angle around the beam pipe. The pseudorapidity is defined in terms of the polar angle $\theta$ as $\eta = -\ln\tan(\theta/2)$, and the transverse energy $E_{\mathrm{T}}$ by $E_{\mathrm{T}} = E\sin\theta$.



JHEP10(2013)130

between the ID and the muon system. In the pseudorapidity region $|\eta| < 3.2$, high-granularity liquid-argon (LAr) electromagnetic (EM) sampling calorimeters are used. An iron/scintillator-tile calorimeter provides hadronic coverage for $|\eta| < 1.7$. The end-cap and forward regions, spanning $1.5 < |\eta| < 4.9$, are instrumented with LAr calorimeters for both EM and hadronic measurements.

The data sample used in this analysis was taken during the period from March to December 2012 with the LHC operating at a $pp$ centre-of-mass energy of $\sqrt{s} = 8$ TeV. Application of data-quality requirements results in an integrated luminosity of $20.3 \pm 0.6\,\text{fb}^{-1}$, where the luminosity is measured using techniques similar to those described in ref. [27], with a preliminary calibration of the luminosity scale derived from beam-overlap scans performed in November 2012. The analysis makes use of dedicated multi-jet triggers, the final step of which required either at least five jets with $E_{\text{T}} > 55$ GeV or at least six jets with $E_{\text{T}} > 45$ GeV, where the jets must have $|\eta| < 3.2$. The final level of the trigger selection is based on a jet algorithm and calibration method closely matched to those used in the signal region selections. In all cases the trigger efficiency is greater than 99% for events satisfying the jet multiplicity selection criteria for the signal regions described in section 4. Events selected with single-lepton triggers and prescaled multi-jet triggers are used for background determination in control regions.

## 3 Physics object selection

Jets are reconstructed using the anti-$k_t$ jet clustering algorithm with radius parameter $R = 0.4$. The inputs to this algorithm are the energies and positions of clusters of calorimeter cells, where the clusters are formed starting from cells with energies significantly above the noise level [28]. Jet momenta are constructed by performing a four-vector sum over these clusters of calorimeter cells, treating each as an $(E, \mathbf{p})$ four-vector with zero mass. The local cluster weighting (LCW) calibration method [29] is used to classify clusters as being of either electromagnetic or hadronic origin and, based on this classification, applies specific energy corrections derived from a combination of Monte Carlo simulation and data [28]. A further calibration is applied to the corrected jet energies to relate the response of the calorimeter to the true jet energy [28]. The jets are corrected for energy from additional proton-proton collisions (pile-up) using a method, proposed in ref. [30], which estimates the pile-up activity in any given event, as well as the sensitivity of any given jet to pile-up. The method subtracts a contribution from the jet energy equal to the product of the jet area and the average energy density of the event. All jets are required to satisfy $p_{\text{T}} > 20$ GeV and $|\eta| < 2.8$. More stringent requirements on $p_{\text{T}}$ and on $|\eta|$ are made when defining signal regions as described in section 4.

Jets with heavy-flavour content are identified using a tagging algorithm that uses both impact parameter and secondary vertex information [31]. This $b$-tagging algorithm is applied to all jets that satisfy both $|\eta| < 2.5$ and $p_{\text{T}} > 40$ GeV. The parameters of the algorithm are chosen such that 70% of $b$-jets and about 1% of light-flavour or gluon jets are selected in $t\bar{t}$ events in Monte Carlo simulations [32]. Jets initiated by charm quarks are tagged with about 20% efficiency.



JHEP10(2013)130

Electrons are required to have $p_{\mathrm{T}} > 10$ GeV and $|\eta| < 2.47$. They must satisfy 'medium' electron shower shape and track selection criteria based upon those described in ref. [33], but modified to reduce the impact of pile-up and to match tightened trigger requirements. They must be separated by at least $\Delta R = 0.4$ from any jet, where $\Delta R = \sqrt{(\Delta\eta)^2 + (\Delta\phi)^2}$. Events containing electrons passing these criteria are vetoed when forming signal regions. Additional requirements are applied to electrons when defining leptonic control regions used to aid in the estimate of the SM background contributions, as described in section 5.4; in this case, electrons must have $p_{\mathrm{T}} > 25$ GeV, must satisfy the 'tight' criteria of ref. [33], must have transverse and longitudinal impact parameters within 5 standard deviations and 0.4 mm, respectively, of the primary vertex, and are required to be well isolated.[3]

Muons are required to have $p_{\mathrm{T}} > 10$ GeV and $|\eta| < 2.5$, to satisfy track quality selection criteria, and to be separated by at least $\Delta R = 0.4$ from the nearest jet candidate. Events containing muons passing these criteria are vetoed when forming signal regions. When defining leptonic control regions, muons must have $p_{\mathrm{T}} > 25$ GeV, $|\eta| < 2.4$, transverse and longitudinal impact parameters within 5 standard deviations and 0.4 mm, respectively, of the primary vertex and they must be isolated.[4]

The missing transverse momentum two-vector $\mathbf{p}_{\mathrm{T}}^{\mathrm{miss}}$ is calculated from the negative vector sum of the transverse momenta of all calorimeter energy clusters with $|\eta| < 4.5$ and of all muons [34]. Clusters associated with either electrons or photons with $p_{\mathrm{T}} > 10$ GeV, and those associated with jets with $p_{\mathrm{T}} > 20$ GeV and $|\eta| < 4.5$ make use of the calibrations of these respective objects. For jets the calibration includes the area-based pile-up correction described above. Clusters not associated with such objects are calibrated using both calorimeter and tracker information. The magnitude of $\mathbf{p}_{\mathrm{T}}^{\mathrm{miss}}$, conventionally denoted by $E_{\mathrm{T}}^{\mathrm{miss}}$, is used to distinguish signal and background regions.

## 4 Event selection

Following the physics object reconstruction described in section 3, events are discarded if they contain any jet that fails quality criteria designed to suppress detector noise and non-collision backgrounds, or if they lack a reconstructed primary vertex with five or more associated tracks. Events containing isolated electron or muon candidates are also vetoed as described in section 3. The remaining events are then analysed in two complementary analysis streams, both of which require large jet multiplicities and significant $E_{\mathrm{T}}^{\mathrm{miss}}$. The selections of the two streams are verified to have good sensitivity to decays such as those in eqs. (1.1)–(1.4), but are kept generic to ensure sensitivity in a broad set of models with large jet multiplicity and $E_{\mathrm{T}}^{\mathrm{miss}}$ in the final state.

[3] The electron isolation requirements are based on nearby tracks and calorimeter clusters, as follows. The scalar sum of transverse momenta of tracks, other than the track from the electron itself, in a cone of radius $\Delta R = 0.3$ around the electron is required to be smaller than 16% of the electron's $p_{\mathrm{T}}$. The scalar sum of calorimeter transverse energy around the electron in the same cone, excluding the electron itself, is required to be smaller than 18% of the electron's $p_{\mathrm{T}}$.

[4] The scalar sum of the transverse momenta of the tracks, other than the track from the muon itself, within a cone of $\Delta R = 0.3$ around the muon must be less than 12% of the muon's $p_{\mathrm{T}}$, and the scalar sum of calorimeter transverse energy in the same cone, excluding that from the muon, must be less than 12% of the muon's $p_{\mathrm{T}}$.



JHEP10(2013)130

### 4.1 The multi-jet + flavour stream

In the multi-jet + flavour stream the number of jets with $|\eta| < 2$ and $p_{\mathrm{T}}$ above the threshold $p_{\mathrm{T}}^{\mathrm{min}} = 50$ GeV is determined. Events with exactly eight or exactly nine such jets are selected, and the sample is further subdivided according to the number of the jets (0, 1 or $\geq$2) with $p_{\mathrm{T}} > 40\,\mathrm{GeV}$ and $|\eta| < 2.5$ which satisfy the $b$-tagging criteria. The $b$-tagged jets may belong to the set of jets with $p_{\mathrm{T}}$ greater than $p_{\mathrm{T}}^{\mathrm{min}}$, but this is not a requirement. Events with ten or more jets are retained in a separate category, without any further subdivision.

A similar procedure is followed for the higher jet-$p_{\mathrm{T}}$ threshold of $p_{\mathrm{T}}^{\mathrm{min}} = 80$ GeV. Signal regions are defined for events with exactly seven jets or at least eight jets. Both categories are again subdivided according to the number of jets (0, 1 or $\geq$2) that are $b$-tagged. Here again, the $b$-tagged jets do not necessarily satisfy the $p_{\mathrm{T}}^{\mathrm{min}}$ requirement.

In all cases the final selection variable is $E_{\mathrm{T}}^{\mathrm{miss}}/\sqrt{H_{\mathrm{T}}}$, the ratio of the $E_{\mathrm{T}}^{\mathrm{miss}}$ to the square root of the scalar sum $H_{\mathrm{T}}$ of the transverse momenta of all jets with $p_{\mathrm{T}} > 40$ GeV and $|\eta| < 2.8$. This ratio is closely related to the significance of the $E_{\mathrm{T}}^{\mathrm{miss}}$ relative to the resolution due to stochastic variations in the measured jet energies [34]. The value of $E_{\mathrm{T}}^{\mathrm{miss}}/\sqrt{H_{\mathrm{T}}}$ is required to be larger than 4 $\mathrm{GeV}^{1/2}$ for all signal regions.

### 4.2 The multi-jet + $M_J^{\Sigma}$ stream

Analysis of the multi-jet + $M_J^{\Sigma}$ stream proceeds as follows. The number of ($R = 0.4$) jets with $p_{\mathrm{T}}$ above 50 GeV is determined, this time using a larger pseudorapidity acceptance of $|\eta| < 2.8$. Events with at least eight, at least nine or at least ten such jets are retained, and a category is created for each of those multiplicity thresholds. The four-momenta of the $R = 0.4$ jets satisfying $p_{\mathrm{T}} > 20\,\mathrm{GeV}$ and $|\eta| < 2.8$ are then used as inputs to a second iteration of the anti-$k_t$ jet algorithm, this time using the larger distance parameter $R = 1.0$. The resulting larger objects are denoted as composite jets. The selection variable $M_J^{\Sigma}$ is then defined to be the sum of the masses $m_j^{R=1.0}$ of the composite jets

$$M_J^{\Sigma} \equiv \sum_j m_j^{R=1.0},$$

where the sum is over the composite jets that satisfy $p_{\mathrm{T}}^{R=1.0} > 100$ GeV and $|\eta^{R=1.0}| < 1.5$. Signal regions are defined for two different $M_J^{\Sigma}$ thresholds. Again the final selection requires that $E_{\mathrm{T}}^{\mathrm{miss}}/\sqrt{H_{\mathrm{T}}} > 4$ $\mathrm{GeV}^{1/2}$.

### 4.3 Summary of signal regions

The nineteen resulting signal regions are summarized in table 1. Within the multi-jet + flavour stream the seven signal regions defined with $p_{\mathrm{T}}^{\mathrm{min}} = 50$ GeV are mutually disjoint. The same is true for the six signal regions defined with the threshold of 80 GeV. However, the two sets of signal regions overlap; an event found in one of the $p_{\mathrm{T}}^{\mathrm{min}} = 80$ GeV signal regions may also be found in one of the $p_{\mathrm{T}}^{\mathrm{min}} = 50$ GeV signal regions. The multi-jet + $M_J^{\Sigma}$ stream has six inclusive signal regions; for example an event which has at least ten $R = 0.4$ jets with $p_{\mathrm{T}} > 50$ GeV, $M_J^{\Sigma} > 420\,\mathrm{GeV}$ and $E_{\mathrm{T}}^{\mathrm{miss}}/\sqrt{H_{\mathrm{T}}} > 4$ $\mathrm{GeV}^{1/2}$ will be found in all six multi-jet + $M_J^{\Sigma}$ regions. These overlaps are treated in the results of the analysis as described in section 6.



JHEP10(2013)130

| | **Multi-jet + flavour stream** | | | | | | | | | | **Multi-jet + $M_J^\Sigma$ stream** | | |
|---|---|---|---|---|---|---|---|---|---|---|---|---|---|
| Identifier | **8j50** | | | **9j50** | | | **≥ 10j50** | **7j80** | | | **≥ 8j80** | | | **≥ 8j50** | **≥ 9j50** | **≥ 10j50** |
| Jet $\lvert\eta\rvert$ | $< 2.0$ | | | | | | | $< 2.0$ | | | | | | $< 2.8$ | | |
| Jet $p_{\mathrm{T}}$ | $> 50$ GeV | | | | | | | $> 80$ GeV | | | | | | $> 50$ GeV | | |
| Jet count | $= 8$ | | | $= 9$ | | | $\geq 10$ | $= 7$ | | | $\geq 8$ | | | $\geq 8$ | $\geq 9$ | $\geq 10$ |
| $b$-jets ($p_{\mathrm{T}} > 40$ GeV, $\lvert\eta\rvert < 2.5$) | 0 | 1 | $\geq 2$ | 0 | 1 | $\geq 2$ | — | 0 | 1 | $\geq 2$ | 0 | 1 | $\geq 2$ | — | | |
| $M_J^\Sigma$ [GeV] | — | | | | | | | — | | | | | | $> 340$ and $> 420$ for each case | | |
| $E_{\mathrm{T}}^{\mathrm{miss}}/\sqrt{H_{\mathrm{T}}}$ | $> 4$ GeV$^{1/2}$ | | | | | | | $> 4$ GeV$^{1/2}$ | | | | | | $> 4$ GeV$^{1/2}$ | | |

**Table 1**. Definition of the nineteen signal regions. The jet $\lvert\eta\rvert$, $p_{\mathrm{T}}$ and multiplicity all refer to the $R = 0.4$ jets. Composite jets with the larger radius parameter $R = 1.0$ are used in the multi-jet + $M_J^\Sigma$ stream when constructing $M_J^\Sigma$. A long dash '—' indicates that no requirement is made.

JHEP10(2013)130

## 5 Standard model background determination

Two background categories are considered in this search: (1) multi-jet production, including purely strong interaction processes and fully hadronic decays of $t\bar{t}$, and hadronic decays of $W$ and $Z$ bosons in association with jets, and (2) processes with leptons in the final states, collectively referred to as leptonic backgrounds. The latter consist of semileptonic and fully leptonic decays of $t\bar{t}$, including $t\bar{t}$ production in association with a boson; leptonically decaying $W$ or $Z$ bosons produced in association with jets; and single top quark production.

The major backgrounds (multi-jet, $t\bar{t}$, $W+$jets, and $Z+$jets) are determined with the aid of control regions, which are defined such that they are enriched in the background process(es) of interest, but nevertheless remain kinematically close to the signal regions. The multi-jet background determination is fully data-driven, and the most significant of the other backgrounds use data control regions to normalise simulations. The normalisations of the event yields predicted by the simulations are adjusted simultaneously in all the control regions using a binned fit described in section 6, and the simulation is used to extrapolate the results into the signal regions. The methods used in the determination of the multi-jet and leptonic backgrounds are described in sections 5.2 and 5.4, respectively.

### 5.1 Monte Carlo simulations

Monte Carlo simulations are used as part of the leptonic background determination process, and to assess the sensitivity to specific SUSY signal models. Most of the leptonic backgrounds are generated using Sherpa-1.4.1 [35] with the CT10 [36] set of parton distribution functions (PDF). For $t\bar{t}$ production, up to four additional partons are modelled in the matrix element. Samples of $W$ + jets and $Z$ + jets events are generated with up to five additional partons in the matrix element, except for processes involving $b$-quarks for which up to four additional partons are included. In all cases, additional jets are generated via parton showering. The leptonic $W$ + jets, $Z$ + jets and $t\bar{t}$ backgrounds are normalised according to their inclusive theoretical cross sections [37, 38]. In the case of $t\bar{t}$ production, to account for higher-order terms which are not present in the Sherpa Monte Carlo simulation, the fraction of events initiated by gluon fusion, relative to other processes, is modified to improve the agreement with data in $t\bar{t}$-enriched validation regions described in section 5.4. This corresponds to applying a scale factor of 1.37 to the processes initiated by gluon fusion and a corresponding factor to the other processes to keep the total $t\bar{t}$ cross section the same. The estimation of the leptonic backgrounds in the signal regions is described in detail in section 5.4.

Smaller background contributions are also modelled for the following processes: single top quark production in association with a $W$ boson in the $s$-channel (MC@NLO 4.06 [39–42] / Herwig 6.520 [43] / Jimmy 4.31 [44]), $t$-channel single top quark production (AcerMC3.8 [45] / Pythia-6.426 [46]), and $t\bar{t}$ production in association with a $W$ or $Z$ boson (Madgraph-5.1.4.8 [47] / Pythia-6.426).

Supersymmetric production processes are generated using Herwig++2.5.2 [48] and Madgraph-5.1.4.8 with the PDF set CTEQ6L1 [49]. The cross sections are calculated



JHEP10(2013)130

to next-to-leading order in the strong coupling constant $\alpha_S$, including the resummation of soft gluon emission at next-to-leading-logarithmic accuracy (NLO+NLL) [50–54].

For each process, the nominal cross section and its uncertainty are taken from an envelope of cross-section predictions using different PDF sets and factorisation and renormalisation scales, as described in ref. [55]. All Monte Carlo simulated samples also include simulation of pile-up and employ a detector simulation [56] based on GEANT4 [57]. The simulated events are reconstructed with the same algorithms as the data.

### 5.2 Multi-jet background

The dominant background at intermediate values of $E_{\mathrm{T}}^{\mathrm{miss}}$ is multi-jet production including purely strong interaction processes and fully hadronic decays of $t\bar{t}$. The contribution from these processes is determined using collision data and the selection criteria were designed such that multi-jet processes can be accurately determined from supporting measurements.

The background determination method is based on the observation that the $E_{\mathrm{T}}^{\mathrm{miss}}$ resolution of the detector is approximately proportional to $\sqrt{H_{\mathrm{T}}}$ and almost independent of the jet multiplicity in events dominated by jet activity, including hadronic decays of top quarks and gauge bosons [10, 11]. The distribution of the ratio $E_{\mathrm{T}}^{\mathrm{miss}}/\sqrt{H_{\mathrm{T}}}$ therefore has a shape that is almost invariant under changes in the jet multiplicity. The multi-jet backgrounds can be determined using control regions with lower $E_{\mathrm{T}}^{\mathrm{miss}}/\sqrt{H_{\mathrm{T}}}$ and/or lower jet multiplicity than the signal regions. The control regions are assumed to be dominated by Standard Model processes, and that assumption is corroborated by the agreement with Standard Model predictions of multi-jet cross-section measurements for up to six jets [58].

Events containing heavy quarks show a different $E_{\mathrm{T}}^{\mathrm{miss}}/\sqrt{H_{\mathrm{T}}}$ distribution than those containing only light-quark or gluon jets, since semileptonic decays of heavy quarks contain neutrinos. The dependence of $E_{\mathrm{T}}^{\mathrm{miss}}/\sqrt{H_{\mathrm{T}}}$ on the number of heavy quarks is accounted for in the multi-jet + flavour signal regions by using a consistent set of control regions with the same $b$-jet multiplicity as the target signal distribution. The $E_{\mathrm{T}}^{\mathrm{miss}}/\sqrt{H_{\mathrm{T}}}$ distribution is also found to be approximately independent of the $M_J^{\Sigma}$ event variable, so a similar technique is used to obtain the expected multi-jet background contributions to the multi-jet + $M_J^{\Sigma}$ signal regions.

The leading source of variation in $E_{\mathrm{T}}^{\mathrm{miss}}/\sqrt{H_{\mathrm{T}}}$ under changes in the jet multiplicity comes from a contribution to $E_{\mathrm{T}}^{\mathrm{miss}}$ from calorimeter energy deposits not associated with jets and hence not contributing to $H_{\mathrm{T}}$. The effect of this 'soft' energy is corrected for by reweighting the $E_{\mathrm{T}}^{\mathrm{miss}}/\sqrt{H_{\mathrm{T}}}$ distribution separately for each jet multiplicity in the signal region, to provide the same $\sum \mathrm{E}_{\mathrm{T}}^{\mathrm{CellOut}}/H_{\mathrm{T}}$ distribution, where $\sum \mathrm{E}_{\mathrm{T}}^{\mathrm{CellOut}}$ is the scalar sum of $E_{\mathrm{T}}$ over all clusters of calorimeter cells not associated with jets having $p_{\mathrm{T}} > 20$ GeV or electron, or muon candidates.

For example, to obtain the multi-jet contribution to the multi-jet + flavour stream 9j50 signal region with exactly one $b$-jet, the procedure is as follows. A template of the shape of the $E_{\mathrm{T}}^{\mathrm{miss}}/\sqrt{H_{\mathrm{T}}}$ distribution is formed from events which have exactly six jets with $p_{\mathrm{T}} > 50\,\mathrm{GeV}$, and exactly one $b$-jet (which is not required to be one of the six previous jets). The expected contribution from leptonic backgrounds is then subtracted, so that the template provides the expected distribution resulting from the detector resolution,



JHEP10(2013)130

together with any contribution to the resolution from semileptonic $b$-quark decays. The nine-jet background prediction for the signal region ($E_{\mathrm{T}}^{\mathrm{miss}}/\sqrt{H_{\mathrm{T}}} > 4$ GeV$^{1/2}$) with exactly one $b$-jet is then given by

$$N_{\text{predicted}}^{\text{multi-jet}} = \left(N_{\text{data}}^{A,\ n^{\text{jet}}=9} - N_{\text{leptonic MC}}^{A,\ n^{\text{jet}}=9}\right) \times \left(\frac{N_{\text{data}}^{B,\ n^{\text{jet}}=6} - N_{\text{leptonic MC}}^{B,\ n^{\text{jet}}=6}}{N_{\text{data}}^{A,\ n^{\text{jet}}=6} - N_{\text{leptonic MC}}^{A,\ n^{\text{jet}}=6}}\right), \qquad (5.1)$$

where $A \equiv E_{\mathrm{T}}^{\mathrm{miss}}/\sqrt{H_{\mathrm{T}}} < 1.5$ GeV$^{1/2}$, $B \equiv E_{\mathrm{T}}^{\mathrm{miss}}/\sqrt{H_{\mathrm{T}}} > 4$ GeV$^{1/2}$, and each of the counts $N$ is determined after requiring the same $b$-jet multiplicity as for the target signal region (i.e. exactly one $b$-jet in this example). Equation 5.1 is applied separately to each of ten bins (of width 0.1) in $\sum \mathrm{E}_{\mathrm{T}}^{\mathrm{CellOut}}/H_{\mathrm{T}}$ to find the prediction for that bin, and then the contributions of the ten bins summed to provide the $\sum \mathrm{E}_{\mathrm{T}}^{\mathrm{CellOut}}/H_{\mathrm{T}}$-weighted multi-jet prediction.

An analogous procedure is used to obtain the expected multi-jet contribution to each of the other multi-jet + flavour stream signal regions by using the appropriate $p_{\mathrm{T}}^{\mathrm{min}}$, jet multiplicity, and $b$-jet multiplicity as required by the target signal region. In each case the shape of the $E_{\mathrm{T}}^{\mathrm{miss}}/\sqrt{H_{\mathrm{T}}}$ distribution is obtained from a 'template' with exactly six (five) jets for signal regions with $p_{\mathrm{T}}^{\mathrm{min}} = 50\,(80)$ GeV. The distributions of $E_{\mathrm{T}}^{\mathrm{miss}}/\sqrt{H_{\mathrm{T}}}$ for multi-jet + flavour stream control regions are shown in figure 1.

The procedure in the multi-jet + $M_J^{\Sigma}$ stream is similar: the same jet $p_{\mathrm{T}}^{\mathrm{min}}$, jet multiplicity and $M_J^{\Sigma}$ criteria are used when forming the template and control regions that are required for the target signal region. $E_{\mathrm{T}}^{\mathrm{miss}}/\sqrt{H_{\mathrm{T}}}$ distributions for control regions with exactly seven jets with $p_{\mathrm{T}}$>50 GeV and additional $M_J^{\Sigma}$ selection criteria applied are shown in figure 2. Leptonic backgrounds are subtracted, and $\sum \mathrm{E}_{\mathrm{T}}^{\mathrm{CellOut}}/H_{\mathrm{T}}$ weighting is applied. For all cases in the multi-jet + $M_J^{\Sigma}$ stream the $E_{\mathrm{T}}^{\mathrm{miss}}/\sqrt{H_{\mathrm{T}}}$ template shape is determined from a sample which has exactly six jets with $p_{\mathrm{T}} > 50$ GeV.

Variations in the shape of the $E_{\mathrm{T}}^{\mathrm{miss}}/\sqrt{H_{\mathrm{T}}}$ distribution under changes in the jet multiplicity are later used to quantify the systematic uncertainty associated with the method, as described in section 5.3.

### 5.3 Systematic uncertainties in the multi-jet background determination

The multi-jet background determination method is validated by measuring the accuracy of the predicted $E_{\mathrm{T}}^{\mathrm{miss}}/\sqrt{H_{\mathrm{T}}}$ template for regions with jet multiplicities and/or $E_{\mathrm{T}}^{\mathrm{miss}}/\sqrt{H_{\mathrm{T}}}$ smaller than those chosen for the signal regions. The consistency of the prediction with the number of observed events (*closure*) is tested in regions with $E_{\mathrm{T}}^{\mathrm{miss}}/\sqrt{H_{\mathrm{T}}}$ [ GeV$^{1/2}$] in the ranges (1.5, 2.0), (2.0, 2.5), and (2.5, 3.5) for jet multiplicities of exactly seven, eight and nine, and in the range (1.5, 2.0) and (2.0, 3.5) for ≥10 jets. The tests are performed separately for 0, 1 and ≥ 2 $b$-tagged jets. In addition, the method is tested for events with exactly six (five) jets with $p_{\mathrm{T}}^{\mathrm{min}} = 50$ GeV (80 GeV) across the full range of $E_{\mathrm{T}}^{\mathrm{miss}}/\sqrt{H_{\mathrm{T}}}$ in this case using a template obtained from events with exactly five (four) jets. The five-jet (four-jet) events are obtained using a prescaled trigger for which only a fraction of the total luminosity is available. Agreement is found both for signal region jet multiplicities at intermediate values of $E_{\mathrm{T}}^{\mathrm{miss}}/\sqrt{H_{\mathrm{T}}}$ and also for the signal region $E_{\mathrm{T}}^{\mathrm{miss}}/\sqrt{H_{\mathrm{T}}}$ selection at lower



JHEP10(2013)130

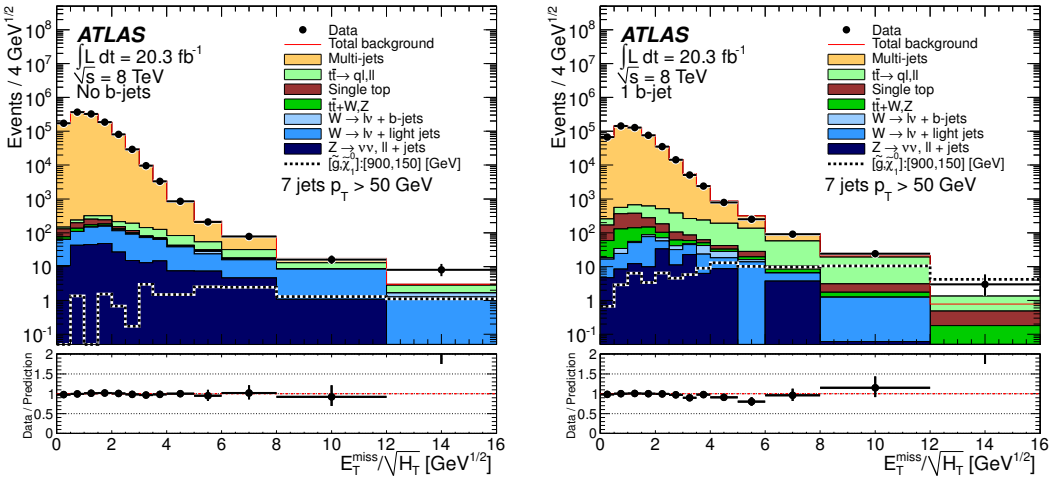


(a) No $b$-jets




(b) Exactly one $b$-jet

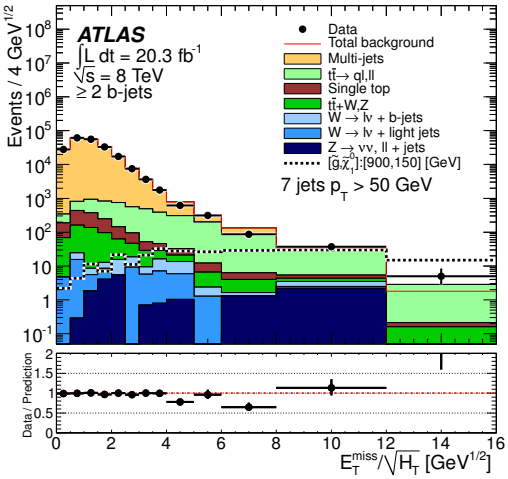


(c) At least two $b$-jets

**Figure 1**. Distribution of $E_{\mathrm{T}}^{\mathrm{miss}}/\sqrt{H_{\mathrm{T}}}$ for the control regions with exactly seven jets with $p_{\mathrm{T}} \geq 50$ GeV and $|\eta| < 2.0$, for different $b$-jet multiplicities. The multi-jet prediction is determined from an $E_{\mathrm{T}}^{\mathrm{miss}}/\sqrt{H_{\mathrm{T}}}$ template obtained from events with exactly six jets. It is normalised to the data in the region $E_{\mathrm{T}}^{\mathrm{miss}}/\sqrt{H_{\mathrm{T}}} < 1.5$ GeV$^{1/2}$ after subtraction of the leptonic backgrounds. The most important leptonic backgrounds are also shown, based on Monte Carlo simulations. Variable bin sizes are used with bin widths (in units of GeV$^{1/2}$) of 0.5 (up to $E_{\mathrm{T}}^{\mathrm{miss}}/\sqrt{H_{\mathrm{T}}} = 4$ GeV$^{1/2}$), 1 (from 4 to 6), 2 (from 6 to 8) and 4 thereafter. For reference and comparison, a supersymmetric model is used where gluinos of mass 900 GeV are pair produced and each decay as in eq. (1.2) to a $t\bar{t}$ pair and a $\tilde{\chi}_1^0$ with a mass of 150 GeV. The model is referred to as '$[\tilde{g}, \tilde{\chi}_1^0] : [900, 150]$ [GeV]'.

JHEP10(2013)130

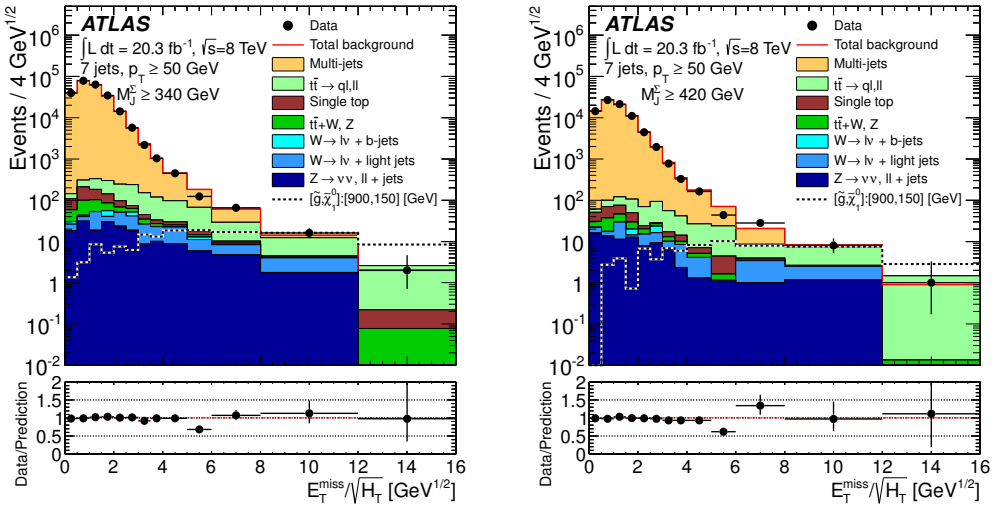


(a) $M_J^{\Sigma} \geq 340$ GeV (b) $M_J^{\Sigma} \geq 420$ GeV

**Figure 2**. Distribution of $E_{\mathrm{T}}^{\mathrm{miss}}/\sqrt{H_{\mathrm{T}}}$ for control regions with exactly seven jets with $p_{\mathrm{T}} \geq 50$ GeV, and satisfying the same requirements as the multi-jet + $M_J^{\Sigma}$ stream signal regions, other than that on $E_{\mathrm{T}}^{\mathrm{miss}}/\sqrt{H_{\mathrm{T}}}$ itself. The multi-jet prediction was determined from an $E_{\mathrm{T}}^{\mathrm{miss}}/\sqrt{H_{\mathrm{T}}}$ template obtained from events with exactly six jets. Other details are as for figure 1.

multiplicity. A symmetrical systematic uncertainty on each signal region is constructed by taking the largest deviation in any of the closure regions with the same jet multiplicity or lower, for the same $b$-tagging requirements. Typical closure uncertainties are in the range 5% to 15%; they can grow as large as ∼50% for the tightest signal regions, due to larger statistical variations in the corresponding control regions.

Additional systematic uncertainties result from modelling of the heavy-flavour content (25%), which is assessed by using combinations of the templates of different $b$-tagged jet multiplicity to vary the purity of the different samples. The closure in simulation of samples with high heavy-flavour content is also tested. The leptonic backgrounds that are subtracted when forming the template have an uncertainty associated with them (5–20%, depending on the signal region). Furthermore, other uncertainties taken into account are due to the scale choice of the cutoff for the soft energy term, $\sum \mathrm{E}_{\mathrm{T}}^{\mathrm{CellOut}}$, (3–15%) and the trigger efficiency (<1%) in the region where the template is formed.

### 5.4 Leptonic backgrounds

The leptonic backgrounds are defined to be those which involve the leptonic decays $W \to \ell\nu$ or $Z \to \nu\nu$. Contributions are determined for partly hadronic (i.e. semileptonic or dileptonic) $t\bar{t}$, single top, $W$ and $Z$ production, and diboson production, each in association with jets. The category excludes semileptonic decays of charm and bottom quarks, which are considered within the multi-jet category (section 5.2). The leptonic backgrounds which contribute most to the signal regions are $t\bar{t}$ and $W$ + jets. In each case, events can evade the lepton veto, either via hadronic $\tau$ decays or when electrons or muons are produced but not reconstructed.



JHEP10(2013)130

| **Single-lepton validation region** | |
|---|---|
| Lepton $p_{\mathrm{T}}$ | $> 25\,\mathrm{GeV}$ |
| Lepton multiplicity | Exactly one, $\ell \in \{e, \mu\}$ |
| $E_{\mathrm{T}}^{\mathrm{miss}}$ | $> 30\,\mathrm{GeV}$ |
| $E_{\mathrm{T}}^{\mathrm{miss}}/\sqrt{H_{\mathrm{T}}}$ | $> 2.0\ \mathrm{GeV}^{1/2}$ |
| $m_{\mathrm{T}}$ | $< 120\,\mathrm{GeV}$ |
| Jet $p_{\mathrm{T}}$ | As for signal regions (table 1) |
| Jet multiplicity | |
| $b$-jet multiplicity | |
| $M_J^{\Sigma}$ | |
| **Control region (additional criteria)** | |
| Jet multiplicity | Unit increment if $p_{\mathrm{T}}^{\ell} > p_{\mathrm{T}}^{\mathrm{min}}$ |
| $E_{\mathrm{T}}^{\mathrm{miss}}/\sqrt{H_{\mathrm{T}}\ (+p_{\mathrm{T}}^{\ell})}$ | $> 4.0\ \mathrm{GeV}^{1/2}$ |

**Table 2**. The selection criteria for the validation and control regions for the $t\bar{t}$ and $W+\mathrm{jets}$ backgrounds. In the control region the lepton is recast as a jet so it contributes to $H_{\mathrm{T}}$ if $p_{\mathrm{T}}^{\ell} > 40\,\mathrm{GeV}$ and to the jet multiplicity count if $p_{\mathrm{T}}^{\ell} > p_{\mathrm{T}}^{\mathrm{min}}$.

The predictions employ the Monte Carlo simulations described in section 5.1. When predictions are taken directly from the Monte Carlo simulations, the leptonic background event yields are subject to large theoretical uncertainties associated with the use of a leading-order Monte Carlo simulation generator. These include scale variations as well as changes in the number of partons present in the matrix element calculation, and uncertainties in the response of the detector. To reduce these uncertainties the background predictions are, where possible, normalised to data using control regions and cross-checked against data in other validation regions. These control regions and validation regions are designed to be distinct from, but kinematically close to, the signal regions, and orthogonal to them by requiring an identified lepton candidate.

The validation and control regions for the $t\bar{t}$ and $W+\mathrm{jets}$ backgrounds are defined in table 2. In single-lepton regions, a single lepton ($e$ or $\mu$) is required, with sufficient $p_{\mathrm{T}}$ to allow the leptonic trigger to be employed. Modest requirements on $E_{\mathrm{T}}^{\mathrm{miss}}$ and $E_{\mathrm{T}}^{\mathrm{miss}}/\sqrt{H_{\mathrm{T}}}$ reduce the background from fake leptons. An upper limit on

$$m_{\mathrm{T}} = \sqrt{2\left(|\mathbf{p}_{\mathrm{T}}^{\mathrm{miss}}||\mathbf{p}_{\mathrm{T}}^{\ell}| - \mathbf{p}_{\mathrm{T}}^{\mathrm{miss}} \cdot \mathbf{p}_{\mathrm{T}}^{\ell}\right)},$$

where $\mathbf{p}_{\mathrm{T}}^{\ell}$ is the transverse momentum vector of the lepton, decreases possible contamination from non-Standard-Model processes.

Since it is dominantly through hadronic $\tau$ decays that $W$ bosons and $t\bar{t}$ pairs contribute to the signal regions, the corresponding control regions are created by recasting the muon or electron as a jet. If the electron or muon has sufficient $p_{\mathrm{T}}$ (without any additional calibration), it is considered as an additional 'jet' and it can contribute to the jet multiplicity count, as well as to $H_{\mathrm{T}}$ and hence to the selection variable $E_{\mathrm{T}}^{\mathrm{miss}}/\sqrt{H_{\mathrm{T}}}$. The same jet



JHEP10(2013)130

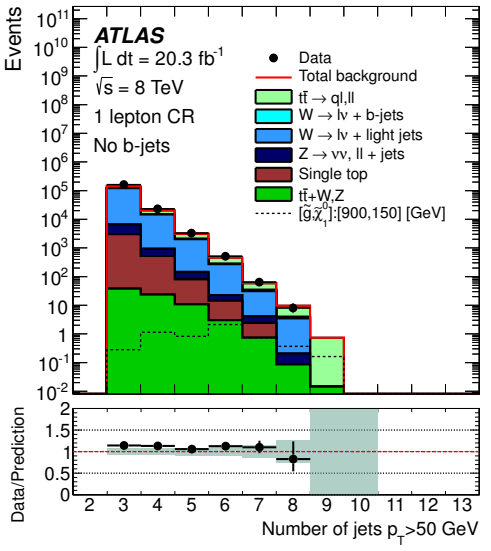


(a) No $b$-jets

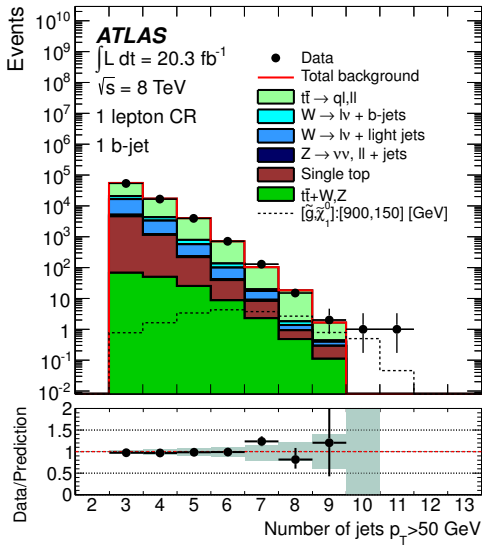


(b) Exactly one $b$-jet

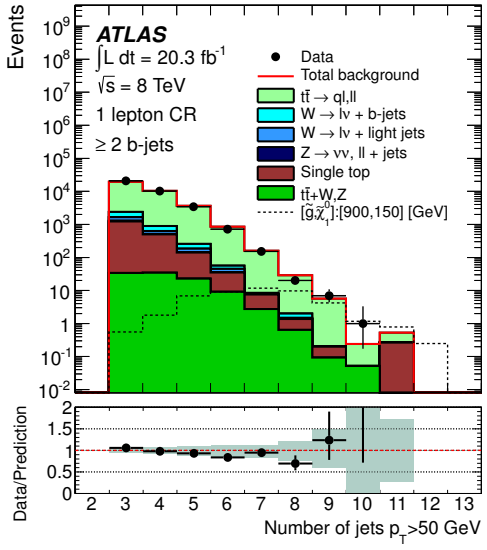


(c) $\geq$2 $b$-jets

**Figure 3**. Jet multiplicity distributions for $p_{\mathrm{T}}^{\mathrm{min}} = 50$ GeV jets in the one-lepton $t\bar{t}$ and $W$ + jets control regions (CR) for different $b$-jet multiplicities. Monte Carlo simulation predictions are before fitting to data. Other details are as for figure 1. The band in the ratio plot indicates the experimental uncertainties on the Monte Carlo simulation prediction and also includes the Monte Carlo simulation statistical uncertainty. Additional theoretical uncertainties are not shown.

JHEP10(2013)130

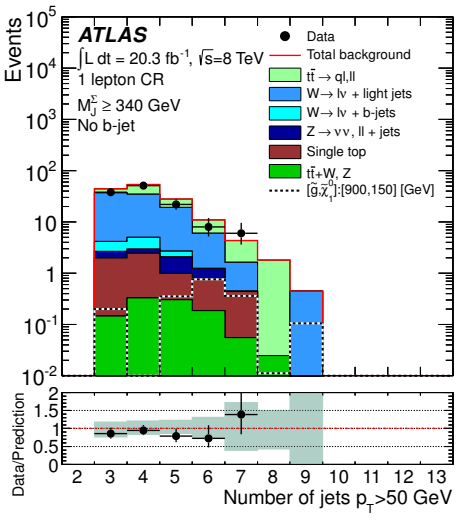


(a) $M_J^{\Sigma}$>340 GeV, no $b$-jets

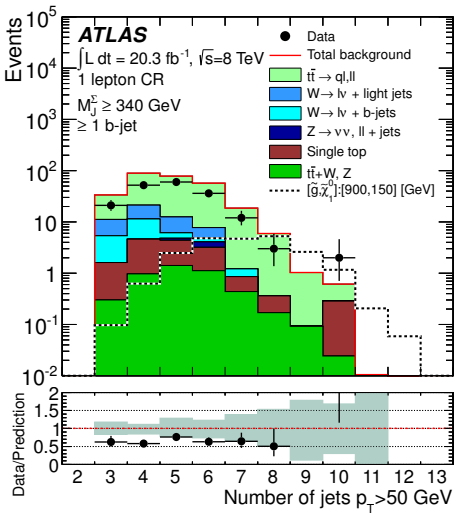


(b) $M_J^{\Sigma}$>340 GeV, $\geq$1 $b$-jets

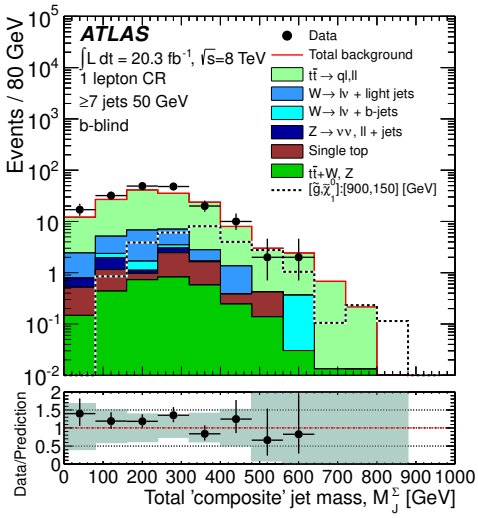


(c) $M_J^{\Sigma}$ distribution, $\geq$7j50 selection applied

**Figure 4**. Jet multiplicity distributions for $p_{\mathrm{T}}^{\mathrm{min}} = 50$ GeV jets in the one-lepton $t\bar{t}$ and $W$ + jets control regions (CR) for different $b$-jet multiplicities and a selection on $M_J^{\Sigma} > 340$ GeV (4(a))–(4(b)), and the $M_J^{\Sigma}$ distribution for an inclusive selection of seven jets with $p_{\mathrm{T}}^{\mathrm{min}} = 50$ GeV (4(c)). Other details are as for figure 3.

JHEP10(2013)130

| **Two-lepton validation region** | |
|---|---|
| Lepton $p_{\mathrm{T}}$ | $> 25\,\mathrm{GeV}$ |
| Lepton multiplicity | Exactly two, $e\,e$ or $\mu\,\mu$ |
| $m_{\ell\ell}$ | 80 GeV to 100 GeV |
| Jet $p_{\mathrm{T}}$ | As for signal regions (table 1) |
| Jet multiplicity | |
| $b$-jet multiplicity | |
| $M_J^{\Sigma}$ | |
| **Control region (additional criteria)** | |
| $\lvert\mathbf{p}_{\mathrm{T}}^{\mathrm{miss}} + \mathbf{p}_{\mathrm{T}}^{\ell_1} + \mathbf{p}_{\mathrm{T}}^{\ell_2}\rvert/\sqrt{H_{\mathrm{T}}}$ | $> 4.0\ \mathrm{GeV}^{1/2}$ |

**Table 3**. The selection criteria for the validation and control regions for the $Z$ + jets background.

multiplicity as the signal region is required for the equivalent control regions. Additionally, the same criteria for $E_{\mathrm{T}}^{\mathrm{miss}}/\sqrt{H_{\mathrm{T}}}$, $M_J^{\Sigma}$ and the number of $b$-tagged jets are required. For the $M_J^{\Sigma}$ stream these control regions are further split into regions with no $b$-tagged jets and those with $b$-tagged jets to allow separation of contributions from $W$+jets and $t\bar{t}$ events. Provided the expected number of Standard Model events in the corresponding control region is greater than two, the number of observed events in that control region is used in a fit to determine the Standard Model background as described in section 6. Distributions of jet multiplicity for the leptonic control regions can be found in figures 3–4. In figure 4 the $M_J^{\Sigma}$ distribution for a leptonic control region is also shown.

The $Z$+jets control regions require two same-flavour leptons with an invariant mass consistent with that of the $Z$ boson. To create control regions that emulate the signal regions, the lepton transverse momenta are added to the missing momentum two-vector and then the requirement $E_{\mathrm{T}}^{\mathrm{miss}}/\sqrt{H_{\mathrm{T}}} > 4\ \mathrm{GeV}^{1/2}$ is applied. This emulates the situation expected for the $Z \to \nu\nu$ background. The details of the selection criteria are given in table 3. This selection, but with relaxed jet multiplicity criteria, is used to validate the Monte Carlo simulation description of this process; however, insufficient events remain at high jet multiplicity, so the estimation of this background is taken from Monte Carlo simulations.

### 5.5 Systematic uncertainties in the leptonic background determination

Systematic uncertainties on the leptonic backgrounds originate from both detector-related and theoretical sources from the Monte Carlo simulation modelling. Experimental uncertainties are dominated by those on the jet energy scale, jet energy resolution and, in the case of the flavour stream, $b$-tagging efficiency. Other less important uncertainties result from the modelling of the pile-up, the lepton identification and the soft energy term in the $E_{\mathrm{T}}^{\mathrm{miss}}$ calculation; these make negligible contributions to the total systematic uncertainty.

The ATLAS jet energy scale and resolution are determined using in-situ techniques [28, 59]. The jet energy scale uncertainty includes uncertainties associated with the quark-gluon composition of the sample, the heavy-flavour fraction and pile-up uncer-



JHEP10(2013)130

tainties. The uncertainties are derived for $R = 0.4$ jets and propagated to all objects and selections used in the analysis. The sources of the jet energy scale uncertainty are treated as correlated between the various Standard Model backgrounds as well as with the signal contributions when setting exclusion limits. The uncertainties on the yields due to those on the jet energy scale and resolution range typically between 20% and 30%. The $b$-tagging efficiency uncertainties are treated in a similar way when setting limits and have typical values of $\approx 10\%$. They are derived from data samples tagged with muons associated with jets, using techniques described in refs. [31, 32].

For the $t\bar{t}$ background, theoretical uncertainties are evaluated by comparing the particle-level predictions of the nominal Sherpa samples with additional samples in which some of the parameter settings were varied. These include variations of the factorisation scale, the matching scale of the matrix element to the parton shower, the number of partons in the matrix element and the PDFs. Alpgen [60] samples are also generated with the renormalisation scale associated with $\alpha_S$ in the matrix element calculation varied up and down by a factor of two relative to the original scale $k_t$ between two partons [61]. Finally, samples with and without weighting of events initiated by gluon fusion relative to other processes are used to provide a systematic uncertainty on this procedure. The two latter sources of systematic uncertainty are the dominant ones with typical values of 25–30% each, leading to a total theoretical uncertainty on the $t\bar{t}$ background of $\approx 40\%$.

Alternative samples are generated similarly for the other smaller backgrounds with different parameters and/or generators to assess the associated theoretical uncertainties, which are found to be similar to those for the $t\bar{t}$ background.

## 6 Results

Figures 5–8 show the $E_{\mathrm{T}}^{\mathrm{miss}}/\sqrt{H_{\mathrm{T}}}$ distributions for all the signal regions of both analysis streams. In order to check the consistency of the data with the background-only and signal hypotheses, a simultaneous profile maximum likelihood fit [62] is performed in the control and signal regions, for each of the analysis streams separately. Poisson likelihood functions are used for event counts in signal and control regions. Systematic uncertainties are treated as nuisance parameters. They are assumed to follow Gaussian distributions and their effect is propagated to the likelihood function. A control region is taken into account in the fit if there are at least two expected events associated with it. The fits differ significantly between the two analysis streams, as described in the following sections.

When evaluating a supersymmetric signal model for exclusion, any signal contamination in the control regions is taken into account for each signal point in the control-region fits performed for each signal hypothesis. Separately, each signal region (one at a time), along with all control regions, is also fitted under the background-only hypothesis. This fit is used to characterise the agreement in each signal region with the background-only hypothesis, and to extract visible cross-section limits and upper limits on the production of events from new physics. For these limits, possible signal contamination in the control regions is neglected.



JHEP10(2013)130

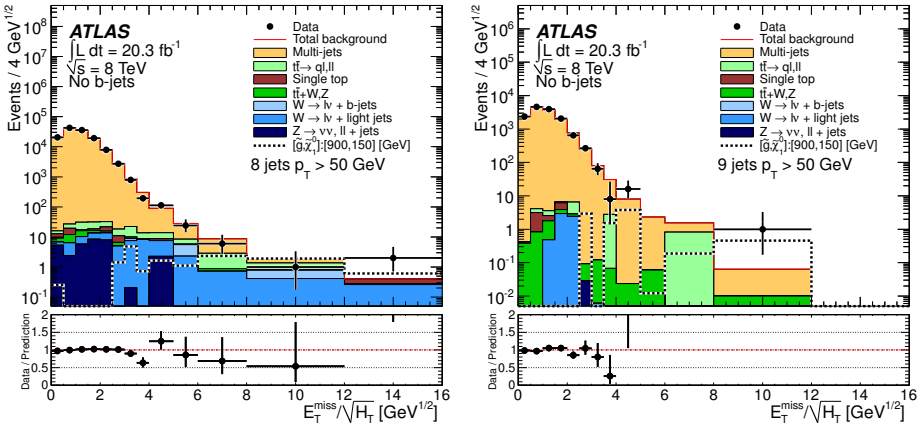


(a) 8j50, no $b$-jets

(b) 9j50, no $b$-jets

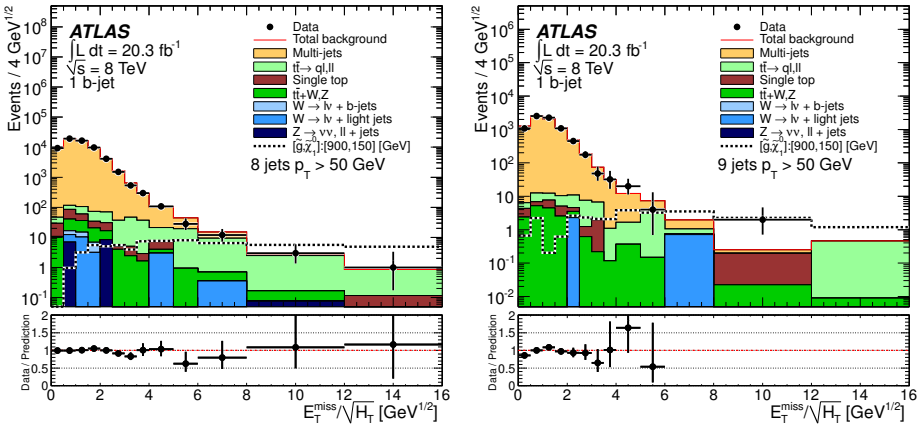


(c) 8j50, exactly one $b$-jet

(d) 9j50, exactly one $b$-jet

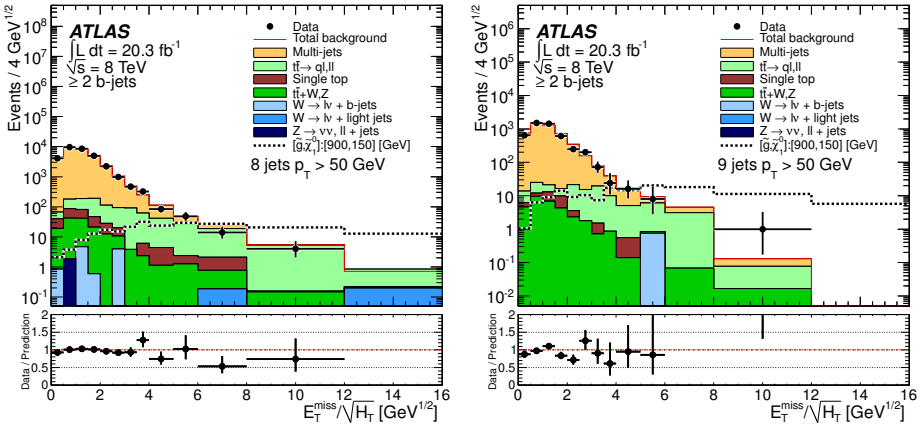


(e) 8j50, $\geq 2$ $b$-jets

(f) 9j50, $\geq 2$ $b$-jets

**Figure 5**. $E_{\mathrm{T}}^{\mathrm{miss}}/\sqrt{H_{\mathrm{T}}}$ distributions for the multi-jet + flavour stream with $p_{\mathrm{T}}^{\mathrm{min}} = 50\,\mathrm{GeV}$, and either exactly eight jets (left) or exactly nine jets (right) with the signal region selection, other than that on $E_{\mathrm{T}}^{\mathrm{miss}}/\sqrt{H_{\mathrm{T}}}$ itself. The $b$-jet multiplicity increases from no $b$-jets (top) to exactly one $b$-jet (middle) to at least two $b$-jets (bottom). Other details are as for figure 1.



JHEP10(2013)130

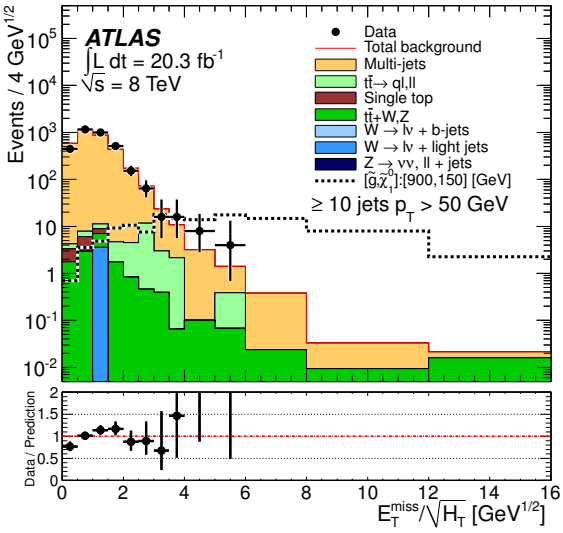


**Figure 6**. $E_{\mathrm{T}}^{\mathrm{miss}}/\sqrt{H_{\mathrm{T}}}$ distribution for the multi-jet + flavour stream with $p_{\mathrm{T}}^{\mathrm{min}} = 50\,\mathrm{GeV}$, and at least ten jets. The complete $\geq$ 10j50 selection has been applied, other than the final $E_{\mathrm{T}}^{\mathrm{miss}}/\sqrt{H_{\mathrm{T}}}$ requirement. Other details are as for figure 1.

### 6.1 Simultaneous fit in the multi-jet + flavour stream

The seven $p_{\mathrm{T}}^{\mathrm{min}} = 50$ GeV signal regions (and similarly the six $p_{\mathrm{T}}^{\mathrm{min}} = 80$ GeV signal regions) are fitted to the background and signal predictions. Correlations from sample to sample and region to region are taken into account, separately for the $p_{\mathrm{T}}^{\mathrm{min}} = 50$ GeV and $p_{\mathrm{T}}^{\mathrm{min}} = 80$ GeV signal regions. Systematic uncertainties arising from the same source are treated as fully correlated.

The fit considers several independent background components:

- $t\bar{t}$ and $W$ + jets. One control region is defined for each signal region, as described in table 2; the normalisation of each background component is allowed to vary freely in the fit.

- Less significant backgrounds ($Z$ + jets, $t\bar{t} + W$, $t\bar{t} + Z$, and single top) are determined using Monte Carlo simulations. These are individually allowed to vary within their uncertainties.

- Multi-jet background. Being data-driven, it is not constrained in the fit by any control region. It is constrained in the signal regions by its uncertainties, which are described in section 5.3.

The systematic effects, described in sections 5.3 and 5.5, are treated as nuisance parameters in the fit. For the signal, the dominant systematic effects are included in the fit; these are the jet energy scale and resolution uncertainties, the $b$-tagging efficiency uncertainties, and the theoretical uncertainties.



JHEP10(2013)130

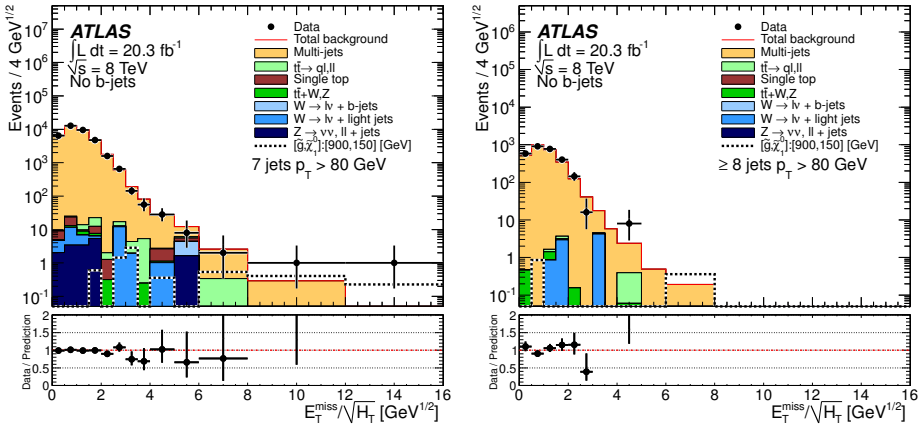


(a) 7j80, no $b$-jets




(b) 8j80, no $b$-jets

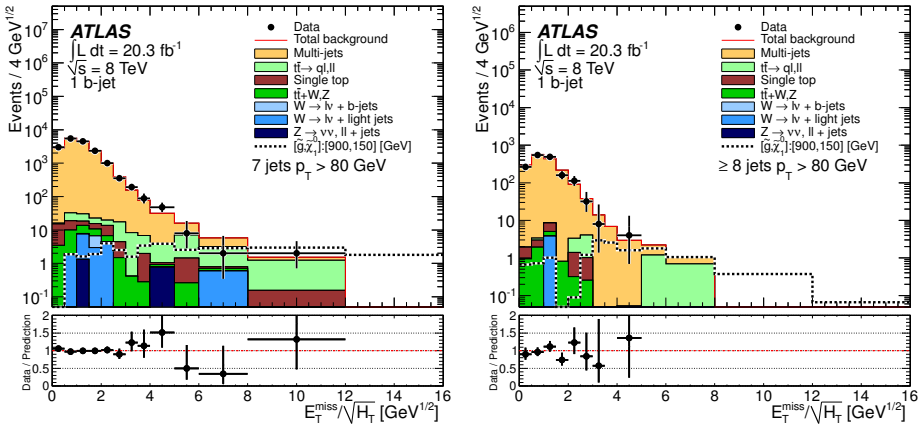


(c) 7j80, exactly one $b$-jet




(d) 8j80, exactly one $b$-jet

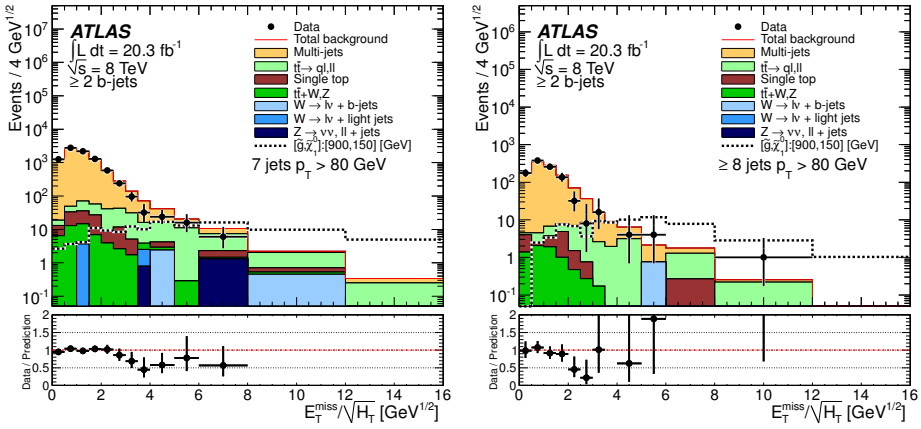


(e) 7j80, $\geq 2$ $b$-jets




(f) 8j80, $\geq 2$ $b$-jets

**Figure 7**. $E_{\mathrm{T}}^{\mathrm{miss}}/\sqrt{H_{\mathrm{T}}}$ distributions for the multi-jet + flavour stream with $p_{\mathrm{T}}^{\mathrm{min}} = 80\,\mathrm{GeV}$. The complete signal region selections were applied, other than the final $E_{\mathrm{T}}^{\mathrm{miss}}/\sqrt{H_{\mathrm{T}}}$ requirement. Other details are as for figure 1.

JHEP10(2013)130

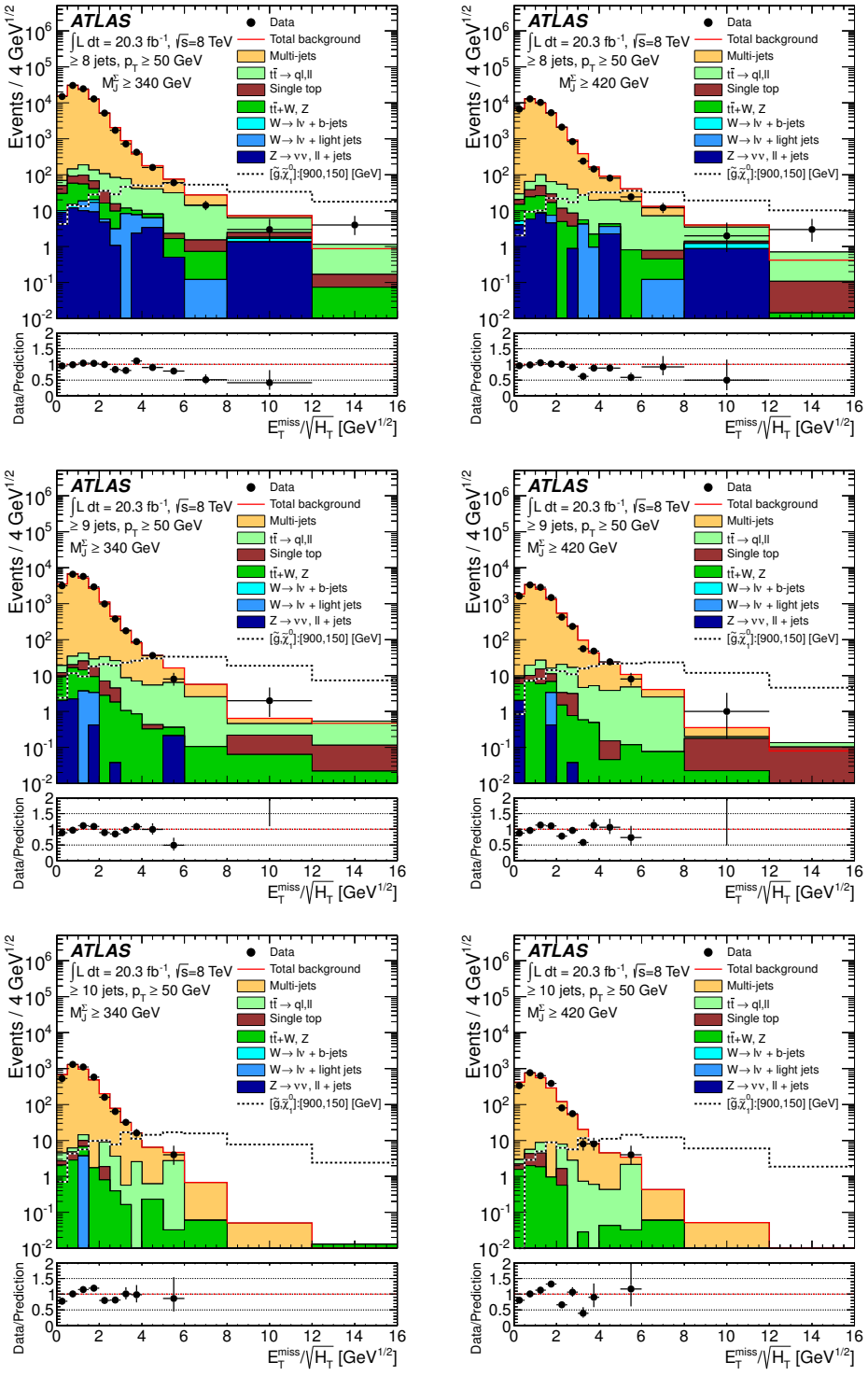


**Figure 8**. $E_{\mathrm{T}}^{\mathrm{miss}}/\sqrt{H_{\mathrm{T}}}$ distributions for the multi-jet + $M_J^{\Sigma}$ stream with the signal region selection, other than the final $E_{\mathrm{T}}^{\mathrm{miss}}/\sqrt{H_{\mathrm{T}}}$ requirement. The figures on the left are for events with $M_J^{\Sigma} > 340\,\mathrm{GeV}$, while those on the right are for $M_J^{\Sigma} > 420\,\mathrm{GeV}$. The minimum multiplicity requirement for $p_{\mathrm{T}}^{\mathrm{min}} = 50$ GeV, $R = 0.4$ jets increases from eight (top) to nine (middle) and finally to ten jets (bottom). Other details are as for figure 1.



JHEP10(2013)130

### 6.2 Simultaneous fit in the multi-jet + $M_J^\Sigma$ stream

For the multi-jet + $M_J^\Sigma$ signal regions, a separate fit is performed on each signal region to adjust the normalisation of the $t\bar{t}$ and $W$ + jets backgrounds using control regions, as defined in table 2.

The systematic uncertainties affecting the background, described in sections 5.3 and 5.5, and signal predictions are treated as nuisance parameters in the fit. The dominant sources of uncertainty are considered for the signal predictions: the jet energy scale, the jet energy resolution, and the theoretical uncertainties.

### 6.3 Fit results

Tables 4–7 summarise the fit results; the number of events observed in each of the signal regions, as well as their Standard Model background expectations, are reported before and after the fit to the control regions. In each of the signal regions, agreement is found between the Standard Model prediction and the data. The fit results are checked for stability and consistency with the background modelling based on the predictions described in sections 5.2 and 5.4. There is no indication of a systematic mis-modelling of any of the major backgrounds; the fitted values are in all cases consistent with the Monte Carlo simulation predictions.

In addition to the event yields, the probability ($p_0$-value) that a background-only pseudo-experiment is more signal-like than the observed data is given for each individual signal region. To obtain these $p_0$-values, the fit in the signal region proceeds in the same way as the control-region-only fit, except that the number of events observed in the signal region is included as an input to the fit. Then, an additional parameter for the non-Standard-Model signal strength, constrained to be non-negative, is fitted. The significance ($\sigma$) of the agreement between data and the Standard Model prediction is given. No significant deviations from the Standard Model prediction are found. The 95% confidence level (CL) upper limit on the number of events ($N_{\mathrm{BSM}}^{95\%}$) and the cross section times acceptance times efficiency ($\sigma_{\mathrm{BSM,max}}^{95\%} \cdot A \cdot \epsilon$) from non-Standard-Model production are also provided, neglecting in the fit possible signal contamination in the control regions.

## 7 Interpretation

In the absence of significant discrepancies, exclusion limits at 95% CL are set in the context of several simplified supersymmetric models and an mSUGRA/CMSSM model, all described in section 1. Theoretical uncertainties on the SUSY signals are estimated as described in section 5.1. Combined experimental systematic uncertainties on the signal yield from the jet energy scale, resolution, and $b$-tagging efficiency in the case of the flavour stream, range from 15% to 25%. Acceptance and efficiency values, uncertainties and other information per signal region are tabulated in HepData [63].

The limit for each signal region is obtained by comparing the observed event count with that expected from Standard Model background plus SUSY signal processes. All uncertainties on the Standard Model expectation are used, including those which are correlated between signal and background (for instance jet energy scale uncertainties) and all



JHEP10(2013)130

| Signal region | **8j50** | | | **9j50** | | | **10j50** |
|---|---|---|---|---|---|---|---|
| $b$-jets | 0 | 1 | $\geq 2$ | 0 | 1 | $\geq 2$ | — |
| Observed events | 40 | 44 | 44 | 5 | 8 | 7 | 3 |
| Total events after fit | $35 \pm 4$ | $40 \pm 10$ | $50 \pm 10$ | $3.3 \pm 0.7$ | $6.1 \pm 1.7$ | $8.0 \pm 2.7$ | $1.37 \pm 0.35$ |
| Fitted $t\bar{t}$ | $2.7 \pm 0.9$ | $11.8 \pm 3.0$ | $23.0 \pm 5.0$ | $0.36 \pm 0.18$ | $1.5 \pm 0.5$ | $3.2 \pm 1.1$ | $0.06^{+0.09}_{-0.06}$ |
| Fitted $W$+jets | $2.0^{+2.6}_{-2.0}$ | $0.62^{+0.81}_{-0.62}$ | $0.20^{+0.28}_{-0.20}$ | – | $0.24^{+0.65}_{-0.24}$ | – | – |
| Fitted others | $2.9^{+1.8}_{-1.8}$ | $1.7^{+1.5}_{-1.2}$ | $2.8^{+2.3}_{-2.0}$ | $0.03 \pm 0.03$ | $0.38 \pm 0.25$ | $0.40^{+0.60}_{-0.24}$ | $0.08 \pm 0.08$ |
| Total events before fit | 36 | 48 | 59 | 3.4 | 6.6 | 8.9 | 1.39 |
| $t\bar{t}$ before fit | 3.5 | 15 | 30 | 0.41 | 1.8 | 4 | 0.08 |
| $W$+jets before fit | 2.9 | 1.0 | 0.29 | – | 0.40 | – | – |
| Others before fit | 2.4 | 1.8 | 2.8 | 0.03 | 0.34 | 0.4 | 0.08 |
| Multi-jets | $27 \pm 3$ | $30 \pm 10$ | $26 \pm 10$ | $3.0 \pm 0.6$ | $4.0 \pm 1.4$ | $4.4 \pm 2.2$ | $1.23 \pm 0.32$ |
| $N^{95\%}_{\mathrm{BSM}}$ (exp) | 16 | 23 | 26 | 5 | 7 | 8 | 4 |
| $N^{95\%}_{\mathrm{BSM}}$ (obs) | 20 | 23 | 22 | 7 | 9 | 7 | 6 |
| $\sigma^{95\%}_{\mathrm{BSM,max}} \cdot A \cdot \epsilon$ (exp) [fb] | 0.8 | 1.2 | 1.3 | 0.26 | 0.36 | 0.40 | 0.19 |
| $\sigma^{95\%}_{\mathrm{BSM,max}} \cdot A \cdot \epsilon$ (obs) [fb] | 0.97 | 1.1 | 1.1 | 0.34 | 0.43 | 0.37 | 0.29 |
| $p_0$ | 0.24 | 0.5 | 0.7 | 0.21 | 0.28 | 0.6 | 0.13 |
| Significance ($\sigma$) | 0.7 | −0.02 | −0.6 | 0.8 | 0.6 | −0.28 | 1.14 |

**Table 4**. Number of observed and expected (fitted) events for the seven $p_{\mathrm{T}}^{\mathrm{min}} = 50$ GeV signal regions of the multi-jet + flavour stream. The category indicated by 'others' includes the contributions from $Z+$jets, $t\bar{t}+W$, $t\bar{t}+Z$, and single top. The table also contains for each signal region the probability, $p_0$, that a background-only pseudo-experiment is more signal-like than the observed data; the significance, $\sigma$, of the agreement between data and the Standard Model prediction; the 95% CL upper limit on the number of events, $N^{95\%}_{\mathrm{BSM}}$, originating from sources other than the Standard Model; and the corresponding cross section times acceptance times efficiency, $\sigma^{95\%}_{\mathrm{BSM,max}} \cdot A \cdot \epsilon$.



JHEP10(2013)130

| Signal region | **7j80** | | | **8j80** | | |
|---|---|---|---|---|---|---|
| $b$-jets | 0 | 1 | $\geq 2$ | 0 | 1 | $\geq 2$ |
| Observed events | 12 | 17 | 13 | 2 | 1 | 3 |
| Total fitted events | $11.0 \pm 2.2$ | $17 \pm 6$ | $25 \pm 10$ | $0.9 \pm 0.6$ | $1.5 \pm 0.9$ | $3.3 \pm 2.2$ |
| Fitted $t\bar{t}$ | $0.00^{+0.26}_{-0.00}$ | $5.0 \pm 4.0$ | $12 \pm 9$ | $0.10^{+0.14}_{-0.10}$ | $0.32^{+0.67}_{-0.32}$ | $1.5^{+1.9}_{-1.5}$ |
| Fitted $W$+jets | $0.07^{+0.38}_{-0.07}$ | $0.29^{+0.37}_{-0.29}$ | – | – | – | – |
| Fitted others | $1.9^{+1.1}_{-0.9}$ | $0.71^{+0.31}_{-0.25}$ | $2.6^{+1.7}_{-1.1}$ | $0.02 \pm 0.02$ | $0.02 \pm 0.02$ | $0.32^{+0.36}_{-0.21}$ |
| Total events before fit | 11.7 | 16 | 23 | 0.8 | 1.8 | 3.3 |
| $t\bar{t}$ before fit | 0.34 | 4 | 10 | 0.08 | 0.6 | 1.5 |
| $W$+jets before fit | 0.46 | 0.29 | – | – | – | – |
| Others before fit | 1.8 | 0.89 | 3.0 | 0.02 | 0.02 | 0.35 |
| Multi-jets | $9.1 \pm 1.6$ | $11 \pm 4$ | $10 \pm 4$ | $0.75 \pm 0.56$ | $1.2 \pm 0.5$ | $1.4 \pm 1.0$ |
| $N^{95}_{\mathrm{BSM}}$ (exp) | 10 | 17 | 14 | 4 | 4 | 6 |
| $N^{95}_{\mathrm{BSM}}$ (obs) | 10 | 16 | 12 | 5 | 3.5 | 6 |
| $\sigma^{95\%}_{\mathrm{BSM,max}} \cdot A \cdot \epsilon$ (exp) [fb] | 0.5 | 0.8 | 0.7 | 0.18 | 0.18 | 0.31 |
| $\sigma^{95\%}_{\mathrm{BSM,max}} \cdot A \cdot \epsilon$ (obs) [fb] | 0.5 | 0.8 | 0.6 | 0.24 | 0.17 | 0.31 |
| $p_0$ | 0.5 | 0.6 | 0.8 | 0.19 | 0.6 | 0.5 |
| Significance ($\sigma$) | 0.05 | $-0.14$ | $-1.0$ | 0.9 | $-0.28$ | $-0.06$ |

**Table 5**. As for table 4 but for the six signal regions for which $p_{\mathrm{T}}^{\mathrm{min}} = 80$ GeV.

| Signal region | **8j50** | |
|---|---|---|
| $M_J^{\Sigma}$ [GeV] | 340 | 420 |
| Observed events | 69 | 37 |
| Total events after fit | $75 \pm 19$ | $45 \pm 14$ |
| Fitted $t\bar{t}$ | $17 \pm 11$ | $16 \pm 13$ |
| Fitted $W$+jets | $0.8^{+1.3}_{-0.8}$ | $0.4^{+0.7}_{-0.4}$ |
| Fitted others | $5.2^{+4.0}_{-2.5}$ | $2.8^{+2.9}_{-1.6}$ |
| Total events before fit | 85 | 44 |
| $t\bar{t}$ before fit | 27 | 14 |
| $W$+jets before fit | 0.8 | 0.4 |
| Others before fit | 5 | 2.8 |
| Multi-jets | $52 \pm 15$ | $27 \pm 7$ |
| $N^{95\%}_{\mathrm{BSM}}$ (exp) | 40 | 23 |
| $N^{95\%}_{\mathrm{BSM}}$ (obs) | 35 | 20 |
| $\sigma^{95\%}_{\mathrm{BSM,max}} \cdot A \cdot \epsilon$ (exp) [fb] | 1.9 | 1.1 |
| $\sigma^{95\%}_{\mathrm{BSM,max}} \cdot A \cdot \epsilon$ (obs) [fb] | 1.7 | 1.0 |
| $p_0$ | 0.60 | 0.7 |
| Significance ($\sigma$) | $-0.27$ | $-0.6$ |

**Table 6**. As for table 4 but for the signal regions in the multi-jet + $M_J^{\Sigma}$ stream for which the number of events in the control regions allowed background determination using a fit.



JHEP10(2013)130

| Signal region | **9j50** | | **10j50** | |
|---|---|---|---|---|
| $M_J^{\Sigma}$ [GeV] | 340 | 420 | 340 | 420 |
| Observed events | 13 | 9 | 1 | 1 |
| Total events | $17 \pm 7$ | $11 \pm 5$ | $3.2^{+3.7}_{-3.2}$ | $2.2 \pm 2.0$ |
| $t\bar{t}$ | $5 \pm 4$ | $3.4^{+3.6}_{-3.4}$ | $0.8^{+0.8}_{-0.8}$ | $0.6^{+0.9}_{-0.6}$ |
| $W$+jets | – | – | – | – |
| Others | $0.58^{+0.54}_{-0.33}$ | $0.39^{+0.32}_{-0.30}$ | $0.12 \pm 0.12$ | $0.06 \pm 0.06$ |
| Multi-jets | $12 \pm 4$ | $7.0 \pm 2.3$ | $2.3^{+3.6}_{-2.3}$ | $1.6^{+1.8}_{-1.6}$ |
| $N_{\mathrm{BSM}}^{95\%}$ (exp) | 13 | 11 | 5 | 5 |
| $N_{\mathrm{BSM}}^{95\%}$ (obs) | 11 | 10 | 4 | 4 |
| $\sigma_{\mathrm{BSM,max}}^{95\%} \cdot A \cdot \epsilon$ (exp) [fb] | 0.7 | 0.5 | 0.23 | 0.23 |
| $\sigma_{\mathrm{BSM,max}}^{95\%} \cdot A \cdot \epsilon$ (obs) [fb] | 0.5 | 0.5 | 0.2 | 0.2 |
| $p_0$ | 0.7 | 0.6 | 0.8 | 0.7 |
| Significance ($\sigma$) | $-0.6$ | $-0.34$ | $-0.8$ | $-0.6$ |

**Table 7**. As for table 4 but for the signal regions in the multi-jet + $M_J^{\Sigma}$ stream for which the number of events in the control regions did not allow background determination using a fit and therefore the leptonic background is extracted directly from Monte Carlo simulations.

but theoretical cross-section uncertainties (PDF and scale) on the signal expectation. The resulting exclusion regions are obtained using the $CL_s$ prescription [64]. For the multi-jet + flavour stream a simultaneous fit is performed in all the signal regions for each of the two values of $p_{\mathrm{T}}^{\mathrm{min}}$, and the two fit results are combined using the better expected limit per point in the parameter space, as described in section 6.1. For the multi-jet + $M_J^{\Sigma}$ stream the signal region with the best expected limit at each point in parameter space is used. The stream with the better expected limit at each point in parameter space is chosen when combining the two streams. The multi-jet + flavour stream typically has stronger expected exclusion limits than the multi-jet + $M_J^{\Sigma}$ stream. However, in models with large numbers of objects in the final state, and more so in boosted topologies, the multi-jet + $M_J^{\Sigma}$ stream becomes competitive. Limits on sparticle masses quoted in the text are those from the lower edge of the $1\sigma$ signal cross-section band rather than the central value of the observed limit.

As shown in the rest of this section, the analysis substantially extends previous published exclusion limits on various models, from ATLAS [11, 12] and CMS [13, 65].

**'Gluino-stop (off-shell)' model.** The analysis result is interpreted in a simplified model that contains only a gluino octet and a neutralino $\tilde{\chi}_1^0$ within kinematic reach, and decaying with unit probability according to eq. 1.2, via an off-shell $\tilde{t}$-squark. The results are presented in the $(m_{\tilde{g}}, m_{\tilde{\chi}_1^0})$ plane in figure 9, which shows the combined exclusion. Within the context of this simplified model, the 95% CL exclusion bound on the gluino mass is 1.1 TeV for the lightest neutralino mass up to 350 GeV.



JHEP10(2013)130

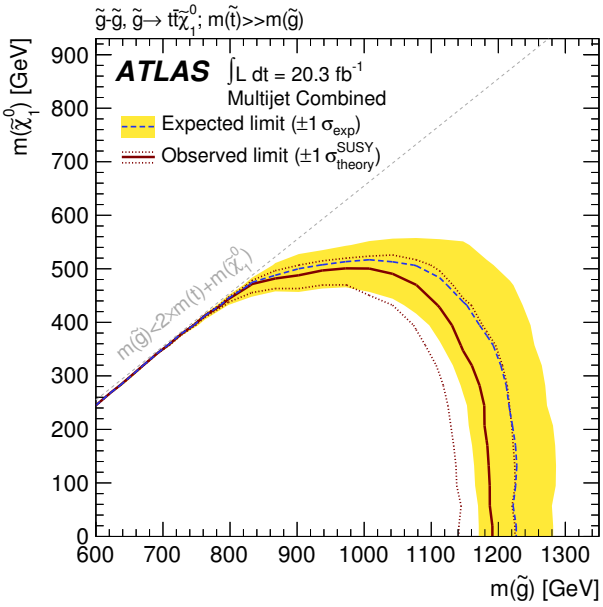


**Figure 9**. 95% CL exclusion curve for the simplified gluino-stop (off-shell) model. The dashed grey and solid red curves show the 95% CL expected and observed limits, respectively, including all uncertainties except the theoretical signal cross-section uncertainty (PDF and scale). The shaded yellow band around the expected limit shows the $\pm 1\sigma$ result. The $\pm 1\sigma$ lines around the observed limit represent the result produced when moving the signal cross section by $\pm 1\sigma$ (as defined by the PDF and scale uncertainties). The diagonal dashed line is the kinematic limit for this decay channel.

**'Gluino-stop (on-shell)' model.** In this simplified model, each gluino of a pair decays as $\tilde{g} \rightarrow \tilde{t}+\bar{t}$; $\tilde{t} \rightarrow \tilde{\chi}_1^0+t$. The mass of $\tilde{\chi}_1^0$ is fixed to 60 GeV. The results are presented in the $(m_{\tilde{g}}, m_{\tilde{t}})$ plane in figure 10 which shows the combined exclusion limits. Within the context of this simplified model, the 95% CL exclusion bound on the gluino mass is 1.15 TeV for stop masses up to 750 GeV.

**'Gluino-squark (via $\tilde{\chi}_1^{\pm}$)' model.** In this simplified model, each gluino of a pair decays promptly via an off-shell squark as $\tilde{g} \rightarrow \bar{q}+q'+\tilde{\chi}_1^{\pm} \rightarrow \bar{q}+q'+W^{\pm}+\tilde{\chi}_1^0$. Two versions of this model are evaluated, and the combined exclusion results are shown in figure 11. In figure 11a, the fractional mass splitting, x, defined as $\mathrm{x} = (\mathrm{m}_{\tilde{\chi}_1^{\pm}} - \mathrm{m}_{\tilde{\chi}_1^0})/(\mathrm{m}_{\tilde{\mathrm{g}}} - \mathrm{m}_{\tilde{\chi}_1^0})$, is set to 1/2, while the $\tilde{\chi}_1^0$ mass varies, and the results are shown in the $(m_{\tilde{g}}, m_{\tilde{\chi}_1^0})$ plane. In the second case, the $\tilde{\chi}_1^0$ mass is fixed to 60 GeV while x varies, and the results are presented in the $(m_{\tilde{g}}, \mathrm{x})$ plane. Gluino masses are excluded below 1 TeV at 95% CL, for $\tilde{\chi}_1^0$ masses below 200 GeV, in the case of $\mathrm{x} = 1/2$.

**'Gluino-squark (via $\tilde{\chi}_1^{\pm}$ and $\tilde{\chi}_2^0$)' model.** In this simplified model, each gluino of a pair decays promptly via an off-shell squark as $\tilde{g} \rightarrow \bar{q}+q'+\tilde{\chi}_1^{\pm} \rightarrow \bar{q}+q'+W^{\pm}+\tilde{\chi}_2^0 \rightarrow \bar{q}+q'+W^{\pm}+Z^0+\tilde{\chi}_1^0$. The intermediate particle masses, $m_{\tilde{\chi}_1^{\pm}}$ and $m_{\tilde{\chi}_2^0}$, are set to $(m_{\tilde{g}}+m_{\tilde{\chi}_1^0})/2$ and $(m_{\tilde{\chi}_1^{\pm}}+m_{\tilde{\chi}_1^0})/2$, respectively. The results are presented in the $(m_{\tilde{g}}, m_{\tilde{\chi}_1^0})$ plane in figure 12, which shows the combined exclusion limits for this model. Gluino masses are excluded below 1.1 TeV at 95% CL, for $\tilde{\chi}_1^0$ masses below 300 GeV.



JHEP10(2013)130

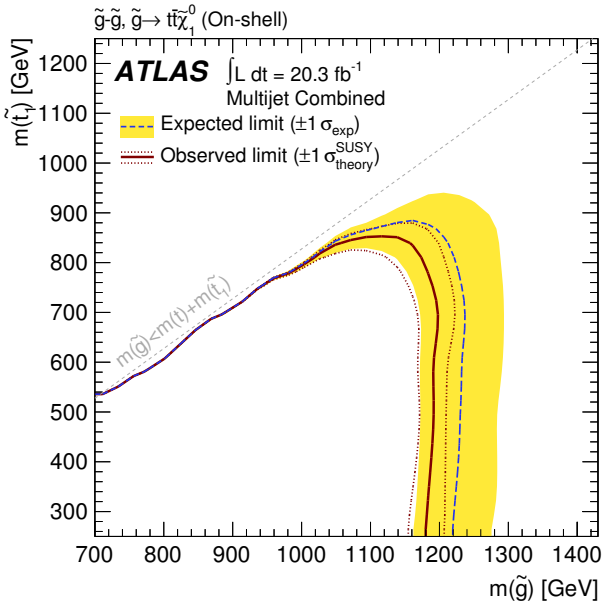


**Figure 10**. 95% CL exclusion curve for the simplified gluino-stop (on-shell) model, where the gluino decays as $\tilde{g} \rightarrow \tilde{t} + \bar{t}$ and the stop as $\tilde{t} \rightarrow \tilde{\chi}_1^0 + t$, with $m_{\tilde{\chi}_1^0} = 60$ GeV. Other details are as in figure 9.

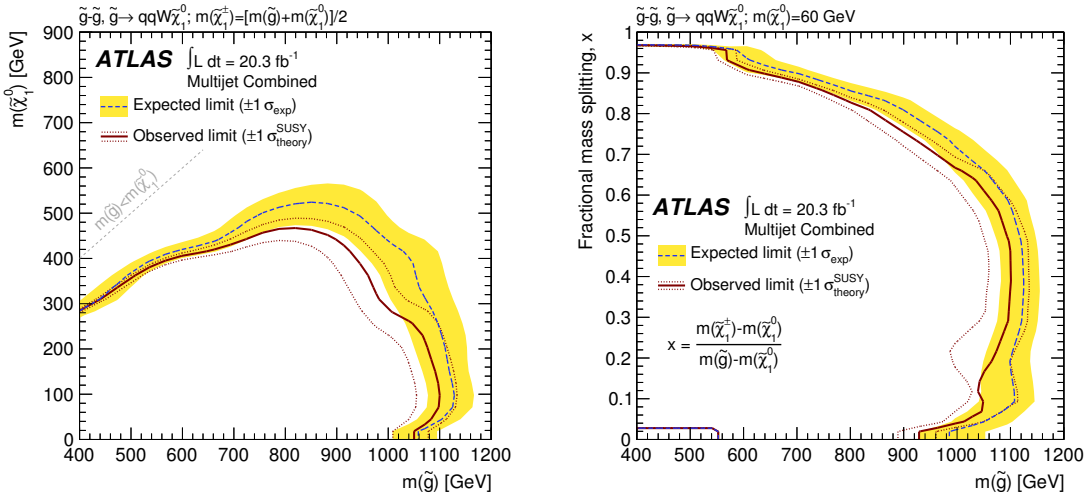


(a) x = 1/2 (b) $m_{\tilde{\chi}_1^0} = 60$ GeV

**Figure 11**. 95% CL exclusion curve for the simplified gluino-squark (via $\tilde{\chi}_1^\pm$) model, for the two versions of the model; fixed x = 1/2, where $x = (m_{\tilde{\chi}_1^\pm} - m_{\tilde{\chi}_1^0})/(m_{\tilde{g}} - m_{\tilde{\chi}_1^0})$, and varying $\tilde{\chi}_1^0$ mass on the left, and $\tilde{\chi}_1^0$ mass fixed to 60 GeV and varying x on the right. The region with gluino masses between 400 GeV and 550 GeV at small x has no signal Monte Carlo simulation. Other details are as in figure 9.

JHEP10(2013)130

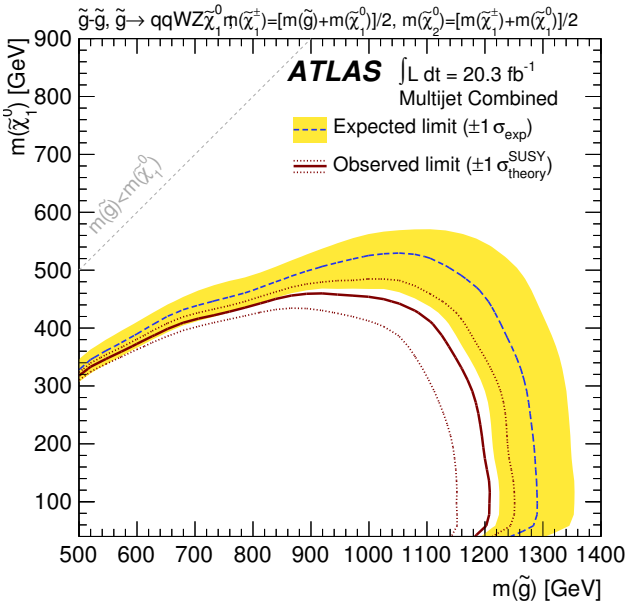


**Figure 12**. 95% CL exclusion curve for the simplified gluino-squark (via $\tilde{\chi}_1^{\pm}$ and $\tilde{\chi}_2^0$) model. Other details are as in figure 9.

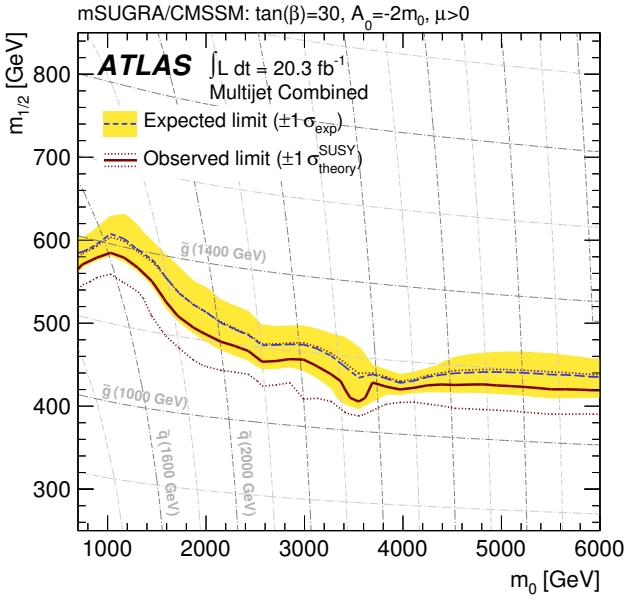


**Figure 13**. 95% CL exclusion curve for the mSUGRA/CMSSM model, generated with parameters $\tan\beta = 30$, $A_0 = -2m_0$ and $\mu > 0$. Other details are as in figure 9.

**mSUGRA/CMSSM.** An mSUGRA/CMSSM model with parameters $\tan\beta = 30$, $A_0 = -2m_0$ and $\mu > 0$ is also used to interpret the analysis results. The exclusion limits are presented in the $(m_0, m_{1/2})$ plane in figure 13. For large universal scalar mass $m_0$, gluino masses smaller than 1.1 TeV are excluded at 95% CL.



JHEP10(2013)130

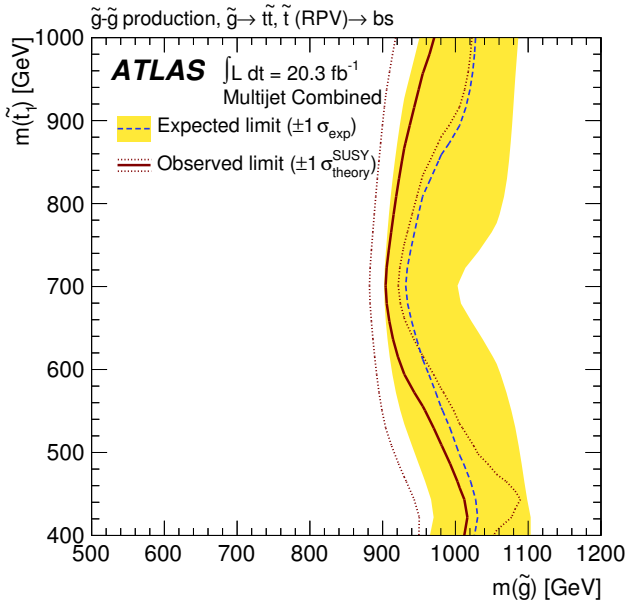


**Figure 14**. 95% CL exclusion curve for the simplified gluino-stop (RPV) model. Other details are as in figure 9.

**'Gluino-stop (RPV)' model.** In this simplified model, each gluino of a pair decays as $\tilde{g} \rightarrow \tilde{t} + \bar{t}$; and the $\tilde{t}$-squark decays via the R-parity- and baryon-number-violating decay $\tilde{t} \rightarrow \bar{s} + \bar{b}$. The results are presented in the $(m_{\tilde{g}}, m_{\tilde{t}})$ plane in figure 14. Within the context of this simplified model, the 95% CL exclusion bound on the gluino mass is 900 GeV for $\tilde{t}$-squark masses ranging from 400 GeV to 1 TeV.

## 8 Conclusion

A search is presented for new phenomena with large jet multiplicities (from 7 to $\geq$10) and missing transverse momentum using 20.3 fb$^{-1}$ of 8 TeV $pp$ collision data collected by the ATLAS experiment at the Large Hadron Collider. The sensitivity to new physics is enhanced by considering the number of $b$-tagged jets and the scalar sum of masses of radius $R = 1.0$ jets in the event, reconstructed using the anti-$k_t$ clustering algorithm. The Standard Model predictions are found to be consistent with the data. The results are interpreted in the context of an mSUGRA/CMSSM model and various simplified models resulting in final states with large jet multiplicity and $E_{\mathrm{T}}^{\mathrm{miss}}$. The exclusion limits substantially extend previous results. For example, in a model where both of the pair-produced gluinos decay via $\tilde{g} \rightarrow t + \bar{t} + \tilde{\chi}_1^0$, gluino masses smaller than 1.1 TeV are excluded for neutralino masses below 350 GeV.

## Acknowledgments

We thank CERN for the very successful operation of the LHC, as well as the support staff from our institutions without whom ATLAS could not be operated efficiently.



JHEP10(2013)130

We acknowledge the support of ANPCyT, Argentina; YerPhI, Armenia; ARC, Australia; BMWF and FWF, Austria; ANAS, Azerbaijan; SSTC, Belarus; CNPq and FAPESP, Brazil; NSERC, NRC and CFI, Canada; CERN; CONICYT, Chile; CAS, MOST and NSFC, China; COLCIENCIAS, Colombia; MSMT CR, MPO CR and VSC CR, Czech Republic; DNRF, DNSRC and Lundbeck Foundation, Denmark; EPLANET, ERC and NSRF, European Union; IN2P3-CNRS, CEA-DSM/IRFU, France; GNSF, Georgia; BMBF, DFG, HGF, MPG and AvH Foundation, Germany; GSRT and NSRF, Greece; ISF, MINERVA, GIF, DIP and Benoziyo Center, Israel; INFN, Italy; MEXT and JSPS, Japan; CNRST, Morocco; FOM and NWO, Netherlands; BRF and RCN, Norway; MNiSW, Poland; GRICES and FCT, Portugal; MERYS (MECTS), Romania; MES of Russia and ROSATOM, Russian Federation; JINR; MSTD, Serbia; MSSR, Slovakia; ARRS and MIZŠ, Slovenia; DST/NRF, South Africa; MICINN, Spain; SRC and Wallenberg Foundation, Sweden; SER, SNSF and Cantons of Bern and Geneva, Switzerland; NSC, Taiwan; TAEK, Turkey; STFC, the Royal Society and Leverhulme Trust, United Kingdom; DOE and NSF, United States of America.

The crucial computing support from all WLCG partners is acknowledged gratefully, in particular from CERN and the ATLAS Tier-1 facilities at TRIUMF (Canada), NDGF (Denmark, Norway, Sweden), CC-IN2P3 (France), KIT/GridKA (Germany), INFN-CNAF (Italy), NL-T1 (Netherlands), PIC (Spain), ASGC (Taiwan), RAL (UK) and BNL (USA) and in the Tier-2 facilities worldwide.

**Open Access.** This article is distributed under the terms of the Creative Commons Attribution License which permits any use, distribution and reproduction in any medium, provided the original author(s) and source are credited.

## References

[1] P. Fayet, *Supersymmetry and weak, electromagnetic and strong interactions*, *Phys. Lett.* **B 64** (1976) 159 [INSPIRE].

[2] P. Fayet, *Spontaneously broken supersymmetric theories of weak, electromagnetic and strong interactions*, *Phys. Lett.* **B 69** (1977) 489 [INSPIRE].

[3] G.R. Farrar and P. Fayet, *Phenomenology of the production, decay and detection of new hadronic states associated with supersymmetry*, *Phys. Lett.* **B 76** (1978) 575 [INSPIRE].

[4] P. Fayet, *Relations between the masses of the superpartners of leptons and quarks, the goldstino couplings and the neutral currents*, *Phys. Lett.* **B 84** (1979) 416 [INSPIRE].

[5] S. Dimopoulos and H. Georgi, *Softly broken supersymmetry and* SU(5), *Nucl. Phys.* **B 193** (1981) 150 [INSPIRE].

[6] H. Goldberg, *Constraint on the photino mass from cosmology*, *Phys. Rev. Lett.* **50** (1983) 1419 [*Erratum ibid.* **103** (2009) 099905] [INSPIRE].

[7] J.R. Ellis, J. Hagelin, D.V. Nanopoulos, K.A. Olive and M. Srednicki, *Supersymmetric relics from the Big Bang*, *Nucl. Phys.* **B 238** (1984) 453 [INSPIRE].

[8] L. Evans and P. Bryant, *LHC machine*, 2008 *JINST* **3** S08001 [INSPIRE].

[9] ATLAS collaboration, *The ATLAS experiment at the CERN Large Hadron Collider*, 2008 *JINST* **3** S08003 [INSPIRE].



JHEP10(2013)130

[10] ATLAS collaboration, *Search for new phenomena in final states with large jet multiplicities and missing transverse momentum using $\sqrt{s} = 7$ TeV pp collisions with the ATLAS detector*, *JHEP* **11** (2011) 099 [arXiv:1110.2299] [INSPIRE].

[11] ATLAS collaboration, *Hunt for new phenomena using large jet multiplicities and missing transverse momentum with ATLAS in 4.7 $fb^{-1}$ of $\sqrt{s} = 7$ TeV proton-proton collisions*, *JHEP* **07** (2012) 167 [arXiv:1206.1760] [INSPIRE].

[12] ATLAS collaboration, *Search for top and bottom squarks from gluino pair production in final states with missing transverse energy and at least three b-jets with the ATLAS detector*, *Eur. Phys. J.* **C 72** (2012) 2174 [arXiv:1207.4686] [INSPIRE].

[13] CMS collaboration, *Search for supersymmetry in hadronic final states with missing transverse energy using the variables $\alpha_T$ and b-quark multiplicity in pp collisions at 8 TeV*, *Eur. Phys. J.* **C 73** (2013) 2568 [arXiv:1303.2985] [INSPIRE].

[14] CMS collaboration, *Inclusive search for supersymmetry using the razor variables in pp collisions at $\sqrt{s} = 7$ TeV*, *Phys. Rev. Lett.* **111** (2013) 081802 [arXiv:1212.6961] [INSPIRE].

[15] CMS collaboration, *Search for new physics in the multijet and missing transverse momentum final state in proton-proton collisions at $\sqrt{s} = 7$ TeV*, *Phys. Rev. Lett.* **109** (2012) 171803 [arXiv:1207.1898] [INSPIRE].

[16] A.H. Chamseddine, R.L. Arnowitt and P. Nath, *Locally supersymmetric grand unification*, *Phys. Rev. Lett.* **49** (1982) 970 [INSPIRE].

[17] R. Barbieri, S. Ferrara and C.A. Savoy, *Gauge models with spontaneously broken local supersymmetry*, *Phys. Lett.* **B 119** (1982) 343 [INSPIRE].

[18] L.E. Ibáñez, *Locally supersymmetric* SU(5) *grand unification*, *Phys. Lett.* **B 118** (1982) 73 [INSPIRE].

[19] L.J. Hall, J.D. Lykken and S. Weinberg, *Supergravity as the messenger of supersymmetry breaking*, *Phys. Rev.* **D 27** (1983) 2359 [INSPIRE].

[20] N. Ohta, *Grand unified theories based on local supersymmetry*, *Prog. Theor. Phys.* **70** (1983) 542 [INSPIRE].

[21] G.L. Kane, C.F. Kolda, L. Roszkowski and J.D. Wells, *Study of constrained minimal supersymmetry*, *Phys. Rev.* **D 49** (1994) 6173 [hep-ph/9312272] [INSPIRE].

[22] M. Cacciari, G.P. Salam and G. Soyez, *The anti-$k_t$ jet clustering algorithm*, *JHEP* **04** (2008) 063 [arXiv:0802.1189] [INSPIRE].

[23] M. Cacciari and G.P. Salam, *Dispelling the $N^3$ myth for the $k_t$ jet-finder*, *Phys. Lett.* **B 641** (2006) 57 [hep-ph/0512210] [INSPIRE].

[24] A. Hook, E. Izaguirre, M. Lisanti and J.G. Wacker, *High multiplicity searches at the LHC using jet masses*, *Phys. Rev.* **D 85** (2012) 055029 [arXiv:1202.0558] [INSPIRE].

[25] ATLAS collaboration, *Observation of a new particle in the search for the standard model Higgs boson with the ATLAS detector at the LHC*, *Phys. Lett.* **B 716** (2012) 1 [arXiv:1207.7214] [INSPIRE].

[26] CMS collaboration, *Observation of a new boson at a mass of 125 GeV with the CMS experiment at the LHC*, *Phys. Lett.* **B 716** (2012) 30 [arXiv:1207.7235] [INSPIRE].

[27] ATLAS collaboration, *Improved luminosity determination in pp collisions at $\sqrt{s} = 7$ TeV using the ATLAS detector at the LHC*, *Eur. Phys. J.* **C 73** (2013) 2518 [arXiv:1302.4393] [INSPIRE].

JHEP10(2013)130

[28] ATLAS collaboration, *Jet energy measurement with the ATLAS detector in proton-proton collisions at* $\sqrt{s} = 7$ *TeV*, *Eur. Phys. J.* **C 73** (2013) 2304 [arXiv:1112.6426] [INSPIRE].

[29] C. Issever, K. Borras and D. Wegener, *An improved weighting algorithm to achieve software compensation in a fine grained LAr calorimeter*, *Nucl. Instrum. Meth.* **A 545** (2005) 803 [physics/0408129] [INSPIRE].

[30] M. Cacciari and G.P. Salam, *Pileup subtraction using jet areas*, *Phys. Lett.* **B 659** (2008) 119 [arXiv:0707.1378] [INSPIRE].

[31] ATLAS collaboration, *Commissioning of the ATLAS high-performance b-tagging algorithms in the 7 TeV collision data*, ATLAS-CONF-2011-102 (2011).

[32] ATLAS collaboration, *Measuring the b-tag efficiency in a top-pair sample with* $4.7\,fb^{-1}$ *of data from the ATLAS detector*, ATLAS-CONF-2012-097 (2012).

[33] ATLAS collaboration, *Electron performance measurements with the ATLAS detector using the 2010 LHC proton-proton collision data*, *Eur. Phys. J.* **C 72** (2012) 1909 [arXiv:1110.3174] [INSPIRE].

[34] ATLAS collaboration, *Performance of missing transverse momentum reconstruction in proton-proton collisions at 7 TeV with ATLAS*, *Eur. Phys. J.* **C 72** (2012) 1844 [arXiv:1108.5602] [INSPIRE].

[35] T. Gleisberg et al., *Event generation with SHERPA 1.1*, *JHEP* **02** (2009) 007 [arXiv:0811.4622] [INSPIRE].

[36] H.-L. Lai et al., *New parton distributions for collider physics*, *Phys. Rev.* **D 82** (2010) 074024 [arXiv:1007.2241] [INSPIRE].

[37] M. Aliev et al., *HATHOR: HAdronic Top and Heavy quarks crOss section calculatoR*, *Comput. Phys. Commun.* **182** (2011) 1034 [arXiv:1007.1327] [INSPIRE].

[38] S. Catani, L. Cieri, G. Ferrera, D. de Florian and M. Grazzini, *Vector boson production at hadron colliders: a fully exclusive QCD calculation at NNLO*, *Phys. Rev. Lett.* **103** (2009) 082001 [arXiv:0903.2120] [INSPIRE].

[39] S. Frixione and B.R. Webber, *Matching NLO QCD computations and parton shower simulations*, *JHEP* **06** (2002) 029 [hep-ph/0204244] [INSPIRE].

[40] S. Frixione, F. Stoeckli, P. Torrielli, B.R. Webber and C.D. White, *The MCaNLO 4.0 event generator*, arXiv:1010.0819 [INSPIRE].

[41] S. Frixione, E. Laenen, P. Motylinski and B.R. Webber, *Single-top production in MC@NLO*, *JHEP* **03** (2006) 092 [hep-ph/0512250] [INSPIRE].

[42] S. Frixione, E. Laenen, P. Motylinski, B.R. Webber and C.D. White, *Single-top hadroproduction in association with a W boson*, *JHEP* **07** (2008) 029 [arXiv:0805.3067] [INSPIRE].

[43] G. Corcella et al., *HERWIG 6.5 release note*, hep-ph/0210213 [INSPIRE].

[44] J. Butterworth, J.R. Forshaw and M. Seymour, *Multiparton interactions in photoproduction at HERA*, *Z. Phys.* **C 72** (1996) 637 [hep-ph/9601371] [INSPIRE].

[45] B.P. Kersevan and E. Richter-Was, *The Monte Carlo event generator AcerMC version 2.0 with interfaces to PYTHIA 6.2 and HERWIG 6.5*, hep-ph/0405247 [INSPIRE].

[46] T. Sjöstrand, S. Mrenna and P.Z. Skands, *PYTHIA 6.4 physics and manual*, *JHEP* **05** (2006) 026 [hep-ph/0603175] [INSPIRE].

[47] J. Alwall, M. Herquet, F. Maltoni, O. Mattelaer and T. Stelzer, *MadGraph 5: going beyond*, *JHEP* **06** (2011) 128 [arXiv:1106.0522] [INSPIRE].



JHEP10(2013)130

[48] M. Bähr et al., *HERWIG++ physics and manual*, *Eur. Phys. J.* **C 58** (2008) 639 [arXiv:0803.0883] [INSPIRE].

[49] J. Pumplin et al., *New generation of parton distributions with uncertainties from global QCD analysis*, *JHEP* **07** (2002) 012 [hep-ph/0201195] [INSPIRE].

[50] W. Beenakker, R. Hopker, M. Spira and P. Zerwas, *Squark and gluino production at hadron colliders*, *Nucl. Phys.* **B 492** (1997) 51 [hep-ph/9610490] [INSPIRE].

[51] A. Kulesza and L. Motyka, *Threshold resummation for squark-antisquark and gluino-pair production at the LHC*, *Phys. Rev. Lett.* **102** (2009) 111802 [arXiv:0807.2405] [INSPIRE].

[52] A. Kulesza and L. Motyka, *Soft gluon resummation for the production of gluino-gluino and squark-antisquark pairs at the LHC*, *Phys. Rev.* **D 80** (2009) 095004 [arXiv:0905.4749] [INSPIRE].

[53] W. Beenakker et al., *Soft-gluon resummation for squark and gluino hadroproduction*, *JHEP* **12** (2009) 041 [arXiv:0909.4418] [INSPIRE].

[54] W. Beenakker et al., *Squark and gluino hadroproduction*, *Int. J. Mod. Phys.* **A 26** (2011) 2637 [arXiv:1105.1110] [INSPIRE].

[55] M. Krämer et al., *Supersymmetry production cross sections in pp collisions at* $\sqrt{s} = 7$ *TeV*, arXiv:1206.2892 [INSPIRE].

[56] ATLAS collaboration, *The ATLAS simulation infrastructure*, *Eur. Phys. J.* **C 70** (2010) 823 [arXiv:1005.4568] [INSPIRE].

[57] GEANT4 collaboration, S. Agostinelli et al., *GEANT4: a simulation toolkit*, *Nucl. Instrum. Meth.* **A 506** (2003) 250 [INSPIRE].

[58] ATLAS collaboration, *Measurement of multi-jet cross sections in proton-proton collisions at a 7 TeV center-of-mass energy*, *Eur. Phys. J.* **C 71** (2011) 1763 [arXiv:1107.2092] [INSPIRE].

[59] ATLAS collaboration, *Jet energy scale and its systematic uncertainty for jets produced in proton-proton collisions at* $\sqrt{s} = 7$ *TeV and measured with the ATLAS detector*, ATLAS-CONF-2010-056 (2010).

[60] M.L. Mangano, M. Moretti, F. Piccinini, R. Pittau and A.D. Polosa, *ALPGEN, a generator for hard multiparton processes in hadronic collisions*, *JHEP* **07** (2003) 001 [hep-ph/0206293] [INSPIRE].

[61] B. Cooper et al., *Importance of a consistent choice of* $\alpha_s$ *in the matching of ALPGEN and PYTHIA*, *Eur. Phys. J.* **C 72** (2012) 2078 [arXiv:1109.5295] [INSPIRE].

[62] G. Cowan, K. Cranmer, E. Gross and O. Vitells, *Asymptotic formulae for likelihood-based tests of new physics*, *Eur. Phys. J.* **C 71** (2011) 1554 [arXiv:1007.1727] [INSPIRE].

[63] HepData, http://hepdata.cedar.ac.uk/view/red6095.

[64] A. Read, *Presentation of search results: the* $CL_s$ *technique*, *J. Phys.* **G 28** (2002) 2693.

[65] CMS collaboration, *Interpretation of searches for supersymmetry with simplified models*, arXiv:1301.2175 [INSPIRE].

JHEP10(2013)130

## The ATLAS collaboration

G. Aad[48], T. Abajyan[21], B. Abbott[112], J. Abdallah[12], S. Abdel Khalek[116], O. Abdinov[11], R. Aben[106], B. Abi[113], M. Abolins[89], O.S. AbouZeid[159], H. Abramowicz[154], H. Abreu[137], Y. Abulaiti[147a,147b], B.S. Acharya[165a,165b,a], L. Adamczyk[38a], D.L. Adams[25], T.N. Addy[56], J. Adelman[177], S. Adomeit[99], T. Adye[130], S. Aefsky[23], T. Agatonovic-Jovin[13b], J.A. Aguilar-Saavedra[125b,b], M. Agustoni[17], S.P. Ahlen[22], A. Ahmad[149], M. Ahsan[41], G. Aielli[134a,134b], T.P.A. Åkesson[80], G. Akimoto[156], A.V. Akimov[95], M.A. Alam[76], J. Albert[170], S. Albrand[55], M.J. Alconada Verzini[70], M. Aleksa[30], I.N. Aleksandrov[64], F. Alessandria[90a], C. Alexa[26a], G. Alexander[154], G. Alexandre[49], T. Alexopoulos[10], M. Alhroob[165a,165c], M. Aliev[16], G. Alimonti[90a], L. Alio[84], J. Alison[31], B.M.M. Allbrooke[18], L.J. Allison[71], P.P. Allport[73], S.E. Allwood-Spiers[53], J. Almond[83], A. Aloisio[103a,103b], R. Alon[173], A. Alonso[36], F. Alonso[70], A. Altheimer[35], B. Alvarez Gonzalez[89], M.G. Alviggi[103a,103b], K. Amako[65], Y. Amaral Coutinho[24a], C. Amelung[23], V.V. Ammosov[129,*], S.P. Amor Dos Santos[125a], A. Amorim[125a,c], S. Amoroso[48], N. Amram[154], C. Anastopoulos[30], L.S. Ancu[17], N. Andari[30], T. Andeen[35], C.F. Anders[58b], G. Anders[58a], K.J. Anderson[31], A. Andreazza[90a,90b], V. Andrei[58a], X.S. Anduaga[70], S. Angelidakis[9], P. Anger[44], A. Angerami[35], F. Anghinolfi[30], A.V. Anisenkov[108], N. Anjos[125a], A. Annovi[47], A. Antonaki[9], M. Antonelli[47], A. Antonov[97], J. Antos[145b], F. Anulli[133a], M. Aoki[102], L. Aperio Bella[18], R. Apolle[119,d], G. Arabidze[89], I. Aracena[144], Y. Arai[65], A.T.H. Arce[45], S. Arfaoui[149], J-F. Arguin[94], S. Argyropoulos[42], E. Arik[19a,*], M. Arik[19a], A.J. Armbruster[88], O. Arnaez[82], V. Arnal[81], O. Arslan[21], A. Artamonov[96], G. Artoni[23], D. Arutinov[21], S. Asai[156], N. Asbah[94], S. Ask[28], B. Åsman[147a,147b], L. Asquith[6], K. Assamagan[25], R. Astalos[145a], A. Astbury[170], M. Atkinson[166], N.B. Atlay[142], B. Auerbach[6], E. Auge[116], K. Augsten[127], M. Aurousseau[146b], G. Avolio[30], D. Axen[169], G. Azuelos[94,e], Y. Azuma[156], M.A. Baak[30], C. Bacci[135a,135b], A.M. Bach[15], H. Bachacou[137], K. Bachas[155], M. Backes[30], M. Backhaus[21], J. Backus Mayes[144], E. Badescu[26a], P. Bagiacchi[133a,133b], P. Bagnaia[133a,133b], Y. Bai[33a], D.C. Bailey[159], T. Bain[35], J.T. Baines[130], O.K. Baker[177], S. Baker[77], P. Balek[128], F. Balli[137], E. Banas[39], Sw. Banerjee[174], D. Banfi[30], A. Bangert[151], V. Bansal[170], H.S. Bansil[18], L. Barak[173], S.P. Baranov[95], T. Barber[48], E.L. Barberio[87], D. Barberis[50a,50b], M. Barbero[84], D.Y. Bardin[64], T. Barillari[100], M. Barisonzi[176], T. Barklow[144], N. Barlow[28], B.M. Barnett[130], R.M. Barnett[15], A. Baroncelli[135a], G. Barone[49], A.J. Barr[119], F. Barreiro[81], J. Barreiro Guimarães da Costa[57], R. Bartoldus[144], A.E. Barton[71], V. Bartsch[150], A. Basye[166], R.L. Bates[53], L. Batkova[145a], J.R. Batley[28], M. Battistin[30], F. Bauer[137], H.S. Bawa[144,f], S. Beale[99], T. Beau[79], P.H. Beauchemin[162], R. Beccherle[50a], P. Bechtle[21], H.P. Beck[17], K. Becker[176], S. Becker[99], M. Beckingham[139], K.H. Becks[176], A.J. Beddall[19c], A. Beddall[19c], S. Bedikian[177], V.A. Bednyakov[64], C.P. Bee[84], L.J. Beemster[106], T.A. Beermann[176], M. Begel[25], C. Belanger-Champagne[86], P.J. Bell[49], W.H. Bell[49], G. Bella[154], L. Bellagamba[20a], A. Bellerive[29], M. Bellomo[30], A. Belloni[57], O.L. Beloborodova[108,g], K. Belotskiy[97], O. Beltramello[30], O. Benary[154], D. Benchekroun[136a], K. Bendtz[147a,147b], N. Benekos[166], Y. Benhammou[154], E. Benhar Noccioli[49], J.A. Benitez Garcia[160b], D.P. Benjamin[45], J.R. Bensinger[23], K. Benslama[131], S. Bentvelsen[106], D. Berge[30], E. Bergeaas Kuutmann[16], N. Berger[5], F. Berghaus[170], E. Berglund[106], J. Beringer[15], C. Bernard[22], P. Bernat[77], R. Bernhard[48], C. Bernius[78], F.U. Bernlochner[170], T. Berry[76], C. Bertella[84], F. Bertolucci[123a,123b], M.I. Besana[90a], G.J. Besjes[105], O. Bessidskaia[147a,147b], N. Besson[137], S. Bethke[100], W. Bhimji[46], R.M. Bianchi[124], L. Bianchini[23], M. Bianco[72a,72b], O. Biebel[99], S.P. Bieniek[77], K. Bierwagen[54], J. Biesiada[15], M. Biglietti[135a], J. Bilbao De Mendizabal[49], H. Bilokon[47], M. Bindi[20a,20b], S. Binet[116], A. Bingul[19c], C. Bini[133a,133b], B. Bittner[100], C.W. Black[151], J.E. Black[144], K.M. Black[22], D. Blackburn[139], R.E. Blair[6], J.-B. Blanchard[137], T. Blazek[145a], I. Bloch[42], C. Blocker[23], J. Blocki[39], W. Blum[82,*], U. Blumenschein[54], G.J. Bobbink[106], V.S. Bobrovnikov[108], S.S. Bocchetta[80], A. Bocci[45], C.R. Boddy[119], M. Boehler[48], J. Boek[176], T.T. Boek[176], N. Boelaert[36], J.A. Bogaerts[30], A.G. Bogdanchikov[108], A. Bogouch[91,*], C. Bohm[147a], J. Bohm[126], V. Boisvert[76], T. Bold[38a], V. Boldea[26a], N.M. Bolnet[137], M. Bomben[79], M. Bona[75], M. Boonekamp[137], S. Bordoni[79],

JHEP10(2013)130

C. Borer[17], A. Borisov[129], G. Borissov[71], M. Borri[83], S. Borroni[42], J. Bortfeldt[99], V. Bortolotto[135a,135b], K. Bos[106], D. Boscherini[20a], M. Bosman[12], H. Boterenbrood[106], J. Bouchami[94], J. Boudreau[124], E.V. Bouhova-Thacker[71], D. Boumediene[34], C. Bourdarios[116], N. Bousson[84], S. Boutouil[136d], A. Boveia[31], J. Boyd[30], I.R. Boyko[64], I. Bozovic-Jelisavcic[13b], J. Bracinik[18], P. Branchini[135a], A. Brandt[8], G. Brandt[15], O. Brandt[54], U. Bratzler[157], B. Brau[85], J.E. Brau[115], H.M. Braun[176,*], S.F. Brazzale[165a,165c], B. Brelier[159], J. Bremer[30], K. Brendlinger[121], R. Brenner[167], S. Bressler[173], T.M. Bristow[46], D. Britton[53], F.M. Brochu[28], I. Brock[21], R. Brock[89], F. Broggi[90a], C. Bromberg[89], J. Bronner[100], G. Brooijmans[35], T. Brooks[76], W.K. Brooks[32b], E. Brost[115], G. Brown[83], J. Brown[55], P.A. Bruckman de Renstrom[39], D. Bruncko[145b], R. Bruneliere[48], S. Brunet[60], A. Bruni[20a], G. Bruni[20a], M. Bruschi[20a], L. Bryngemark[80], T. Buanes[14], Q. Buat[55], F. Bucci[49], J. Buchanan[119], P. Buchholz[142], R.M. Buckingham[119], A.G. Buckley[46], S.I. Buda[26a], I.A. Budagov[64], B. Budick[109], F. Buehrer[48], L. Bugge[118], O. Bulekov[97], A.C. Bundock[73], M. Bunse[43], T. Buran[118,*], H. Burckhart[30], S. Burdin[73], T. Burgess[14], S. Burke[130], E. Busato[34], V. Büscher[82], P. Bussey[53], C.P. Buszello[167], B. Butler[57], J.M. Butler[22], C.M. Buttar[53], J.M. Butterworth[77], W. Buttinger[28], M. Byszewski[10], S. Cabrera Urbán[168], D. Caforio[20a,20b], O. Cakir[4a], P. Calafiura[15], G. Calderini[79], P. Calfayan[99], R. Calkins[107], L.P. Caloba[24a], R. Caloi[133a,133b], D. Calvet[34], S. Calvet[34], R. Camacho Toro[49], P. Camarri[134a,134b], D. Cameron[118], L.M. Caminada[15], R. Caminal Armadans[12], S. Campana[30], M. Campanelli[77], V. Canale[103a,103b], F. Canelli[31], A. Canepa[160a], J. Cantero[81], R. Cantrill[76], T. Cao[40], M.D.M. Capeans Garrido[30], I. Caprini[26a], M. Caprini[26a], D. Capriotti[100], M. Capua[37a,37b], R. Caputo[82], R. Cardarelli[134a], T. Carli[30], G. Carlino[103a], L. Carminati[90a,90b], S. Caron[105], E. Carquin[32b], G.D. Carrillo-Montoya[146c], A.A. Carter[75], J.R. Carter[28], J. Carvalho[125a,h], D. Casadei[77], M.P. Casado[12], C. Caso[50a,50b,*], E. Castaneda-Miranda[174], A. Castelli[106], V. Castillo Gimenez[168], N.F. Castro[125a], G. Cataldi[72a], P. Catastini[57], A. Catinaccio[30], J.R. Catmore[30], A. Cattai[30], G. Cattani[134a,134b], S. Caughron[89], V. Cavaliere[166], D. Cavalli[90a], M. Cavalli-Sforza[12], V. Cavasinni[123a,123b], F. Ceradini[135a,135b], B. Cerio[45], A.S. Cerqueira[24b], A. Cerri[15], L. Cerrito[75], F. Cerutti[15], A. Cervelli[17], S.A. Cetin[19b], A. Chafaq[136a], D. Chakraborty[107], I. Chalupkova[128], K. Chan[3], P. Chang[166], B. Chapleau[86], J.D. Chapman[28], J.W. Chapman[88], D.G. Charlton[18], V. Chavda[83], C.A. Chavez Barajas[30], S. Cheatham[86], S. Chekanov[6], S.V. Chekulaev[160a], G.A. Chelkov[64], M.A. Chelstowska[88], C. Chen[63], H. Chen[25], S. Chen[33c], X. Chen[174], Y. Chen[35], Y. Cheng[31], A. Cheplakov[64], R. Cherkaoui El Moursli[136e], V. Chernyatin[25,*], E. Cheu[7], L. Chevalier[137], V. Chiarella[47], G. Chiefari[103a,103b], J.T. Childers[30], A. Chilingarov[71], G. Chiodini[72a], A.S. Chisholm[18], R.T. Chislett[77], A. Chitan[26a], M.V. Chizhov[64], G. Choudalakis[31], S. Chouridou[9], B.K.B. Chow[99], I.A. Christidi[77], A. Christov[48], D. Chromek-Burckhart[30], M.L. Chu[152], J. Chudoba[126], G. Ciapetti[133a,133b], A.K. Ciftci[4a], R. Ciftci[4a], D. Cinca[62], V. Cindro[74], A. Ciocio[15], M. Cirilli[88], P. Cirkovic[13b], Z.H. Citron[173], M. Citterio[90a], M. Ciubancan[26a], A. Clark[49], P.J. Clark[46], R.N. Clarke[15], J.C. Clemens[84], B. Clement[55], C. Clement[147a,147b], Y. Coadou[84], M. Cobal[165a,165c], A. Coccaro[139], J. Cochran[63], S. Coelli[90a], L. Coffey[23], J.G. Cogan[144], J. Coggeshall[166], J. Colas[5], B. Cole[35], S. Cole[107], A.P. Colijn[106], C. Collins-Tooth[53], J. Collot[55], T. Colombo[120a,120b], G. Colon[85], G. Compostella[100], P. Conde Muiño[125a], E. Coniavitis[167], M.C. Conidi[12], S.M. Consonni[90a,90b], V. Consorti[48], S. Constantinescu[26a], C. Conta[120a,120b], G. Conti[57], F. Conventi[103a,i], M. Cooke[15], B.D. Cooper[77], A.M. Cooper-Sarkar[119], N.J. Cooper-Smith[76], K. Copic[15], T. Cornelissen[176], M. Corradi[20a], F. Corriveau[86,j], A. Corso-Radu[164], A. Cortes-Gonzalez[12], G. Cortiana[100], G. Costa[90a], M.J. Costa[168], D. Costanzo[140], D. Côté[8], G. Cottin[32a], L. Courneyea[170], G. Cowan[76], B.E. Cox[83], K. Cranmer[109], S. Crépé-Renaudin[55], F. Crescioli[79], M. Crispin Ortuzar[119], M. Cristinziani[21], G. Crosetti[37a,37b], C.-M. Cuciuc[26a], C. Cuenca Almenar[177], T. Cuhadar Donszelmann[140], J. Cummings[177], M. Curatolo[47], C. Cuthbert[151], H. Czirr[142], P. Czodrowski[44], Z. Czyczula[177], S. D'Auria[53], M. D'Onofrio[73], A. D'Orazio[133a,133b], M.J. Da Cunha Sargedas De Sousa[125a], C. Da Via[83], W. Dabrowski[38a], A. Dafinca[119], T. Dai[88], F. Dallaire[94], C. Dallapiccola[85], M. Dam[36], D.S. Damiani[138], A.C. Daniells[18], V. Dao[105], G. Darbo[50a], G.L. Darlea[26c],

JHEP10(2013)130

S. Darmora[8], J.A. Dassoulas[42], W. Davey[21], C. David[170], T. Davidek[128], E. Davies[119,d], M. Davies[94], O. Davignon[79], A.R. Davison[77], Y. Davygora[58a], E. Dawe[143], I. Dawson[140], R.K. Daya-Ishmukhametova[23], K. De[8], R. de Asmundis[103a], S. De Castro[20a,20b], S. De Cecco[79], J. de Graat[99], N. De Groot[105], P. de Jong[106], C. De La Taille[116], H. De la Torre[81], F. De Lorenzi[63], L. De Nooij[106], D. De Pedis[133a], A. De Salvo[133a], U. De Sanctis[165a,165c], A. De Santo[150], J.B. De Vivie De Regie[116], G. De Zorzi[133a,133b], W.J. Dearnaley[71], R. Debbe[25], C. Debenedetti[46], B. Dechenaux[55], D.V. Dedovich[64], J. Degenhardt[121], J. Del Peso[81], T. Del Prete[123a,123b], T. Delemontex[55], M. Deliyergiyev[74], A. Dell'Acqua[30], L. Dell'Asta[22], M. Della Pietra[103a,i], D. della Volpe[103a,103b], M. Delmastro[5], P.A. Delsart[55], C. Deluca[106], S. Demers[177], M. Demichev[64], A. Demilly[79], B. Demirkoz[12,k], S.P. Denisov[129], D. Derendarz[39], J.E. Derkaoui[136d], F. Derue[79], P. Dervan[73], K. Desch[21], P.O. Deviveiros[106], A. Dewhurst[130], B. DeWilde[149], S. Dhaliwal[106], R. Dhullipudi[78,l], A. Di Ciaccio[134a,134b], L. Di Ciaccio[5], C. Di Donato[103a,103b], A. Di Girolamo[30], B. Di Girolamo[30], S. Di Luise[135a,135b], A. Di Mattia[153], B. Di Micco[135a,135b], R. Di Nardo[47], A. Di Simone[48], R. Di Sipio[20a,20b], M.A. Diaz[32a], E.B. Diehl[88], J. Dietrich[42], T.A. Dietzsch[58a], S. Diglio[87], K. Dindar Yagci[40], J. Dingfelder[21], F. Dinut[26a], C. Dionisi[133a,133b], P. Dita[26a], S. Dita[26a], F. Dittus[30], F. Djama[84], T. Djobava[51b], M.A.B. do Vale[24c], A. Do Valle Wemans[125a,m], T.K.O. Doan[5], D. Dobos[30], E. Dobson[77], J. Dodd[35], C. Doglioni[49], T. Doherty[53], T. Dohmae[156], Y. Doi[65,*], J. Dolejsi[128], Z. Dolezal[128], B.A. Dolgoshein[97,*], M. Donadelli[24d], J. Donini[34], J. Dopke[30], A. Doria[103a], A. Dos Anjos[174], A. Dotti[123a,123b], M.T. Dova[70], A.T. Doyle[53], M. Dris[10], J. Dubbert[88], S. Dube[15], E. Dubreuil[34], E. Duchovni[173], G. Duckeck[99], D. Duda[176], A. Dudarev[30], F. Dudziak[63], L. Duflot[116], M-A. Dufour[86], L. Duguid[76], M. Dührssen[30], M. Dunford[58a], H. Duran Yildiz[4a], M. Düren[52], M. Dwuznik[38a], J. Ebke[99], W. Edson[2], C.A. Edwards[76], N.C. Edwards[46], W. Ehrenfeld[21], T. Eifert[144], G. Eigen[14], K. Einsweiler[15], E. Eisenhandler[75], T. Ekelof[167], M. El Kacimi[136c], M. Ellert[167], S. Elles[5], F. Ellinghaus[82], K. Ellis[75], N. Ellis[30], J. Elmsheuser[99], M. Elsing[30], D. Emeliyanov[130], Y. Enari[156], O.C. Endner[82], R. Engelmann[149], A. Engl[99], J. Erdmann[177], A. Ereditato[17], D. Eriksson[147a], J. Ernst[2], M. Ernst[25], J. Ernwein[137], D. Errede[166], S. Errede[166], E. Ertel[82], M. Escalier[116], H. Esch[43], C. Escobar[124], X. Espinal Curull[12], B. Esposito[47], F. Etienne[84], A.I. Etienvre[137], E. Etzion[154], D. Evangelakou[54], H. Evans[60], L. Fabbri[20a,20b], C. Fabre[30], G. Facini[30], R.M. Fakhrutdinov[129], S. Falciano[133a], Y. Fang[33a], M. Fanti[90a,90b], A. Farbin[8], A. Farilla[135a], T. Farooque[159], S. Farrell[164], S.M. Farrington[171], P. Farthouat[30], F. Fassi[168], P. Fassnacht[30], D. Fassouliotis[9], B. Fatholahzadeh[159], A. Favareto[90a,90b], L. Fayard[116], P. Federic[145a], O.L. Fedin[122], W. Fedorko[169], M. Fehling-Kaschek[48], L. Feligioni[84], C. Feng[33d], E.J. Feng[6], H. Feng[88], A.B. Fenyuk[129], J. Ferencei[145b], W. Fernando[6], S. Ferrag[53], J. Ferrando[53], V. Ferrara[42], A. Ferrari[167], P. Ferrari[106], R. Ferrari[120a], D.E. Ferreira de Lima[53], A. Ferrer[168], D. Ferrere[49], C. Ferretti[88], A. Ferretto Parodi[50a,50b], M. Fiascaris[31], F. Fiedler[82], A. Filipčič[74], M. Filipuzzi[42], F. Filthaut[105], M. Fincke-Keeler[170], K.D. Finelli[45], M.C.N. Fiolhais[125a,h], L. Fiorini[168], A. Firan[40], J. Fischer[176], M.J. Fisher[110], E.A. Fitzgerald[23], M. Flechl[48], I. Fleck[142], P. Fleischmann[175], S. Fleischmann[176], G.T. Fletcher[140], G. Fletcher[75], T. Flick[176], A. Floderus[80], L.R. Flores Castillo[174], A.C. Florez Bustos[160b], M.J. Flowerdew[100], T. Fonseca Martin[17], A. Formica[137], A. Forti[83], D. Fortin[160a], D. Fournier[116], H. Fox[71], P. Francavilla[12], M. Franchini[20a,20b], S. Franchino[30], D. Francis[30], M. Franklin[57], S. Franz[61], M. Fraternali[120a,120b], S. Fratina[121], S.T. French[28], C. Friedrich[42], F. Friedrich[44], D. Froidevaux[30], J.A. Frost[28], C. Fukunaga[157], E. Fullana Torregrosa[128], B.G. Fulsom[144], J. Fuster[168], C. Gabaldon[30], O. Gabizon[173], A. Gabrielli[20a,20b], A. Gabrielli[133a,133b], S. Gadatsch[106], T. Gadfort[25], S. Gadomski[49], G. Gagliardi[50a,50b], P. Gagnon[60], C. Galea[99], B. Galhardo[125a], E.J. Gallas[119], V. Gallo[17], B.J. Gallop[130], P. Gallus[127], G. Galster[36], K.K. Gan[110], R.P. Gandrajula[62], Y.S. Gao[144,f], A. Gaponenko[15], F.M. Garay Walls[46], F. Garberson[177], C. García[168], J.E. García Navarro[168], M. Garcia-Sciveres[15], R.W. Gardner[31], N. Garelli[144], V. Garonne[30], C. Gatti[47], G. Gaudio[120a], B. Gaur[142], L. Gauthier[94], P. Gauzzi[133a,133b], I.L. Gavrilenko[95], C. Gay[169], G. Gaycken[21], E.N. Gazis[10], P. Ge[33d,n], Z. Gecse[169], C.N.P. Gee[130], D.A.A. Geerts[106], Ch. Geich-Gimbel[21], K. Gellerstedt[147a,147b], C. Gemme[50a], A. Gemmell[53], M.H. Genest[55],

JHEP10(2013)130

S. Gentile[133a,133b], M. George[54], S. George[76], D. Gerbaudo[164], A. Gershon[154], H. Ghazlane[136b], N. Ghodbane[34], B. Giacobbe[20a], S. Giagu[133a,133b], V. Giangiobbe[12], P. Giannetti[123a,123b], F. Gianotti[30], B. Gibbard[25], S.M. Gibson[76], M. Gilchriese[15], T.P.S. Gillam[28], D. Gillberg[30], A.R. Gillman[130], D.M. Gingrich[3,e], N. Giokaris[9], M.P. Giordani[165c], R. Giordano[103a,103b], F.M. Giorgi[16], P. Giovannini[100], P.F. Giraud[137], D. Giugni[90a], C. Giuliani[48], M. Giunta[94], B.K. Gjelsten[118], I. Gkialas[155,o], L.K. Gladilin[98], C. Glasman[81], J. Glatzer[21], A. Glazov[42], G.L. Glonti[64], M. Goblirsch-Kolb[100], J.R. Goddard[75], J. Godfrey[143], J. Godlewski[30], M. Goebel[42], C. Goeringer[82], S. Goldfarb[88], T. Golling[177], D. Golubkov[129], A. Gomes[125a,c], L.S. Gomez Fajardo[42], R. Gonçalo[76], J. Goncalves Pinto Firmino Da Costa[42], L. Gonella[21], S. González de la Hoz[168], G. Gonzalez Parra[12], M.L. Gonzalez Silva[27], S. Gonzalez-Sevilla[49], J.J. Goodson[149], L. Goossens[30], P.A. Gorbounov[96], H.A. Gordon[25], I. Gorelov[104], G. Gorfine[176], B. Gorini[30], E. Gorini[72a,72b], A. Gorišek[74], E. Gornicki[39], A.T. Goshaw[6], C. Gössling[43], M.I. Gostkin[64], I. Gough Eschrich[164], M. Gouighri[136a], D. Goujdami[136c], M.P. Goulette[49], A.G. Goussiou[139], C. Goy[5], S. Gozpinar[23], H.M.X. Grabas[137], L. Graber[54], I. Grabowska-Bold[38a], P. Grafström[20a,20b], K-J. Grahn[42], E. Gramstad[118], F. Grancagnolo[72a], S. Grancagnolo[16], V. Grassi[149], V. Gratchev[122], H.M. Gray[30], J.A. Gray[149], E. Graziani[135a], O.G. Grebenyuk[122], T. Greenshaw[73], Z.D. Greenwood[78,l], K. Gregersen[36], I.M. Gregor[42], P. Grenier[144], J. Griffiths[8], N. Grigalashvili[64], A.A. Grillo[138], K. Grimm[71], S. Grinstein[12,p], Ph. Gris[34], Y.V. Grishkevich[98], J.-F. Grivaz[116], J.P. Grohs[44], A. Grohsjean[42], E. Gross[173], J. Grosse-Knetter[54], J. Groth-Jensen[173], K. Grybel[142], F. Guescini[49], D. Guest[177], O. Gueta[154], C. Guicheney[34], E. Guido[50a,50b], T. Guillemin[116], S. Guindon[2], U. Gul[53], J. Gunther[127], J. Guo[35], S. Gupta[119], P. Gutierrez[112], N.G. Gutierrez Ortiz[53], N. Guttman[154], O. Gutzwiller[174], C. Guyot[137], C. Gwenlan[119], C.B. Gwilliam[73], A. Haas[109], C. Haber[15], H.K. Hadavand[8], P. Haefner[21], Z. Hajduk[39], H. Hakobyan[178], D. Hall[119], G. Halladjian[62], K. Hamacher[176], P. Hamal[114], K. Hamano[87], M. Hamer[54], A. Hamilton[146a,q], S. Hamilton[162], L. Han[33b], K. Hanagaki[117], K. Hanawa[156], M. Hance[15], C. Handel[82], P. Hanke[58a], J.R. Hansen[36], J.B. Hansen[36], J.D. Hansen[36], P.H. Hansen[36], P. Hansson[144], K. Hara[161], A.S. Hard[174], T. Harenberg[176], S. Harkusha[91], D. Harper[88], R.D. Harrington[46], O.M. Harris[139], J. Hartert[48], F. Hartjes[106], A. Harvey[56], S. Hasegawa[102], Y. Hasegawa[141], S. Hassani[137], S. Haug[17], M. Hauschild[30], R. Hauser[89], M. Havranek[21], C.M. Hawkes[18], R.J. Hawkings[30], A.D. Hawkins[80], T. Hayashi[161], D. Hayden[89], C.P. Hays[119], H.S. Hayward[73], S.J. Haywood[130], S.J. Head[18], T. Heck[82], V. Hedberg[80], L. Heelan[8], S. Heim[121], B. Heinemann[15], S. Heisterkamp[36], J. Hejbal[126], L. Helary[22], C. Heller[99], M. Heller[30], S. Hellman[147a,147b], D. Hellmich[21], C. Helsens[30], J. Henderson[119], R.C.W. Henderson[71], A. Henrichs[177], A.M. Henriques Correia[30], S. Henrot-Versille[116], C. Hensel[54], G.H. Herbert[16], C.M. Hernandez[8], Y. Hernández Jiménez[168], R. Herrberg-Schubert[16], G. Herten[48], R. Hertenberger[99], L. Hervas[30], G.G. Hesketh[77], N.P. Hessey[106], R. Hickling[75], E. Higón-Rodriguez[168], J.C. Hill[28], K.H. Hiller[42], S. Hillert[21], S.J. Hillier[18], I. Hinchliffe[15], E. Hines[121], M. Hirose[117], D. Hirschbuehl[176], J. Hobbs[149], N. Hod[106], M.C. Hodgkinson[140], P. Hodgson[140], A. Hoecker[30], M.R. Hoeferkamp[104], J. Hoffman[40], D. Hoffmann[84], J.I. Hofmann[58a], M. Hohlfeld[82], S.O. Holmgren[147a], J.L. Holzbauer[89], T.M. Hong[121], L. Hooft van Huysduynen[109], J-Y. Hostachy[55], S. Hou[152], A. Hoummada[136a], J. Howard[119], J. Howarth[83], M. Hrabovsky[114], I. Hristova[16], J. Hrivnac[116], T. Hryn'ova[5], P.J. Hsu[82], S.-C. Hsu[139], D. Hu[35], X. Hu[25], Y. Huang[33a], Z. Hubacek[30], F. Hubaut[84], F. Huegging[21], A. Huettmann[42], T.B. Huffman[119], E.W. Hughes[35], G. Hughes[71], M. Huhtinen[30], T.A. Hülsing[82], M. Hurwitz[15], N. Huseynov[64,r], J. Huston[89], J. Huth[57], G. Iacobucci[49], G. Iakovidis[10], I. Ibragimov[142], L. Iconomidou-Fayard[116], J. Idarraga[116], P. Iengo[103a], O. Igonkina[106], Y. Ikegami[65], K. Ikematsu[142], M. Ikeno[65], D. Iliadis[155], N. Ilic[159], T. Ince[100], P. Ioannou[9], M. Iodice[135a], K. Iordanidou[9], V. Ippolito[133a,133b], A. Irles Quiles[168], C. Isaksson[167], M. Ishino[67], M. Ishitsuka[158], R. Ishmukhametov[110], C. Issever[119], S. Istin[19a], A.V. Ivashin[129], W. Iwanski[39], H. Iwasaki[65], J.M. Izen[41], V. Izzo[103a], B. Jackson[121], J.N. Jackson[73], P. Jackson[1], M.R. Jaekel[30], V. Jain[2], K. Jakobs[48], S. Jakobsen[36], T. Jakoubek[126], J. Jakubek[127], D.O. Jamin[152], D.K. Jana[112], E. Jansen[77], H. Jansen[30], J. Janssen[21], M. Janus[171], R.C. Jared[174],

JHEP10(2013)130

G. Jarlskog[80], L. Jeanty[57], G.-Y. Jeng[151], I. Jen-La Plante[31], D. Jennens[87], P. Jenni[30], J. Jentzsch[43], C. Jeske[171], S. Jézéquel[5], M.K. Jha[20a], H. Ji[174], W. Ji[82], J. Jia[149], Y. Jiang[33b], M. Jimenez Belenguer[42], S. Jin[33a], O. Jinnouchi[158], M.D. Joergensen[36], D. Joffe[40], K.E. Johansson[147a], P. Johansson[140], S. Johnert[42], K.A. Johns[7], K. Jon-And[147a,147b], G. Jones[171], R.W.L. Jones[71], T.J. Jones[73], P.M. Jorge[125a], K.D. Joshi[83], J. Jovicevic[148], X. Ju[174], C.A. Jung[43], R.M. Jungst[30], P. Jussel[61], A. Juste Rozas[12,p], M. Kaci[168], A. Kaczmarska[39], P. Kadlecik[36], M. Kado[116], H. Kagan[110], M. Kagan[144], E. Kajomovitz[153], S. Kalinin[176], S. Kama[40], N. Kanaya[156], M. Kaneda[30], S. Kaneti[28], T. Kanno[158], V.A. Kantserov[97], J. Kanzaki[65], B. Kaplan[109], A. Kapliy[31], D. Kar[53], K. Karakostas[10], N. Karastathis[10], M. Karnevskiy[82], S.N. Karpov[64], V. Kartvelishvili[71], A.N. Karyukhin[129], L. Kashif[174], G. Kasieczka[58b], R.D. Kass[110], A. Kastanas[14], Y. Kataoka[156], A. Katre[49], J. Katzy[42], V. Kaushik[7], K. Kawagoe[69], T. Kawamoto[156], G. Kawamura[54], S. Kazama[156], V.F. Kazanin[108], M.Y. Kazarinov[64], R. Keeler[170], P.T. Keener[121], R. Kehoe[40], M. Keil[54], J.S. Keller[139], H. Keoshkerian[5], O. Kepka[126], B.P. Kerševan[74], S. Kersten[176], K. Kessoku[156], J. Keung[159], F. Khalil-zada[11], H. Khandanyan[147a,147b], A. Khanov[113], D. Kharchenko[64], A. Khodinov[97], A. Khomich[58a], T.J. Khoo[28], G. Khoriauli[21], A. Khoroshilov[176], V. Khovanskiy[96], E. Khramov[64], J. Khubua[51b], H. Kim[147a,147b], S.H. Kim[161], N. Kimura[172], O. Kind[16], B.T. King[73], M. King[66], R.S.B. King[119], S.B. King[169], J. Kirk[130], A.E. Kiryunin[100], T. Kishimoto[66], D. Kisielewska[38a], T. Kitamura[66], T. Kittelmann[124], K. Kiuchi[161], E. Kladiva[145b], M. Klein[73], U. Klein[73], K. Kleinknecht[82], M. Klemetti[86], P. Klimek[147a,147b], A. Klimentov[25], R. Klingenberg[43], J.A. Klinger[83], E.B. Klinkby[36], T. Klioutchnikova[30], P.F. Klok[105], E.-E. Kluge[58a], P. Kluit[106], S. Kluth[100], E. Kneringer[61], E.B.F.G. Knoops[84], A. Knue[54], B.R. Ko[45], T. Kobayashi[156], M. Kobel[44], M. Kocian[144], P. Kodys[128], S. Koenig[82], P. Koevesarki[21], T. Koffas[29], E. Koffeman[106], L.A. Kogan[119], S. Kohlmann[176], F. Kohn[54], Z. Kohout[127], T. Kohriki[65], T. Koi[144], H. Kolanoski[16], I. Koletsou[90a], J. Koll[89], A.A. Komar[95], Y. Komori[156], T. Kondo[65], K. Köneke[48], A.C. König[105], T. Kono[65,s], R. Konoplich[109,t], N. Konstantinidis[77], R. Kopeliansky[153], S. Koperny[38a], L. Köpke[82], A.K. Kopp[48], K. Korcyl[39], K. Kordas[155], A. Korn[46], A.A. Korol[108], I. Korolkov[12], E.V. Korolkova[140], V.A. Korotkov[129], O. Kortner[100], S. Kortner[100], V.V. Kostyukhin[21], S. Kotov[100], V.M. Kotov[64], A. Kotwal[45], C. Kourkoumelis[9], V. Kouskoura[155], A. Koutsman[160a], R. Kowalewski[170], T.Z. Kowalski[38a], W. Kozanecki[137], A.S. Kozhin[129], V. Kral[127], V.A. Kramarenko[98], G. Kramberger[74], M.W. Krasny[79], A. Krasznahorkay[109], J.K. Kraus[21], A. Kravchenko[25], S. Kreiss[109], J. Kretzschmar[73], K. Kreutzfeldt[52], N. Krieger[54], P. Krieger[159], K. Kroeninger[54], H. Kroha[100], J. Kroll[121], J. Kroseberg[21], J. Krstic[13a], U. Kruchonak[64], H. Krüger[21], T. Kruker[17], N. Krumnack[63], Z.V. Krumshteyn[64], A. Kruse[174], M.C. Kruse[45], M. Kruskal[22], T. Kubota[87], S. Kuday[4a], S. Kuehn[48], A. Kugel[58c], T. Kuhl[42], V. Kukhtin[64], Y. Kulchitsky[91], S. Kuleshov[32b], M. Kuna[79], J. Kunkle[121], A. Kupco[126], H. Kurashige[66], M. Kurata[161], Y.A. Kurochkin[91], V. Kus[126], E.S. Kuwertz[148], M. Kuze[158], J. Kvita[143], R. Kwee[16], A. La Rosa[49], L. La Rotonda[37a,37b], L. Labarga[81], S. Lablak[136a], C. Lacasta[168], F. Lacava[133a,133b], J. Lacey[29], H. Lacker[16], D. Lacour[79], V.R. Lacuesta[168], E. Ladygin[64], R. Lafaye[5], B. Laforge[79], T. Lagouri[177], S. Lai[48], H. Laier[58a], E. Laisne[55], L. Lambourne[77], C.L. Lampen[7], W. Lampl[7], E. Lançon[137], U. Landgraf[48], M.P.J. Landon[75], V.S. Lang[58a], C. Lange[42], A.J. Lankford[164], F. Lanni[25], K. Lantzsch[30], A. Lanza[120a], S. Laplace[79], C. Lapoire[21], J.F. Laporte[137], T. Lari[90a], A. Larner[119], M. Lassnig[30], P. Laurelli[47], V. Lavorini[37a,37b], W. Lavrijsen[15], P. Laycock[73], B.T. Le[55], O. Le Dortz[79], E. Le Guirriec[84], E. Le Menedeu[12], T. LeCompte[6], F. Ledroit-Guillon[55], C.A. Lee[152], H. Lee[106], J.S.H. Lee[117], S.C. Lee[152], L. Lee[177], G. Lefebvre[79], M. Lefebvre[170], M. Legendre[137], F. Legger[99], C. Leggett[15], A. Lehan[73], M. Lehmacher[21], G. Lehmann Miotto[30], A.G. Leister[177], M.A.L. Leite[24d], R. Leitner[128], D. Lellouch[173], B. Lemmer[54], V. Lendermann[58a], K.J.C. Leney[146c], T. Lenz[106], G. Lenzen[176], B. Lenzi[30], R. Leone[7], K. Leonhardt[44], S. Leontsinis[10], C. Leroy[94], J-R. Lessard[170], C.G. Lester[28], C.M. Lester[121], J. Levêque[5], D. Levin[88], L.J. Levinson[173], A. Lewis[119], G.H. Lewis[109], A.M. Leyko[21], M. Leyton[16], B. Li[33b,u], B. Li[84], H. Li[149], H.L. Li[31], S. Li[45], X. Li[88], Z. Liang[119,v], H. Liao[34], B. Liberti[134a], P. Lichard[30],



JHEP10(2013)130

K. Lie[166], J. Liebal[21], W. Liebig[14], C. Limbach[21], A. Limosani[87], M. Limper[62], S.C. Lin[152,w], F. Linde[106], B.E. Lindquist[149], J.T. Linnemann[89], E. Lipeles[121], A. Lipniacka[14], M. Lisovyi[42], T.M. Liss[166], D. Lissauer[25], A. Lister[169], A.M. Litke[138], B. Liu[152], D. Liu[152], J.B. Liu[33b], K. Liu[33b,x], L. Liu[88], M. Liu[45], M. Liu[33b], Y. Liu[33b], M. Livan[120a,120b], S.S.A. Livermore[119], A. Lleres[55], J. Llorente Merino[81], S.L. Lloyd[75], F. Lo Sterzo[133a,133b], E. Lobodzinska[42], P. Loch[7], W.S. Lockman[138], T. Loddenkoetter[21], F.K. Loebinger[83], A.E. Loevschall-Jensen[36], A. Loginov[177], C.W. Loh[169], T. Lohse[16], K. Lohwasser[48], M. Lokajicek[126], V.P. Lombardo[5], R.E. Long[71], L. Lopes[125a], D. Lopez Mateos[57], B. Lopez Paredes[140], J. Lorenz[99], N. Lorenzo Martinez[116], M. Losada[163], P. Loscutoff[15], M.J. Losty[160a,*], X. Lou[41], A. Lounis[116], K.F. Loureiro[163], J. Love[6], P.A. Love[71], A.J. Lowe[144,f], F. Lu[33a], H.J. Lubatti[139], C. Luci[133a,133b], A. Lucotte[55], D. Ludwig[42], I. Ludwig[48], J. Ludwig[48], F. Luehring[60], W. Lukas[61], L. Luminari[133a], E. Lund[118], J. Lundberg[147a,147b], O. Lundberg[147a,147b], B. Lund-Jensen[148], M. Lungwitz[82], D. Lynn[25], R. Lysak[126], E. Lytken[80], H. Ma[25], L.L. Ma[33d], G. Maccarrone[47], A. Macchiolo[100], B. Maček[74], J. Machado Miguens[125a], D. Macina[30], R. Mackeprang[36], R. Madar[48], R.J. Madaras[15], H.J. Maddocks[71], W.F. Mader[44], A. Madsen[167], M. Maeno[5], T. Maeno[25], L. Magnoni[164], E. Magradze[54], K. Mahboubi[48], J. Mahlstedt[106], S. Mahmoud[73], G. Mahout[18], C. Maiani[137], C. Maidantchik[24a], A. Maio[125a,c], S. Majewski[115], Y. Makida[65], N. Makovec[116], P. Mal[137,y], B. Malaescu[79], Pa. Malecki[39], V.P. Maleev[122], F. Malek[55], U. Mallik[62], D. Malon[6], C. Malone[144], S. Maltezos[10], V.M. Malyshev[108], S. Malyukov[30], J. Mamuzic[13b], L. Mandelli[90a], I. Mandić[74], R. Mandrysch[62], J. Maneira[125a], A. Manfredini[100], L. Manhaes de Andrade Filho[24b], J.A. Manjarres Ramos[137], A. Mann[99], P.M. Manning[138], A. Manousakis-Katsikakis[9], B. Mansoulie[137], R. Mantifel[86], L. Mapelli[30], L. March[168], J.F. Marchand[29], F. Marchese[134a,134b], G. Marchiori[79], M. Marcisovsky[126], C.P. Marino[170], C.N. Marques[125a], F. Marroquim[24a], Z. Marshall[121], L.F. Marti[17], S. Marti-Garcia[168], B. Martin[30], B. Martin[89], J.P. Martin[94], T.A. Martin[171], V.J. Martin[46], B. Martin dit Latour[49], H. Martinez[137], M. Martinez[12,p], S. Martin-Haugh[150], A.C. Martyniuk[170], M. Marx[83], F. Marzano[133a], A. Marzin[112], L. Masetti[82], T. Mashimo[156], R. Mashinistov[95], J. Masik[83], A.L. Maslennikov[108], I. Massa[20a,20b], N. Massol[5], P. Mastrandrea[149], A. Mastroberardino[37a,37b], T. Masubuchi[156], H. Matsunaga[156], T. Matsushita[66], P. Mättig[176], S. Mättig[42], J. Mattmann[82], C. Mattravers[119,d], J. Maurer[84], S.J. Maxfield[73], D.A. Maximov[108,g], R. Mazini[152], L. Mazzaferro[134a,134b], M. Mazzanti[90a], S.P. Mc Kee[88], A. McCarn[166], R.L. McCarthy[149], T.G. McCarthy[29], N.A. McCubbin[130], K.W. McFarlane[56,*], J.A. Mcfayden[140], G. Mchedlidze[51b], T. Mclaughlan[18], S.J. McMahon[130], R.A. McPherson[170,j], A. Meade[85], J. Mechnich[106], M. Mechtel[176], M. Medinnis[42], S. Meehan[31], R. Meera-Lebbai[112], S. Mehlhase[36], A. Mehta[73], K. Meier[58a], C. Meineck[99], B. Meirose[80], C. Melachrinos[31], B.R. Mellado Garcia[146c], F. Meloni[90a,90b], L. Mendoza Navas[163], A. Mengarelli[20a,20b], S. Menke[100], E. Meoni[162], K.M. Mercurio[57], S. Mergelmeyer[21], N. Meric[137], P. Mermod[49], L. Merola[103a,103b], C. Meroni[90a], F.S. Merritt[31], H. Merritt[110], A. Messina[30,z], J. Metcalfe[25], A.S. Mete[164], C. Meyer[82], C. Meyer[31], J-P. Meyer[137], J. Meyer[30], J. Meyer[54], S. Michal[30], R.P. Middleton[130], S. Migas[73], L. Mijović[137], G. Mikenberg[173], M. Mikestikova[126], M. Mikuž[74], D.W. Miller[31], W.J. Mills[169], C. Mills[57], A. Milov[173], D.A. Milstead[147a,147b], D. Milstein[173], A.A. Minaenko[129], M. Miñano Moya[168], I.A. Minashvili[64], A.I. Mincer[109], B. Mindur[38a], M. Mineev[64], Y. Ming[174], L.M. Mir[12], G. Mirabelli[133a], T. Mitani[172], J. Mitrevski[138], V.A. Mitsou[168], S. Mitsui[65], P.S. Miyagawa[140], J.U. Mjörnmark[80], T. Moa[147a,147b], V. Moeller[28], S. Mohapatra[149], W. Mohr[48], R. Moles-Valls[168], A. Molfetas[30], K. Mönig[42], C. Monini[55], J. Monk[36], E. Monnier[84], J. Montejo Berlingen[12], F. Monticelli[70], S. Monzani[20a,20b], R.W. Moore[3], C. Mora Herrera[49], A. Moraes[53], N. Morange[62], J. Morel[54], D. Moreno[82], M. Moreno Llácer[168], P. Morettini[50a], M. Morgenstern[44], M. Morii[57], S. Moritz[82], A.K. Morley[148], G. Mornacchi[30], J.D. Morris[75], L. Morvaj[102], H.G. Moser[100], M. Mosidze[51b], J. Moss[110], R. Mount[144], E. Mountricha[10,aa], S.V. Mouraviev[95,*], E.J.W. Moyse[85], R.D. Mudd[18], F. Mueller[58a], J. Mueller[124], K. Mueller[21], T. Mueller[28], T. Mueller[82], D. Muenstermann[49], Y. Munwes[154], J.A. Murillo Quijada[18], W.J. Murray[130], I. Mussche[106], E. Musto[153], A.G. Myagkov[129,ab], M. Myska[126],

JHEP10(2013)130

O. Nackenhorst[54], J. Nadal[12], K. Nagai[61], R. Nagai[158], Y. Nagai[84], K. Nagano[65], A. Nagarkar[110], Y. Nagasaka[59], M. Nagel[100], A.M. Nairz[30], Y. Nakahama[30], K. Nakamura[65], T. Nakamura[156], I. Nakano[111], H. Namasivayam[41], G. Nanava[21], A. Napier[162], R. Narayan[58b], M. Nash[77,d], T. Nattermann[21], T. Naumann[42], G. Navarro[163], H.A. Neal[88], P.Yu. Nechaeva[95], T.J. Neep[83], A. Negri[120a,120b], G. Negri[30], M. Negrini[20a], S. Nektarijevic[49], A. Nelson[164], T.K. Nelson[144], S. Nemecek[126], P. Nemethy[109], A.A. Nepomuceno[24a], M. Nessi[30,ac], M.S. Neubauer[166], M. Neumann[176], A. Neusiedl[82], R.M. Neves[109], P. Nevski[25], F.M. Newcomer[121], P.R. Newman[18], D.H. Nguyen[6], V. Nguyen Thi Hong[137], R.B. Nickerson[119], R. Nicolaidou[137], B. Nicquevert[30], J. Nielsen[138], N. Nikiforou[35], A. Nikiforov[16], V. Nikolaenko[129,ab], I. Nikolic-Audit[79], K. Nikolics[49], K. Nikolopoulos[18], P. Nilsson[8], Y. Ninomiya[156], A. Nisati[133a], R. Nisius[100], T. Nobe[158], L. Nodulman[6], M. Nomachi[117], I. Nomidis[155], S. Norberg[112], M. Nordberg[30], J. Novakova[128], M. Nozaki[65], L. Nozka[114], K. Ntekas[10], A.-E. Nuncio-Quiroz[21], G. Nunes Hanninger[87], T. Nunnemann[99], E. Nurse[77], B.J. O'Brien[46], F. O'grady[7], D.C. O'Neil[143], V. O'Shea[53], L.B. Oakes[99], F.G. Oakham[29,e], H. Oberlack[100], J. Ocariz[79], A. Ochi[66], M.I. Ochoa[77], S. Oda[69], S. Odaka[65], J. Odier[84], H. Ogren[60], A. Oh[83], S.H. Oh[45], C.C. Ohm[30], T. Ohshima[102], W. Okamura[117], H. Okawa[25], Y. Okumura[31], T. Okuyama[156], A. Olariu[26a], A.G. Olchevski[64], S.A. Olivares Pino[46], M. Oliveira[125a,h], D. Oliveira Damazio[25], E. Oliver Garcia[168], D. Olivito[121], A. Olszewski[39], J. Olszowska[39], A. Onofre[125a,ad], P.U.E. Onyisi[31,ae], C.J. Oram[160a], M.J. Oreglia[31], Y. Oren[154], D. Orestano[135a,135b], N. Orlando[72a,72b], C. Oropeza Barrera[53], R.S. Orr[159], B. Osculati[50a,50b], R. Ospanov[121], G. Otero y Garzon[27], H. Otono[69], J.P. Ottersbach[106], M. Ouchrif[136d], E.A. Ouellette[170], F. Ould-Saada[118], A. Ouraou[137], K.P. Oussoren[106], Q. Ouyang[33a], A. Ovcharova[15], M. Owen[83], S. Owen[140], V.E. Ozcan[19a], N. Ozturk[8], K. Pachal[119], A. Pacheco Pages[12], C. Padilla Aranda[12], S. Pagan Griso[15], E. Paganis[140], C. Pahl[100], F. Paige[25], P. Pais[85], K. Pajchel[118], G. Palacino[160b], C.P. Paleari[7], S. Palestini[30], D. Pallin[34], A. Palma[125a], J.D. Palmer[18], Y.B. Pan[174], E. Panagiotopoulou[10], J.G. Panduro Vazquez[76], P. Pani[106], N. Panikashvili[88], S. Panitkin[25], D. Pantea[26a], A. Papadelis[147a], Th.D. Papadopoulou[10], K. Papageorgiou[155,o], A. Paramonov[6], D. Paredes Hernandez[34], M.A. Parker[28], F. Parodi[50a,50b], J.A. Parsons[35], U. Parzefall[48], S. Pashapour[54], E. Pasqualucci[133a], S. Passaggio[50a], A. Passeri[135a], F. Pastore[135a,135b,*], Fr. Pastore[76], G. Pásztor[49,af], S. Pataraia[176], N.D. Patel[151], J.R. Pater[83], S. Patricelli[103a,103b], T. Pauly[30], J. Pearce[170], M. Pedersen[118], S. Pedraza Lopez[168], M.I. Pedraza Morales[174], S.V. Peleganchuk[108], D. Pelikan[167], H. Peng[33b], B. Penning[31], A. Penson[35], J. Penwell[60], D.V. Perepelitsa[35], T. Perez Cavalcanti[42], E. Perez Codina[160a], M.T. Pérez García-Estañ[168], V. Perez Reale[35], L. Perini[90a,90b], H. Pernegger[30], R. Perrino[72a], V.D. Peshekhonov[64], K. Peters[30], R.F.Y. Peters[54,ag], B.A. Petersen[30], J. Petersen[30], T.C. Petersen[36], E. Petit[5], A. Petridis[147a,147b], C. Petridou[155], E. Petrolo[133a], F. Petrucci[135a,135b], M. Petteni[143], R. Pezoa[32b], A. Phan[87], P.W. Phillips[130], G. Piacquadio[144], E. Pianori[171], A. Picazio[49], E. Piccaro[75], M. Piccinini[20a,20b], S.M. Piec[42], R. Piegaia[27], D.T. Pignotti[110], J.E. Pilcher[31], A.D. Pilkington[77], J. Pina[125a,c], M. Pinamonti[165a,165c,ah], A. Pinder[119], J.L. Pinfold[3], A. Pingel[36], B. Pinto[125a], C. Pizio[90a,90b], M.-A. Pleier[25], V. Pleskot[128], E. Plotnikova[64], P. Plucinski[147a,147b], S. Poddar[58a], F. Podlyski[34], R. Poettgen[82], L. Poggioli[116], D. Pohl[21], M. Pohl[49], G. Polesello[120a], A. Policicchio[37a,37b], R. Polifka[159], A. Polini[20a], C.S. Pollard[45], V. Polychronakos[25], D. Pomeroy[23], K. Pommès[30], L. Pontecorvo[133a], B.G. Pope[89], G.A. Popeneciu[26b], D.S. Popovic[13a], A. Poppleton[30], X. Portell Bueso[12], G.E. Pospelov[100], S. Pospisil[127], I.N. Potrap[64], C.J. Potter[150], C.T. Potter[115], G. Poulard[30], J. Poveda[60], V. Pozdnyakov[64], R. Prabhu[77], P. Pralavorio[84], A. Pranko[15], S. Prasad[30], R. Pravahan[25], S. Prell[63], D. Price[60], J. Price[73], L.E. Price[6], D. Prieur[124], M. Primavera[72a], M. Proissl[46], K. Prokofiev[109], F. Prokoshin[32b], E. Protopapadaki[137], S. Protopopescu[25], J. Proudfoot[6], X. Prudent[44], M. Przybycien[38a], H. Przysiezniak[5], S. Psoroulas[21], E. Ptacek[115], E. Pueschel[85], D. Puldon[149], M. Purohit[25,ai], P. Puzo[116], Y. Pylypchenko[62], J. Qian[88], A. Quadt[54], D.R. Quarrie[15], W.B. Quayle[146c], D. Quilty[53], M. Raas[105], V. Radeka[25], V. Radescu[42], P. Radloff[115], F. Ragusa[90a,90b], G. Rahal[179], S. Rajagopalan[25], M. Rammensee[48], M. Rammes[142], A.S. Randle-Conde[40], C. Rangel-Smith[79],



JHEP10(2013)130

K. Rao[164], F. Rauscher[99], T.C. Rave[48], T. Ravenscroft[53], M. Raymond[30], A.L. Read[118], D.M. Rebuzzi[120a,120b], A. Redelbach[175], G. Redlinger[25], R. Reece[121], K. Reeves[41], A. Reinsch[115], H. Reisin[27], I. Reisinger[43], M. Relich[164], C. Rembser[30], Z.L. Ren[152], A. Renaud[116], M. Rescigno[133a], S. Resconi[90a], B. Resende[137], P. Reznicek[99], R. Rezvani[94], R. Richter[100], E. Richter-Was[38b], M. Ridel[79], P. Rieck[16], M. Rijssenbeek[149], A. Rimoldi[120a,120b], L. Rinaldi[20a], R.R. Rios[40], E. Ritsch[61], I. Riu[12], G. Rivoltella[90a,90b], F. Rizatdinova[113], E. Rizvi[75], S.H. Robertson[86,j], A. Robichaud-Veronneau[119], D. Robinson[28], J.E.M. Robinson[83], A. Robson[53], J.G. Rocha de Lima[107], C. Roda[123a,123b], D. Roda Dos Santos[30], A. Roe[54], S. Roe[30], O. Røhne[118], S. Rolli[162], A. Romaniouk[97], M. Romano[20a,20b], G. Romeo[27], E. Romero Adam[168], N. Rompotis[139], L. Roos[79], E. Ros[168], S. Rosati[133a], K. Rosbach[49], A. Rose[150], M. Rose[76], P.L. Rosendahl[14], O. Rosenthal[142], V. Rossetti[12], E. Rossi[133a,133b], L.P. Rossi[50a], M. Rotaru[26a], I. Roth[173], J. Rothberg[139], D. Rousseau[116], C.R. Royon[137], A. Rozanov[84], Y. Rozen[153], X. Ruan[146c], F. Rubbo[12], I. Rubinskiy[42], N. Ruckstuhl[106], V.I. Rud[98], C. Rudolph[44], M.S. Rudolph[159], F. Rühr[7], A. Ruiz-Martinez[63], L. Rumyantsev[64], Z. Rurikova[48], N.A. Rusakovich[64], A. Ruschke[99], J.P. Rutherfoord[7], N. Ruthmann[48], P. Ruzicka[126], Y.F. Ryabov[122], M. Rybar[128], G. Rybkin[116], N.C. Ryder[119], A.F. Saavedra[151], A. Saddique[3], I. Sadeh[154], H.F-W. Sadrozinski[138], R. Sadykov[64], F. Safai Tehrani[133a], H. Sakamoto[156], G. Salamanna[75], A. Salamon[134a], M. Saleem[112], D. Salek[30], D. Salihagic[100], A. Salnikov[144], J. Salt[168], B.M. Salvachua Ferrando[6], D. Salvatore[37a,37b], F. Salvatore[150], A. Salvucci[105], A. Salzburger[30], D. Sampsonidis[155], A. Sanchez[103a,103b], J. Sánchez[168], V. Sanchez Martinez[168], H. Sandaker[14], H.G. Sander[82], M.P. Sanders[99], M. Sandhoff[176], T. Sandoval[28], C. Sandoval[163], R. Sandstroem[100], D.P.C. Sankey[130], A. Sansoni[47], C. Santoni[34], R. Santonico[134a,134b], H. Santos[125a], I. Santoyo Castillo[150], K. Sapp[124], A. Sapronov[64], J.G. Saraiva[125a], T. Sarangi[174], E. Sarkisyan-Grinbaum[8], B. Sarrazin[21], F. Sarri[123a,123b], G. Sartisohn[176], O. Sasaki[65], Y. Sasaki[156], N. Sasao[67], I. Satsounkevitch[91], G. Sauvage[5,*], E. Sauvan[5], J.B. Sauvan[116], P. Savard[159,e], V. Savinov[124], D.O. Savu[30], C. Sawyer[119], L. Sawyer[78,l], D.H. Saxon[53], J. Saxon[121], C. Sbarra[20a], A. Sbrizzi[3], D.A. Scannicchio[164], M. Scarcella[151], J. Schaarschmidt[116], P. Schacht[100], D. Schaefer[121], A. Schaelicke[46], S. Schaepe[21], S. Schaetzel[58b], U. Schäfer[82], A.C. Schaffer[116], D. Schaile[99], R.D. Schamberger[149], V. Scharf[58a], V.A. Schegelsky[122], D. Scheirich[88], M. Schernau[164], M.I. Scherzer[35], C. Schiavi[50a,50b], J. Schieck[99], C. Schillo[48], M. Schioppa[37a,37b], S. Schlenker[30], E. Schmidt[48], K. Schmieden[30], C. Schmitt[82], C. Schmitt[99], S. Schmitt[58b], B. Schneider[17], Y.J. Schnellbach[73], U. Schnoor[44], L. Schoeffel[137], A. Schoening[58b], A.L.S. Schorlemmer[54], M. Schott[82], D. Schouten[160a], J. Schovancova[126], M. Schram[86], C. Schroeder[82], N. Schroer[58c], M.J. Schultens[21], H.-C. Schultz-Coulon[58a], H. Schulz[16], M. Schumacher[48], B.A. Schumm[138], Ph. Schune[137], A. Schwartzman[144], Ph. Schwegler[100], Ph. Schwemling[137], R. Schwienhorst[89], J. Schwindling[137], T. Schwindt[21], M. Schwoerer[5], F.G. Sciacca[17], E. Scifo[116], G. Sciolla[23], W.G. Scott[130], F. Scutti[21], J. Searcy[88], G. Sedov[42], E. Sedykh[122], S.C. Seidel[104], A. Seiden[138], F. Seifert[44], J.M. Seixas[24a], G. Sekhniaidze[103a], S.J. Sekula[40], K.E. Selbach[46], D.M. Seliverstov[122], G. Sellers[73], M. Seman[145b], N. Semprini-Cesari[20a,20b], C. Serfon[30], L. Serin[116], L. Serkin[54], T. Serre[84], R. Seuster[160a], H. Severini[112], A. Sfyrla[30], E. Shabalina[54], M. Shamim[115], L.Y. Shan[33a], J.T. Shank[22], Q.T. Shao[87], M. Shapiro[15], P.B. Shatalov[96], K. Shaw[165a,165c], P. Sherwood[77], S. Shimizu[66], M. Shimojima[101], T. Shin[56], M. Shiyakova[64], A. Shmeleva[95], M.J. Shochet[31], D. Short[119], S. Shrestha[63], E. Shulga[97], M.A. Shupe[7], S. Shushkevich[42], P. Sicho[126], A. Sidoti[133a], F. Siegert[48], Dj. Sijacki[13a], O. Silbert[173], J. Silva[125a], Y. Silver[154], D. Silverstein[144], S.B. Silverstein[147a], V. Simak[127], O. Simard[5], Lj. Simic[13a], S. Simion[116], E. Simioni[82], B. Simmons[77], R. Simoniello[90a,90b], M. Simonyan[36], P. Sinervo[159], N.B. Sinev[115], V. Sipica[142], G. Siragusa[175], A. Sircar[78], A.N. Sisakyan[64,*], S.Yu. Sivoklokov[98], J. Sjölin[147a,147b], T.B. Sjursen[14], L.A. Skinnari[15], H.P. Skottowe[57], K.Yu. Skovpen[108], P. Skubic[112], M. Slater[18], T. Slavicek[127], K. Sliwa[162], V. Smakhtin[173], B.H. Smart[46], L. Smestad[118], S.Yu. Smirnov[97], Y. Smirnov[97], L.N. Smirnova[98,aj], O. Smirnova[80], K.M. Smith[53], M. Smizanska[71], K. Smolek[127], A.A. Snesarev[95], G. Snidero[75], J. Snow[112], S. Snyder[25], R. Sobie[170,j], J. Sodomka[127], A. Soffer[154],

JHEP10(2013)130

D.A. Soh[152,v], C.A. Solans[30], M. Solar[127], J. Solc[127], E.Yu. Soldatov[97], U. Soldevila[168], E. Solfaroli Camillocci[133a,133b], A.A. Solodkov[129], O.V. Solovyanov[129], V. Solovyev[122], N. Soni[1], A. Sood[15], V. Sopko[127], B. Sopko[127], M. Sosebee[8], R. Soualah[165a,165c], P. Soueid[94], A.M. Soukharev[108], D. South[42], S. Spagnolo[72a,72b], F. Spanò[76], W.R. Spearman[57], R. Spighi[20a], G. Spigo[30], M. Spousta[128,ak], T. Spreitzer[159], B. Spurlock[8], R.D. St. Denis[53], J. Stahlman[121], R. Stamen[58a], E. Stanecka[39], R.W. Stanek[6], C. Stanescu[135a], M. Stanescu-Bellu[42], M.M. Stanitzki[42], S. Stapnes[118], E.A. Starchenko[129], J. Stark[55], P. Staroba[126], P. Starovoitov[42], R. Staszewski[39], A. Staude[99], P. Stavina[145a,*], G. Steele[53], P. Steinbach[44], P. Steinberg[25], I. Stekl[127], B. Stelzer[143], H.J. Stelzer[89], O. Stelzer-Chilton[160a], H. Stenzel[52], S. Stern[100], G.A. Stewart[30], J.A. Stillings[21], M.C. Stockton[86], M. Stoebe[86], K. Stoerig[48], G. Stoicea[26a], S. Stonjek[100], A.R. Stradling[8], A. Straessner[44], J. Strandberg[148], S. Strandberg[147a,147b], A. Strandlie[118], M. Strang[110], E. Strauss[144], M. Strauss[112], P. Strizenec[145b], R. Ströhmer[175], D.M. Strom[115], J.A. Strong[76,*], R. Stroynowski[40], B. Stugu[14], I. Stumer[25,*], J. Stupak[149], P. Sturm[176], N.A. Styles[42], D. Su[144], HS. Subramania[3], R. Subramaniam[78], A. Succurro[12], Y. Sugaya[117], C. Suhr[107], M. Suk[127], V.V. Sulin[95], S. Sultansoy[4c], T. Sumida[67], X. Sun[55], J.E. Sundermann[48], K. Suruliz[140], G. Susinno[37a,37b], M.R. Sutton[150], Y. Suzuki[65], M. Svatos[126], S. Swedish[169], M. Swiatlowski[144], I. Sykora[145a], T. Sykora[128], D. Ta[106], K. Tackmann[42], A. Taffard[164], R. Tafirout[160a], N. Taiblum[154], Y. Takahashi[102], H. Takai[25], R. Takashima[68], H. Takeda[66], T. Takeshita[141], Y. Takubo[65], M. Talby[84], A.A. Talyshev[108,g], J.Y.C. Tam[175], M.C. Tamsett[78,al], K.G. Tan[87], J. Tanaka[156], R. Tanaka[116], S. Tanaka[132], S. Tanaka[65], A.J. Tanasijczuk[143], K. Tani[66], N. Tannoury[84], S. Tapprogge[82], S. Tarem[153], F. Tarrade[29], G.F. Tartarelli[90a], P. Tas[128], M. Tasevsky[126], T. Tashiro[67], E. Tassi[37a,37b], A. Tavares Delgado[125a], Y. Tayalati[136d], C. Taylor[77], F.E. Taylor[93], G.N. Taylor[87], W. Taylor[160b], M. Teinturier[116], F.A. Teischinger[30], M. Teixeira Dias Castanheira[75], P. Teixeira-Dias[76], K.K. Temming[48], H. Ten Kate[30], P.K. Teng[152], S. Terada[65], K. Terashi[156], J. Terron[81], M. Testa[47], R.J. Teuscher[159,j], J. Therhaag[21], T. Theveneaux-Pelzer[34], S. Thoma[48], J.P. Thomas[18], E.N. Thompson[35], P.D. Thompson[18], P.D. Thompson[159], A.S. Thompson[53], L.A. Thomsen[36], E. Thomson[121], M. Thomson[28], W.M. Thong[87], R.P. Thun[88,*], F. Tian[35], M.J. Tibbetts[15], T. Tic[126], V.O. Tikhomirov[95,am], Yu.A. Tikhonov[108,g], S. Timoshenko[97], E. Tiouchichine[84], P. Tipton[177], S. Tisserant[84], T. Todorov[5], S. Todorova-Nova[128], B. Toggerson[164], J. Tojo[69], S. Tokár[145a], K. Tokushuku[65], K. Tollefson[89], L. Tomlinson[83], M. Tomoto[102], L. Tompkins[31], K. Toms[104], A. Tonoyan[14], C. Topfel[17], N.D. Topilin[64], E. Torrence[115], H. Torres[79], E. Torró Pastor[168], J. Toth[84,af], F. Touchard[84], D.R. Tovey[140], H.L. Tran[116], T. Trefzger[175], L. Tremblet[30], A. Tricoli[30], I.M. Trigger[160a], S. Trincaz-Duvoid[79], M.F. Tripiana[70], N. Triplett[25], W. Trischuk[159], B. Trocmé[55], C. Troncon[90a], M. Trottier-McDonald[143], M. Trovatelli[135a,135b], P. True[89], M. Trzebinski[39], A. Trzupek[39], C. Tsarouchas[30], J.C-L. Tseng[119], M. Tsiakiris[106], P.V. Tsiareshka[91], D. Tsionou[137], G. Tsipolitis[10], S. Tsiskaridze[12], V. Tsiskaridze[48], E.G. Tskhadadze[51a], I.I. Tsukerman[96], V. Tsulaia[15], J.-W. Tsung[21], S. Tsuno[65], D. Tsybychev[149], A. Tua[140], A. Tudorache[26a], V. Tudorache[26a], J.M. Tuggle[31], A.N. Tuna[121], S. Turchikhin[98,aj], D. Turecek[127], I. Turk Cakir[4d], R. Turra[90a,90b], P.M. Tuts[35], A. Tykhonov[74], M. Tylmad[147a,147b], M. Tyndel[130], K. Uchida[21], I. Ueda[156], R. Ueno[29], M. Ughetto[84], M. Ugland[14], M. Uhlenbrock[21], F. Ukegawa[161], G. Unal[30], A. Undrus[25], G. Unel[164], F.C. Ungaro[48], Y. Unno[65], D. Urbaniec[35], P. Urquijo[21], G. Usai[8], A. Usanova[61], L. Vacavant[84], V. Vacek[127], B. Vachon[86], S. Vahsen[15], N. Valencic[106], S. Valentinetti[20a,20b], A. Valero[168], L. Valery[34], S. Valkar[128], E. Valladolid Gallego[168], S. Vallecorsa[153], J.A. Valls Ferrer[168], R. Van Berg[121], P.C. Van Der Deijl[106], R. van der Geer[106], H. van der Graaf[106], R. Van Der Leeuw[106], D. van der Ster[30], N. van Eldik[30], P. van Gemmeren[6], J. Van Nieuwkoop[143], I. van Vulpen[106], M. Vanadia[100], W. Vandelli[30], A. Vaniachine[6], P. Vankov[42], F. Vannucci[79], R. Vari[133a], E.W. Varnes[7], T. Varol[85], D. Varouchas[15], A. Vartapetian[8], K.E. Varvell[151], V.I. Vassilakopoulos[56], F. Vazeille[34], T. Vazquez Schroeder[54], J. Veatch[7], F. Veloso[125a], S. Veneziano[133a], A. Ventura[72a,72b], D. Ventura[85], M. Venturi[48], N. Venturi[159], V. Vercesi[120a], M. Verducci[139], W. Verkerke[106], J.C. Vermeulen[106], A. Vest[44],



JHEP10(2013)130

M.C. Vetterli[143,e], I. Vichou[166], T. Vickey[146c,an], O.E. Vickey Boeriu[146c], G.H.A. Viehhauser[119], S. Viel[169], R. Vigne[30], M. Villa[20a,20b], M. Villaplana Perez[168], E. Vilucchi[47], M.G. Vincter[29], V.B. Vinogradov[64], J. Virzi[15], O. Vitells[173], M. Viti[42], I. Vivarelli[48], F. Vives Vaque[3], S. Vlachos[10], D. Vladoiu[99], M. Vlasak[127], A. Vogel[21], P. Vokac[127], G. Volpi[47], M. Volpi[87], G. Volpini[90a], H. von der Schmitt[100], H. von Radziewski[48], E. von Toerne[21], V. Vorobel[128], M. Vos[168], R. Voss[30], J.H. Vossebeld[73], N. Vranjes[137], M. Vranjes Milosavljevic[106], V. Vrba[126], M. Vreeswijk[106], T. Vu Anh[48], R. Vuillermet[30], I. Vukotic[31], Z. Vykydal[127], W. Wagner[176], P. Wagner[21], S. Wahrmund[44], J. Wakabayashi[102], S. Walch[88], J. Walder[71], R. Walker[99], W. Walkowiak[142], R. Wall[177], P. Waller[73], B. Walsh[177], C. Wang[45], H. Wang[174], H. Wang[40], J. Wang[152], J. Wang[33a], K. Wang[86], R. Wang[104], S.M. Wang[152], T. Wang[21], X. Wang[177], A. Warburton[86], C.P. Ward[28], D.R. Wardrope[77], M. Warsinsky[48], A. Washbrook[46], C. Wasicki[42], I. Watanabe[66], P.M. Watkins[18], A.T. Watson[18], I.J. Watson[151], M.F. Watson[18], G. Watts[139], S. Watts[83], A.T. Waugh[151], B.M. Waugh[77], M.S. Weber[17], J.S. Webster[31], A.R. Weidberg[119], P. Weigell[100], J. Weingarten[54], C. Weiser[48], H. Weits[106], P.S. Wells[30], T. Wenaus[25], D. Wendland[16], Z. Weng[152,v], T. Wengler[30], S. Wenig[30], N. Wermes[21], M. Werner[48], P. Werner[30], M. Werth[164], M. Wessels[58a], J. Wetter[162], K. Whalen[29], A. White[8], M.J. White[87], R. White[32b], S. White[123a,123b], D. Whiteson[164], D. Whittington[60], D. Wicke[176], F.J. Wickens[130], W. Wiedenmann[174], M. Wielers[80,d], P. Wienemann[21], C. Wiglesworth[36], L.A.M. Wiik-Fuchs[21], P.A. Wijeratne[77], A. Wildauer[100], M.A. Wildt[42,ao], I. Wilhelm[128], H.G. Wilkens[30], J.Z. Will[99], E. Williams[35], H.H. Williams[121], S. Williams[28], W. Willis[35,*], S. Willocq[85], J.A. Wilson[18], A. Wilson[88], I. Wingerter-Seez[5], S. Winkelmann[48], F. Winklmeier[30], M. Wittgen[144], T. Wittig[43], J. Wittkowski[99], S.J. Wollstadt[82], M.W. Wolter[39], H. Wolters[125a,h], W.C. Wong[41], G. Wooden[88], B.K. Wosiek[39], J. Wotschack[30], M.J. Woudstra[83], K.W. Wozniak[39], K. Wraight[53], M. Wright[53], B. Wrona[73], S.L. Wu[174], X. Wu[49], Y. Wu[88], E. Wulf[35], B.M. Wynne[46], S. Xella[36], M. Xiao[137], C. Xu[33b,aa], D. Xu[33a], L. Xu[33b,ap], B. Yabsley[151], S. Yacoob[146b,aq], M. Yamada[65], H. Yamaguchi[156], Y. Yamaguchi[156], A. Yamamoto[65], K. Yamamoto[63], S. Yamamoto[156], T. Yamamura[156], T. Yamanaka[156], K. Yamauchi[102], Y. Yamazaki[66], Z. Yan[22], H. Yang[33e], H. Yang[174], U.K. Yang[83], Y. Yang[110], Z. Yang[147a,147b], S. Yanush[92], L. Yao[33a], Y. Yasu[65], E. Yatsenko[42], K.H. Yau Wong[21], J. Ye[40], S. Ye[25], A.L. Yen[57], E. Yildirim[42], M. Yilmaz[4b], R. Yoosoofmiya[124], K. Yorita[172], R. Yoshida[6], K. Yoshihara[156], C. Young[144], C.J.S. Young[119], S. Youssef[22], D.R. Yu[15], J. Yu[8], J. Yu[113], L. Yuan[66], A. Yurkewicz[107], B. Zabinski[39], R. Zaidan[62], A.M. Zaitsev[129,ab], S. Zambito[23], L. Zanello[133a,133b], D. Zanzi[100], A. Zaytsev[25], C. Zeitnitz[176], M. Zeman[127], A. Zemla[39], O. Zenin[129], T. Ženiš[145a], D. Zerwas[116], G. Zevi della Porta[57], D. Zhang[88], H. Zhang[89], J. Zhang[6], L. Zhang[152], X. Zhang[33d], Z. Zhang[116], Z. Zhao[33b], A. Zhemchugov[64], J. Zhong[119], B. Zhou[88], N. Zhou[164], C.G. Zhu[33d], H. Zhu[42], J. Zhu[88], Y. Zhu[33b], X. Zhuang[33a], A. Zibell[99], D. Zieminska[60], N.I. Zimin[64], C. Zimmermann[82], R. Zimmermann[21], S. Zimmermann[21], S. Zimmermann[48], Z. Zinonos[123a,123b], M. Ziolkowski[142], R. Zitoun[5], L. Živković[35], G. Zobernig[174], A. Zoccoli[20a,20b], M. zur Nedden[16], G. Zurzolo[103a,103b], V. Zutshi[107], L. Zwalinski[30]

[1] School of Chemistry and Physics, University of Adelaide, Adelaide, Australia
[2] Physics Department, SUNY Albany, Albany NY, United States of America
[3] Department of Physics, University of Alberta, Edmonton AB, Canada
[4] [(a)] Department of Physics, Ankara University, Ankara; [(b)] Department of Physics, Gazi University, Ankara; [(c)] Division of Physics, TOBB University of Economics and Technology, Ankara; [(d)] Turkish Atomic Energy Authority, Ankara, Turkey
[5] LAPP, CNRS/IN2P3 and Université de Savoie, Annecy-le-Vieux, France
[6] High Energy Physics Division, Argonne National Laboratory, Argonne IL, United States of America
[7] Department of Physics, University of Arizona, Tucson AZ, United States of America
[8] Department of Physics, The University of Texas at Arlington, Arlington TX, United States of America
[9] Physics Department, University of Athens, Athens, Greece
[10] Physics Department, National Technical University of Athens, Zografou, Greece



JHEP10(2013)130

[11] Institute of Physics, Azerbaijan Academy of Sciences, Baku, Azerbaijan
[12] Institut de Física d'Altes Energies and Departament de Física de la Universitat Autònoma de Barcelona, Barcelona, Spain
[13] [(a)] Institute of Physics, University of Belgrade, Belgrade; [(b)] Vinca Institute of Nuclear Sciences, University of Belgrade, Belgrade, Serbia
[14] Department for Physics and Technology, University of Bergen, Bergen, Norway
[15] Physics Division, Lawrence Berkeley National Laboratory and University of California, Berkeley CA, United States of America
[16] Department of Physics, Humboldt University, Berlin, Germany
[17] Albert Einstein Center for Fundamental Physics and Laboratory for High Energy Physics, University of Bern, Bern, Switzerland
[18] School of Physics and Astronomy, University of Birmingham, Birmingham, United Kingdom
[19] [(a)] Department of Physics, Bogazici University, Istanbul; [(b)] Department of Physics, Dogus University, Istanbul; [(c)] Department of Physics Engineering, Gaziantep University, Gaziantep, Turkey
[20] [(a)] INFN Sezione di Bologna; [(b)] Dipartimento di Fisica e Astronomia, Università di Bologna, Bologna, Italy
[21] Physikalisches Institut, University of Bonn, Bonn, Germany
[22] Department of Physics, Boston University, Boston MA, United States of America
[23] Department of Physics, Brandeis University, Waltham MA, United States of America
[24] [(a)] Universidade Federal do Rio De Janeiro COPPE/EE/IF, Rio de Janeiro; [(b)] Federal University of Juiz de Fora (UFJF), Juiz de Fora; [(c)] Federal University of Sao Joao del Rei (UFSJ), Sao Joao del Rei; [(d)] Instituto de Fisica, Universidade de Sao Paulo, Sao Paulo, Brazil
[25] Physics Department, Brookhaven National Laboratory, Upton NY, United States of America
[26] [(a)] National Institute of Physics and Nuclear Engineering, Bucharest; [(b)] National Institute for Research and Development of Isotopic and Molecular Technologies, Physics Department, Cluj Napoca; [(c)] University Politehnica Bucharest, Bucharest; [(d)] West University in Timisoara, Timisoara, Romania
[27] Departamento de Física, Universidad de Buenos Aires, Buenos Aires, Argentina
[28] Cavendish Laboratory, University of Cambridge, Cambridge, United Kingdom
[29] Department of Physics, Carleton University, Ottawa ON, Canada
[30] CERN, Geneva, Switzerland
[31] Enrico Fermi Institute, University of Chicago, Chicago IL, United States of America
[32] [(a)] Departamento de Física, Pontificia Universidad Católica de Chile, Santiago; [(b)] Departamento de Física, Universidad Técnica Federico Santa María, Valparaíso, Chile
[33] [(a)] Institute of High Energy Physics, Chinese Academy of Sciences, Beijing; [(b)] Department of Modern Physics, University of Science and Technology of China, Anhui; [(c)] Department of Physics, Nanjing University, Jiangsu; [(d)] School of Physics, Shandong University, Shandong; [(e)] Physics Department, Shanghai Jiao Tong University, Shanghai, China
[34] Laboratoire de Physique Corpusculaire, Clermont Université and Université Blaise Pascal and CNRS/IN2P3, Clermont-Ferrand, France
[35] Nevis Laboratory, Columbia University, Irvington NY, United States of America
[36] Niels Bohr Institute, University of Copenhagen, Kobenhavn, Denmark
[37] [(a)] INFN Gruppo Collegato di Cosenza; [(b)] Dipartimento di Fisica, Università della Calabria, Rende, Italy
[38] [(a)] AGH University of Science and Technology, Faculty of Physics and Applied Computer Science, Krakow; [(b)] Marian Smoluchowski Institute of Physics, Jagiellonian University, Krakow, Poland
[39] The Henryk Niewodniczanski Institute of Nuclear Physics, Polish Academy of Sciences, Krakow, Poland
[40] Physics Department, Southern Methodist University, Dallas TX, United States of America
[41] Physics Department, University of Texas at Dallas, Richardson TX, United States of America
[42] DESY, Hamburg and Zeuthen, Germany

JHEP10(2013)130

[43] Institut für Experimentelle Physik IV, Technische Universität Dortmund, Dortmund, Germany
[44] Institut für Kern- und Teilchenphysik, Technische Universität Dresden, Dresden, Germany
[45] Department of Physics, Duke University, Durham NC, United States of America
[46] SUPA - School of Physics and Astronomy, University of Edinburgh, Edinburgh, United Kingdom
[47] INFN Laboratori Nazionali di Frascati, Frascati, Italy
[48] Fakultät für Mathematik und Physik, Albert-Ludwigs-Universität, Freiburg, Germany
[49] Section de Physique, Université de Genève, Geneva, Switzerland
[50] [(a)] INFN Sezione di Genova; [(b)] Dipartimento di Fisica, Università di Genova, Genova, Italy
[51] [(a)] E. Andronikashvili Institute of Physics, Iv. Javakhishvili Tbilisi State University, Tbilisi; [(b)] High Energy Physics Institute, Tbilisi State University, Tbilisi, Georgia
[52] II Physikalisches Institut, Justus-Liebig-Universität Giessen, Giessen, Germany
[53] SUPA - School of Physics and Astronomy, University of Glasgow, Glasgow, United Kingdom
[54] II Physikalisches Institut, Georg-August-Universität, Göttingen, Germany
[55] Laboratoire de Physique Subatomique et de Cosmologie, Université Joseph Fourier and CNRS/IN2P3 and Institut National Polytechnique de Grenoble, Grenoble, France
[56] Department of Physics, Hampton University, Hampton VA, United States of America
[57] Laboratory for Particle Physics and Cosmology, Harvard University, Cambridge MA, United States of America
[58] [(a)] Kirchhoff-Institut für Physik, Ruprecht-Karls-Universität Heidelberg, Heidelberg; [(b)] Physikalisches Institut, Ruprecht-Karls-Universität Heidelberg, Heidelberg; [(c)] ZITI Institut für technische Informatik, Ruprecht-Karls-Universität Heidelberg, Mannheim, Germany
[59] Faculty of Applied Information Science, Hiroshima Institute of Technology, Hiroshima, Japan
[60] Department of Physics, Indiana University, Bloomington IN, United States of America
[61] Institut für Astro- und Teilchenphysik, Leopold-Franzens-Universität, Innsbruck, Austria
[62] University of Iowa, Iowa City IA, United States of America
[63] Department of Physics and Astronomy, Iowa State University, Ames IA, United States of America
[64] Joint Institute for Nuclear Research, JINR Dubna, Dubna, Russia
[65] KEK, High Energy Accelerator Research Organization, Tsukuba, Japan
[66] Graduate School of Science, Kobe University, Kobe, Japan
[67] Faculty of Science, Kyoto University, Kyoto, Japan
[68] Kyoto University of Education, Kyoto, Japan
[69] Department of Physics, Kyushu University, Fukuoka, Japan
[70] Instituto de Física La Plata, Universidad Nacional de La Plata and CONICET, La Plata, Argentina
[71] Physics Department, Lancaster University, Lancaster, United Kingdom
[72] [(a)] INFN Sezione di Lecce; [(b)] Dipartimento di Matematica e Fisica, Università del Salento, Lecce, Italy
[73] Oliver Lodge Laboratory, University of Liverpool, Liverpool, United Kingdom
[74] Department of Physics, Jožef Stefan Institute and University of Ljubljana, Ljubljana, Slovenia
[75] School of Physics and Astronomy, Queen Mary University of London, London, United Kingdom
[76] Department of Physics, Royal Holloway University of London, Surrey, United Kingdom
[77] Department of Physics and Astronomy, University College London, London, United Kingdom
[78] Louisiana Tech University, Ruston LA, United States of America
[79] Laboratoire de Physique Nucléaire et de Hautes Energies, UPMC and Université Paris-Diderot and CNRS/IN2P3, Paris, France
[80] Fysiska institutionen, Lunds universitet, Lund, Sweden
[81] Departamento de Fisica Teorica C-15, Universidad Autonoma de Madrid, Madrid, Spain
[82] Institut für Physik, Universität Mainz, Mainz, Germany
[83] School of Physics and Astronomy, University of Manchester, Manchester, United Kingdom
[84] CPPM, Aix-Marseille Université and CNRS/IN2P3, Marseille, France
[85] Department of Physics, University of Massachusetts, Amherst MA, United States of America
[86] Department of Physics, McGill University, Montreal QC, Canada
[87] School of Physics, University of Melbourne, Victoria, Australia

JHEP10(2013)130

[88] Department of Physics, The University of Michigan, Ann Arbor MI, United States of America
[89] Department of Physics and Astronomy, Michigan State University, East Lansing MI, United States of America
[90] [(a)] INFN Sezione di Milano; [(b)] Dipartimento di Fisica, Università di Milano, Milano, Italy
[91] B.I. Stepanov Institute of Physics, National Academy of Sciences of Belarus, Minsk, Republic of Belarus
[92] National Scientific and Educational Centre for Particle and High Energy Physics, Minsk, Republic of Belarus
[93] Department of Physics, Massachusetts Institute of Technology, Cambridge MA, United States of America
[94] Group of Particle Physics, University of Montreal, Montreal QC, Canada
[95] P.N. Lebedev Institute of Physics, Academy of Sciences, Moscow, Russia
[96] Institute for Theoretical and Experimental Physics (ITEP), Moscow, Russia
[97] Moscow Engineering and Physics Institute (MEPhI), Moscow, Russia
[98] D.V.Skobeltsyn Institute of Nuclear Physics, M.V.Lomonosov Moscow State University, Moscow, Russia
[99] Fakultät für Physik, Ludwig-Maximilians-Universität München, München, Germany
[100] Max-Planck-Institut für Physik (Werner-Heisenberg-Institut), München, Germany
[101] Nagasaki Institute of Applied Science, Nagasaki, Japan
[102] Graduate School of Science and Kobayashi-Maskawa Institute, Nagoya University, Nagoya, Japan
[103] [(a)] INFN Sezione di Napoli; [(b)] Dipartimento di Scienze Fisiche, Università di Napoli, Napoli, Italy
[104] Department of Physics and Astronomy, University of New Mexico, Albuquerque NM, United States of America
[105] Institute for Mathematics, Astrophysics and Particle Physics, Radboud University Nijmegen/Nikhef, Nijmegen, Netherlands
[106] Nikhef National Institute for Subatomic Physics and University of Amsterdam, Amsterdam, Netherlands
[107] Department of Physics, Northern Illinois University, DeKalb IL, United States of America
[108] Budker Institute of Nuclear Physics, SB RAS, Novosibirsk, Russia
[109] Department of Physics, New York University, New York NY, United States of America
[110] Ohio State University, Columbus OH, United States of America
[111] Faculty of Science, Okayama University, Okayama, Japan
[112] Homer L. Dodge Department of Physics and Astronomy, University of Oklahoma, Norman OK, United States of America
[113] Department of Physics, Oklahoma State University, Stillwater OK, United States of America
[114] Palacký University, RCPTM, Olomouc, Czech Republic
[115] Center for High Energy Physics, University of Oregon, Eugene OR, United States of America
[116] LAL, Université Paris-Sud and CNRS/IN2P3, Orsay, France
[117] Graduate School of Science, Osaka University, Osaka, Japan
[118] Department of Physics, University of Oslo, Oslo, Norway
[119] Department of Physics, Oxford University, Oxford, United Kingdom
[120] [(a)] INFN Sezione di Pavia; [(b)] Dipartimento di Fisica, Università di Pavia, Pavia, Italy
[121] Department of Physics, University of Pennsylvania, Philadelphia PA, United States of America
[122] Petersburg Nuclear Physics Institute, Gatchina, Russia
[123] [(a)] INFN Sezione di Pisa; [(b)] Dipartimento di Fisica E. Fermi, Università di Pisa, Pisa, Italy
[124] Department of Physics and Astronomy, University of Pittsburgh, Pittsburgh PA, United States of America
[125] [(a)] Laboratorio de Instrumentacao e Fisica Experimental de Particulas - LIP, Lisboa, Portugal; [(b)] Departamento de Fisica Teorica y del Cosmos and CAFPE, Universidad de Granada, Granada, Spain
[126] Institute of Physics, Academy of Sciences of the Czech Republic, Praha, Czech Republic
[127] Czech Technical University in Prague, Praha, Czech Republic

JHEP10(2013)130

[128] Faculty of Mathematics and Physics, Charles University in Prague, Praha, Czech Republic
[129] State Research Center Institute for High Energy Physics, Protvino, Russia
[130] Particle Physics Department, Rutherford Appleton Laboratory, Didcot, United Kingdom
[131] Physics Department, University of Regina, Regina SK, Canada
[132] Ritsumeikan University, Kusatsu, Shiga, Japan
[133] [(a)] INFN Sezione di Roma I; [(b)] Dipartimento di Fisica, Università La Sapienza, Roma, Italy
[134] [(a)] INFN Sezione di Roma Tor Vergata; [(b)] Dipartimento di Fisica, Università di Roma Tor Vergata, Roma, Italy
[135] [(a)] INFN Sezione di Roma Tre; [(b)] Dipartimento di Matematica e Fisica, Università Roma Tre, Roma, Italy
[136] [(a)] Faculté des Sciences Ain Chock, Réseau Universitaire de Physique des Hautes Energies - Université Hassan II, Casablanca; [(b)] Centre National de l'Energie des Sciences Techniques Nucleaires, Rabat; [(c)] Faculté des Sciences Semlalia, Université Cadi Ayyad, LPHEA-Marrakech; [(d)] Faculté des Sciences, Université Mohamed Premier and LPTPM, Oujda; [(e)] Faculté des sciences, Université Mohammed V-Agdal, Rabat, Morocco
[137] DSM/IRFU (Institut de Recherches sur les Lois Fondamentales de l'Univers), CEA Saclay (Commissariat à l'Energie Atomique et aux Energies Alternatives), Gif-sur-Yvette, France
[138] Santa Cruz Institute for Particle Physics, University of California Santa Cruz, Santa Cruz CA, United States of America
[139] Department of Physics, University of Washington, Seattle WA, United States of America
[140] Department of Physics and Astronomy, University of Sheffield, Sheffield, United Kingdom
[141] Department of Physics, Shinshu University, Nagano, Japan
[142] Fachbereich Physik, Universität Siegen, Siegen, Germany
[143] Department of Physics, Simon Fraser University, Burnaby BC, Canada
[144] SLAC National Accelerator Laboratory, Stanford CA, United States of America
[145] [(a)] Faculty of Mathematics, Physics & Informatics, Comenius University, Bratislava; [(b)] Department of Subnuclear Physics, Institute of Experimental Physics of the Slovak Academy of Sciences, Kosice, Slovak Republic
[146] [(a)] Department of Physics, University of Cape Town, Cape Town; [(b)] Department of Physics, University of Johannesburg, Johannesburg; [(c)] School of Physics, University of the Witwatersrand, Johannesburg, South Africa
[147] [(a)] Department of Physics, Stockholm University; [(b)] The Oskar Klein Centre, Stockholm, Sweden
[148] Physics Department, Royal Institute of Technology, Stockholm, Sweden
[149] Departments of Physics & Astronomy and Chemistry, Stony Brook University, Stony Brook NY, United States of America
[150] Department of Physics and Astronomy, University of Sussex, Brighton, United Kingdom
[151] School of Physics, University of Sydney, Sydney, Australia
[152] Institute of Physics, Academia Sinica, Taipei, Taiwan
[153] Department of Physics, Technion: Israel Institute of Technology, Haifa, Israel
[154] Raymond and Beverly Sackler School of Physics and Astronomy, Tel Aviv University, Tel Aviv, Israel
[155] Department of Physics, Aristotle University of Thessaloniki, Thessaloniki, Greece
[156] International Center for Elementary Particle Physics and Department of Physics, The University of Tokyo, Tokyo, Japan
[157] Graduate School of Science and Technology, Tokyo Metropolitan University, Tokyo, Japan
[158] Department of Physics, Tokyo Institute of Technology, Tokyo, Japan
[159] Department of Physics, University of Toronto, Toronto ON, Canada
[160] [(a)] TRIUMF, Vancouver BC; [(b)] Department of Physics and Astronomy, York University, Toronto ON, Canada
[161] Faculty of Pure and Applied Sciences, University of Tsukuba, Tsukuba, Japan
[162] Department of Physics and Astronomy, Tufts University, Medford MA, United States of America
[163] Centro de Investigaciones, Universidad Antonio Narino, Bogota, Colombia

JHEP10(2013)130

[164] Department of Physics and Astronomy, University of California Irvine, Irvine CA, United States of America
[165] [(a)] INFN Gruppo Collegato di Udine; [(b)] ICTP, Trieste; [(c)] Dipartimento di Chimica, Fisica e Ambiente, Università di Udine, Udine, Italy
[166] Department of Physics, University of Illinois, Urbana IL, United States of America
[167] Department of Physics and Astronomy, University of Uppsala, Uppsala, Sweden
[168] Instituto de Física Corpuscular (IFIC) and Departamento de Física Atómica, Molecular y Nuclear and Departamento de Ingeniería Electrónica and Instituto de Microelectrónica de Barcelona (IMB-CNM), University of Valencia and CSIC, Valencia, Spain
[169] Department of Physics, University of British Columbia, Vancouver BC, Canada
[170] Department of Physics and Astronomy, University of Victoria, Victoria BC, Canada
[171] Department of Physics, University of Warwick, Coventry, United Kingdom
[172] Waseda University, Tokyo, Japan
[173] Department of Particle Physics, The Weizmann Institute of Science, Rehovot, Israel
[174] Department of Physics, University of Wisconsin, Madison WI, United States of America
[175] Fakultät für Physik und Astronomie, Julius-Maximilians-Universität, Würzburg, Germany
[176] Fachbereich C Physik, Bergische Universität Wuppertal, Wuppertal, Germany
[177] Department of Physics, Yale University, New Haven CT, United States of America
[178] Yerevan Physics Institute, Yerevan, Armenia
[179] Centre de Calcul de l'Institut National de Physique Nucléaire et de Physique des Particules (IN2P3), Villeurbanne, France

[a] Also at Department of Physics, King's College London, London, United Kingdom
[b] Also at Laboratorio de Instrumentacao e Fisica Experimental de Particulas - LIP, Lisboa, Portugal
[c] Also at Faculdade de Ciencias and CFNUL, Universidade de Lisboa, Lisboa, Portugal
[d] Also at Particle Physics Department, Rutherford Appleton Laboratory, Didcot, United Kingdom
[e] Also at TRIUMF, Vancouver BC, Canada
[f] Also at Department of Physics, California State University, Fresno CA, United States of America
[g] Also at Novosibirsk State University, Novosibirsk, Russia
[h] Also at Department of Physics, University of Coimbra, Coimbra, Portugal
[i] Also at Università di Napoli Parthenope, Napoli, Italy
[j] Also at Institute of Particle Physics (IPP), Canada
[k] Also at Department of Physics, Middle East Technical University, Ankara, Turkey
[l] Also at Louisiana Tech University, Ruston LA, United States of America
[m] Also at Dep Fisica and CEFITEC of Faculdade de Ciencias e Tecnologia, Universidade Nova de Lisboa, Caparica, Portugal
[n] Also at Department of Physics and Astronomy, Michigan State University, East Lansing MI, United States of America
[o] Also at Department of Financial and Management Engineering, University of the Aegean, Chios, Greece
[p] Also at Institucio Catalana de Recerca i Estudis Avancats, ICREA, Barcelona, Spain
[q] Also at Department of Physics, University of Cape Town, Cape Town, South Africa
[r] Also at Institute of Physics, Azerbaijan Academy of Sciences, Baku, Azerbaijan
[s] Also at Ochadai Academic Production, Ochanomizu University, Tokyo, Japan
[t] Also at Manhattan College, New York NY, United States of America
[u] Also at Institute of Physics, Academia Sinica, Taipei, Taiwan
[v] Also at School of Physics and Engineering, Sun Yat-sen University, Guanzhou, China
[w] Also at Academia Sinica Grid Computing, Institute of Physics, Academia Sinica, Taipei, Taiwan
[x] Also at Laboratoire de Physique Nucléaire et de Hautes Energies, UPMC and Université Paris-Diderot and CNRS/IN2P3, Paris, France
[y] Also at School of Physical Sciences, National Institute of Science Education and Research, Bhubaneswar, India

JHEP10(2013)130

[z] Also at Dipartimento di Fisica, Università La Sapienza, Roma, Italy
[aa] Also at DSM/IRFU (Institut de Recherches sur les Lois Fondamentales de l'Univers), CEA Saclay (Commissariat à l'Energie Atomique et aux Energies Alternatives), Gif-sur-Yvette, France
[ab] Also at Moscow Institute of Physics and Technology State University, Dolgoprudny, Russia
[ac] Also at Section de Physique, Université de Genève, Geneva, Switzerland
[ad] Also at Departamento de Fisica, Universidade de Minho, Braga, Portugal
[ae] Also at Department of Physics, The University of Texas at Austin, Austin TX, United States of America
[af] Also at Institute for Particle and Nuclear Physics, Wigner Research Centre for Physics, Budapest, Hungary
[ag] Also at DESY, Hamburg and Zeuthen, Germany
[ah] Also at International School for Advanced Studies (SISSA), Trieste, Italy
[ai] Also at Department of Physics and Astronomy, University of South Carolina, Columbia SC, United States of America
[aj] Also at Faculty of Physics, M.V.Lomonosov Moscow State University, Moscow, Russia
[ak] Also at Nevis Laboratory, Columbia University, Irvington NY, United States of America
[al] Also at Physics Department, Brookhaven National Laboratory, Upton NY, United States of America
[am] Also at Moscow Engineering and Physics Institute (MEPhI), Moscow, Russia
[an] Also at Department of Physics, Oxford University, Oxford, United Kingdom
[ao] Also at Institut für Experimentalphysik, Universität Hamburg, Hamburg, Germany
[ap] Also at Department of Physics, The University of Michigan, Ann Arbor MI, United States of America
[aq] Also at Discipline of Physics, University of KwaZulu-Natal, Durban, South Africa
[*] Deceased

JHEP10(2013)130